

Rheological and Physical Properties of AP-101 LAW Pretreated Waste and Melter Feed

P. R. Bredt	B. K. McNamara
B. W. Arey	A. P. Poloski
E. C. Buck	R. G. Swoboda
E. D. Jenson	

March 2003

WTP Project Report

Prepared for Bechtel National, Inc.
under Contract 24590-101-TSA-W000-0004

LEGAL NOTICE

This report was prepared by Battelle Memorial Institute (Battelle) as an account of sponsored research activities. Neither Client nor Battelle nor any person acting on behalf of either:

MAKES ANY WARRANTY OR REPRESENTATION, EXPRESS OR IMPLIED, with respect to the accuracy, completeness, or usefulness of the information contained in this report, or that the use of any information, apparatus, process, or composition disclosed in this report may not infringe privately owned rights; or assumes any liabilities with respect to the use of, or for damages resulting from the use of, any information, apparatus, process, or composition disclosed in this report.

Reference herein to any specific commercial product, process, or service by trade name, trademark, manufacturer, or otherwise, does not necessarily constitute or imply its endorsement, recommendation, or favoring by Battelle. The views and opinions of authors expressed herein do not necessarily state or reflect those of Battelle.

Rheological and Physical Properties of AP-101 LAW Pretreated Waste and Melter Feed

P. R. Bredt B. K. McNamara
B. W. Arey A. P. Poloski
E. C. Buck R. G. Swoboda
E. D. Jenson

March 2003

Prepared for Bechtel National, Inc.
under Contract 24590-101-TSA-W000-0004

Test specification: 24590-LAW-TSP-RT-01-001 Rev 1
Test plan: TP-RPP-WTP-104 Rev 0
Test exceptions: 24590-WTP-TEF-RT-02-064
R&T focus area: Pretreatment & Vitrification
Test Scoping Statement(s): B-17

Battelle - Pacific Northwest Division
Richland, Washington 99352

Completeness of Testing

This report describes the results of work and testing specified by Test Specification 24590-LAW-TSP-RT-01-001 Rev. 1 and Test Plan TP-RPP-WTP-104 Rev. 0. The work and any associated testing followed the quality assurance requirements outlined in the Test Specification/Plan. The descriptions provided in this test report are an accurate account of both the conduct of the work and the data collected. Test plan results are reported. Also reported are any unusual or anomalous occurrences that are different from expected results. The test results and this report have been reviewed and verified.

Approved:

Gordon H. Beeman, Manager
WTP R&T Support Project

Date

Summary

Objectives

This document describes work performed under Battelle – Pacific Northwest Division (PNWD) Test Plan TP-RPP-WTP-104 Rev 0 “AP-101 Melter Feed Rheology Testing”. The objective of this report is to present physical and rheological properties of AP-101 waste that is in a state similar to two streams anticipated in the Waste Treatment Plant (WTP). The first stream considered was the pretreated Low-Activity Waste (LAW) stream that consists of the effluent from the Cesium and Technetium ion exchange columns. The second stream is the LAW melter feed material. This material consists of the pretreated LAW waste stream mixed with a formulation of glass former chemicals.

Conduct of Testing

The measurement of physical properties described in this document were performed in accordance with *Guidelines for Performing Chemical, Physical, and Rheological Properties Measurements* (24590-WTP-GPG-RTD-001 Rev 0). Pretreated AP-101 material at a Na concentration of 4.9 M was the source material for all measurements in this document. Initially, the 4.9 M Na pretreated material was evaporated to several other Na concentrations (6 M, 8 M, and 10 M). It was observed that the material at 4.9 M Na did not contain visible solids. However, solids did precipitate during the evaporation to 6 M, 8 M, and 10 M Na concentrations. These solids were identified to be primarily sodium nitrate and possibly potassium carbonate. The quantity of these phases precipitating increased with increasing sodium concentration. A minor phase, nitrate-cancrinite (nitrate form of $(\text{Na,Ca,K})_7\text{Al}_6\text{Si}_6\text{O}_{24}(\text{CO}_3)_{1.6}\cdot 2.1\text{H}_2\text{O}$), increased in concentration with increasing sodium concentration. The solids at 6 M, 8 M, and 10 M Na appeared similar in chemistry with increasing wt% solids at higher Na concentrations. The 6 M, 8 M, and 10 M Na samples were mixed to suspend the solids and aliquots from each of these samples were drawn. The settling behavior of the solids at 6 M and 8 M Na concentrations were characterized at 25°C and 40°C^a. Next, physical properties were determined for the 6 M, 8 M, and 10 M Na samples at 25°C. Then an additional set of physical properties measurements at 40°C were performed on the 6 M and 8 M Na samples. Lastly, a Haake RS300 rheometer was used to measure the rheological properties of the 4.9 M, 6 M, 8 M, and 10 M Na samples at 25°C and 40°C.

The 6 M and 8 M Na pretreated waste samples were then mixed with project approved glass former chemicals in a formulation consistent with “LAWA-126^b”. This material should be considered representative of the LAW melter feed stream in the WTP. The melter feeds were agitated to suspend the solids and aliquots were drawn from both homogenized samples at room temperature. The settling behavior of these 6 M and 8 M Na melter feed aliquots was measured at 25°C and 40°C. Physical property measurements were then performed on these aliquots at 25°C and 40°C. Next, the samples were allowed to remain undisturbed for a 48-hour period at a temperature of 40°C. A shear vane was used with a Haake RS300 rheometer to determine the 6 M and 8 M Na LAW melter feed settled solids shear strength at 40°C. The rheological properties of the 6 M and 8 M Na LAW melter feeds were measured with a Haake RS300 rheometer at 25°C and 40°C. A series of rheological measurements on the 8 M Na melter feed sample based on mixing/aging times of 1 hour, 1 day, and 1 week were performed. Particle size measurements on the 6 M Na melter feed sample were also performed.

a 40°C was used throughout this testing as it is close to the expected operating temperature of the WTP

b LAWA-126 is a glass formulation developed by Vitreous State Laboratory (VSL) at the Catholic University of America.

Results and Performance Against Objectives

The results from the testing of the AP-101 pretreated waste at 4.9 M, 6 M, 8 M, and 10 M Na concentrations are summarized in Table S.1. Based on rheological characterization, the material appeared to be Newtonian in nature with average viscosities ranging from approximately 2 cP to 12 cP. As expected, the measured viscosity increases with Na concentration and decreases with increased temperature. These viscosity measurements fall within the pretreated LAW bounding conditions of 0.4-15 cP (Poloski et al., 2002). Consistent with visual observations, the amount of undissolved solids appears to increase as the sample is evaporated indicating that the sample is saturated with respect to sodium nitrate and possibly a potassium carbonate. A minor phase, nitrate-cancrinite, increased in concentration with increasing sodium concentration. With this in consideration, the physical properties of these samples appear to be self-consistent.

Table S.1. Summary of AP-101 Pretreated LAW Measurements^a

Description	Units	4.9 <u>M</u> Na	6 <u>M</u> Na	8 <u>M</u> Na	10 <u>M</u> Na
Newtonian Viscosity	cP	25°C: 3.5 40°C: 2.5	25°C: 5.2 40°C: 3.6	25°C: 8.0 40°C: 5.4	25°C: 11.8 40°C: 7.2
Bulk Density	g/mL	1.259	25°C: 1.325 40°C: 1.293	25°C: 1.399 40°C: 1.360	1.461
Density of Settled Solids	g/mL	c	b	b	d
Density of Centrifuged Solids	g/mL	c	b	b	d
Supernatant Density	g/mL	1.259	1.33	1.40	1.45
Average Particle Density	g/mL	c	b	b	d
72 hr Vol% Settled Solids	%	c	25°C: 3.8 40°C: 2.3	25°C: 9.9 40°C: 8.4	d
Vol% Centrifuged Solids	%	c	1.9	6.8	d
Vol% undissolved solids		c	b	b	d
Vol% undissolved solids in settled solids	%	c	b	b	d
Vol% undissolved solids in centrifuged solids	%	c	b	b	d
Wt% settled solids	%	c	b	b	d
Wt% centrifuged solids	%	c	b	b	d
Wt% Total dried Solids	%	d	35.8	25°C: 43.0 40°C: 43.0	49.0
Wt% Dissolved Solids	%	d	35.8	25°C: 42.3 40°C: 42.5	45.3
Wt% Undissolved Solids	%	c	b	25°C: 1.2 40°C: 0.81	6.7
Wt% Undissolved Solids in Settled Solids	%	c	b	b	d
Wt% Undissolved Solids in Centrifuged Solids	%	c	b	b	d
a Unless otherwise stated measurements were taken at 25°C b Too little solids to quantify c No solids visible in 4.9 <u>M</u> Na feed d Not measured as part of scope					

The results from the tests performed on the melter feed material are summarized in Table S.2. The AP-101 melter feed material appeared to be Newtonian in nature with average viscosities ranging from approximately 10 cP to 40 cP depending on Na molarity and measurement temperature. Note that shear strength measurements were performed on the settled solids several times on both samples, and the order of magnitude higher shear strength of the 6 M Na sample over the 8 M Na sample appears valid (see Section 5.0). One possible explanation for this behavior could be the higher degree of precipitated solids in the 8 M Na system. These precipitated solids could disrupt the settled solids “network” resulting in the observed lower shear strength in the 8 M Na sample. Note that the melter feed formulation required a larger quantity of glass former chemicals to be added to the 8 M sample on a per volume basis (see Section 2.0). With this in consideration, the physical properties of these samples appear to be self-consistent. The packing efficiency of the settled solids samples appears to decrease as temperature increases. This is demonstrated by the observed increase in settled solids volume percent at elevated temperatures while the weight percent undissolved solids remains relatively constant.

Table S.2. Summary of AP-101 LAW Melter Feed Measurements

Description	Units	6 M Na	8 M Na
Viscosity	cP	25°C: 13.2	25°C: 39.9
		40°C: 9.7	40°C: 27.0
Settled Solids Shear Strength at 40°C	Pa	790	79
pH (at ambient)	--	12.3	12.5
Bulk Density	g/mL	25°C: 1.645	25°C: 1.742
		40°C: 1.587	40°C: 1.734
Density of Settled Solids	g/mL	25°C: 1.95	25°C: 1.97
		40°C: 1.78	40°C: 1.81
Density of Centrifuged Solids	g/mL	25°C: 2.11	25°C: 2.11
		40°C: 1.99	40°C: 2.04
Supernatant Density	g/mL	25°C: 1.34	25°C: 1.39
		40°C: 1.30	40°C: 1.38
Average Particle Density	g/mL	25°C: 3.10	25°C: 3.01
		40°C: 3.13	40°C: 3.17
72 hr Vol% Settled Solids	%	25°C: 49.9	25°C: 60.3
		40°C: 60.1	40°C: 81.7
Vol% Centrifuged Solids	%	25°C: 39.9	25°C: 49.3
		40°C: 41.4	40°C: 54.3
Vol% Undissolved Solids	%	25°C: 17.5	25°C: 21.8
		40°C: 15.9	40°C: 19.7
Vol% Undissolved Solids in Settled Solids	%	25°C: 34.8	25°C: 36.0
		40°C: 26.8	40°C: 24.2
Vol% Undissolved Solids in Centrifuged Solids	%	25°C: 43.8	25°C: 44.2
		40°C: 38.9	40°C: 36.4
Wt% Settled Solids	%	25°C: 59.5	25°C: 68.6
		40°C: 67.1	40°C: 85.4
Wt% Centrifuged Solids	%	25°C: 51.2	25°C: 59.6
		40°C: 52.1	40°C: 63.7
Wt. % Total Dried Solids	%	25°C: 58.0	25°C: 65.3
		40°C: 58.1	40°C: 65.2
Wt. % Dissolved Solids	%	25°C: 37.3	25°C: 44.1
		40°C: 35.3	40°C: 44.8
Wt. % Undissolved Solids	%	25°C: 32.9	25°C: 37.7
		40°C: 31.4	40°C: 36.0
Wt% Undissolved Solids in Settled Solids	%	25°C: 55.3	25°C: 54.9
		40°C: 46.6	40°C: 47.4
Wt% Undissolved Solids in Centrifuged Solids	%	25°C: 64.3	25°C: 63.2
		40°C: 60.6	40°C: 56.7

Glass former chemicals were continuously mixed with an AP-101 8 M Na pretreated waste sample. At intervals of one hour, one day, and one week, the rheology and pH of the sample was measured. After the one-week interval, the rheological properties of the settled solids portion of the sample were measured. Lastly, the shear strength of the one-week mixed material was measured. Results from these tests are shown in Table S.3.

As expected, at higher temperatures the viscosity of the melter feeds drops. At 25°C the mixing/aging viscosity measurements increase after one day of mixing. At 40°C the mixing/aging viscosity values increase after one week of mixing. While increasing over the one-week mixed/aged

period, the viscosity of the 8 M Na LAW melter feed was less than or comparable to that observed for the 8 M Na LAW melter feed at 25°C and 40°C reported in Table S.2. The material used in the measurements reported in Table S.1 has a mixing/aging history of being mixed for one hour and aged for one month. Since the material in the WTP is not anticipated to be mixed and aged for this extended period, the viscosity of the actual slurry should be bounded by testing described in this report. These measurements fall within the LAW melter feed bounding conditions (Poloski et al., 2002) of Bingham plastic consistency index between 0.4-90 cP and Bingham plastic yield index not to exceed 15 Pa.

The pH of the melter feed sample was also measured during the mixing/aging portion of the study. Results of these measurements are shown in Table S.3. The pH of the sample remains the same as the reported value of 12.5 (see Table S.2) throughout the mixing/aging process.

Rheology of the settled solids portion of the one-week mixed sample indicates Bingham Plastic behavior. Both the consistency and yield indices decrease with increasing temperature. These measurements fall outside the LAW melter feed bounding conditions (Poloski et al., 2002) of Bingham plastic consistency index between 0.4-90 cP and Bingham plastic yield index not to exceed 15 Pa. Shear strength on the settled solids fraction was also measured. The shear strength of the sample exhibits a high degree of sensitivity to temperature with a value of approximately 2600 Pa at ambient temperature and 610 Pa at 40°C. Poloski et al. (2002) demonstrated that design challenges may be faced with materials possessing a shear strength above approximately 625 Pa.

Table S.3. Summary of 8 M Na AP-101 LAW Melter Feed Mixing/Aging Measurements

Description	Units	Ambient (~23°C)	25°C	40°C
Viscosity (1-hr mixing time)	cP	NM	24.7	19.8
Viscosity (1-day mixing time)	cP	NM	30.6	21.6
Viscosity (1-wk mixing time)	cP	NM	31.0	28.7
pH (1-hr mixing time at ambient)	--	12.5	NM	NM
pH (1-day mixing time at ambient)	--	12.5	NM	NM
pH (1-wk mixing time at ambient)	--	12.5	NM	NM
Bingham Plastic Indices of Settled Solids (1-wk mixing time)	--	NM	Consistency (cP): 177.8 Yield (Pa): 21.8	Consistency (cP): 128.2 Yield (Pa): 6.1
Shear Strength of Settled Solids (1-wk mixing time)	Pa	2600	NM	610
NM – Not measured as part of scope.				

The particle size distribution of a 6 M Na melter feed sample was measured. Initially, a calibration check on the particle size instrument was performed. The number basis mean results were within approximately 15% of the NIST traceable values. Due to deterioration of the particle size instrument, the typical 10% difference between the number basis mean results and NIST traceable values of the Duke Scientific particle size standards could not be reached. The particle size distribution from the 6 M Na melter feed sample is shown in Figure S.1. The particle size distribution exhibits two major peaks, one in approximately the 2 to 7 μm range and the other in approximately the 10 to 20 μm range. The resulting mean particle size on a volume, basis is 9.2 μm . Approximately 10 vol% of the particles are below 2.6 μm , 50 vol% (i.e., median value) below 7.6 μm , 90 vol% below 18.2 μm , and 95 vol% below 20.2 μm .

The particle size distribution of a LAWA-126 glass former mix in deionized water sample was also measured. The resulting particle size distribution is shown in Figure S.1. The particle size distribution exhibits two major peaks, one in approximately the 0.5 to 1.5 μm range and the other in approximately the 5 to 40 μm range. The resulting mean particle size on a volume basis is 19.9 μm . Approximately 10 vol% of the particles are below 1.1 μm , 50 vol% (i.e., median value) below 17.2 μm , 90 vol% below 43.8 μm , and 95 vol% below 50.8 μm .

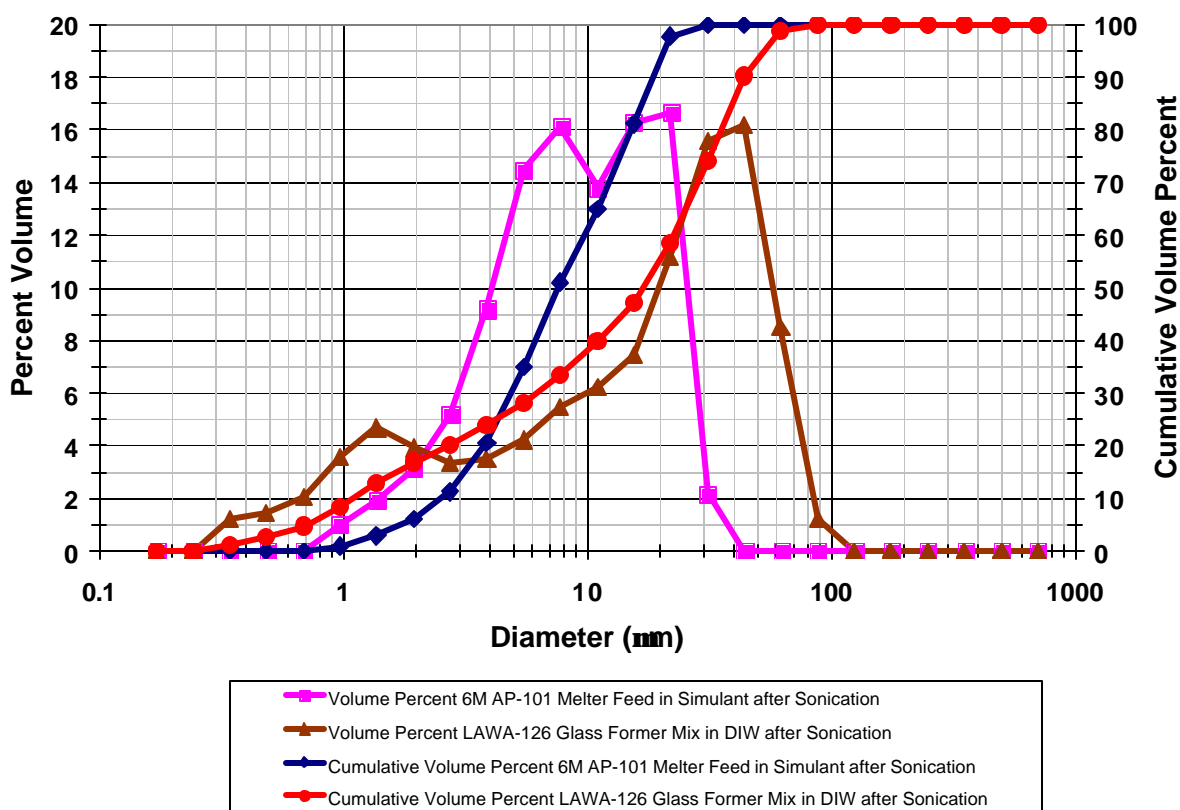


Figure S.1. Summary of AP-101 6 M Na LAW Melter Feed and LAWA-126 Glass Former Mix Particle Size Distribution

Quality Requirements

PNWD implemented the River Protection Project (RPP)-WTP quality requirements by performing work in accordance with the quality assurance project plan (QAPjP) approved by the RPP-WTP Quality Assurance (QA) organization. This work was conducted to the quality requirements of NQA-1-1989 and NQA-2a-1990, Part 2.7 as instituted through PNWD's *Waste Treatment Plant Support Project Quality Assurance Requirements and Description* (WTPSP) Manual.

PNWD addressed verification activities by conducting an Independent Technical Review of the final data report in accordance with procedure QA-RPP-WTP-604. This review verified that the reported results were traceable, that inferences and conclusions were soundly based, and the reported work satisfied the Test Plan objectives.

Issues

The results from this test raise the following issues in regard to processing these materials through the WTP:

- The viscosities of the 4.9 M to 10 M Na pretreated LAW at 40°C are within the pretreated LAW bounding recommendations of 0.4 to 15 cP (Poloski et al., 2002) indicating that the material is relatively easy to transport. Concentration of the pretreated LAW above 10 M Na may lead to transport issues. However, 10 M Na pretreated LAW may not be suitable for processing as this material contains 6.7 wt% undissolved solids. This exceeds the current bounding criteria of 2 wt% set forth on the WTP contract and may be too high of an undissolved solids concentration for plant operation.
- The 6 M and 8 M Na melter feed suspensions at 40°C exhibited Newtonian behavior with viscosities which are easily within the LAW melter feed bounding conditions (Poloski et al., 2002) of a Bingham plastic consistency index between 0.4-90 cP and a Bingham plastic yield index not to exceed 15 Pa. This indicates that the material is relatively easy to transport. Rheological measurements on the settled solids portion of the melter feed produce values outside this acceptable range. If the melter feed is not kept suspended, transport difficulties may arise. The timeframe by which transport difficulties may arise due to loss of process agitation has not been determined.
- The AP-101 LAW melter feed shear strength data indicates that difficulties could arise in operations that involve moving the material from a settled configuration. This is likely to happen during plant upset conditions. Examples of such operations include: 1) resuspending this material from a settled solids configuration in a mixing vessel; and 2) initiating pipeline flow with material that has settled in the pipe. Poloski et al. (2002) established a maximum bounding condition for shear strength at 625 Pa. When shear strength exceeds this value, process difficulties may be encountered. The timeframe by which transport difficulties may arise due to loss of process agitation has not been determined.
 - The settled solids shear strength of the 6 M Na melter feed material is higher than expected (790 Pa at 40°C).
 - The settled solids shear strength of the 8 M Na melter feed sample was an order of magnitude lower than the 6 M Na melter feed sample. This could be a result of mixing the glass formers with the solids that precipitated as the solution was evaporated to 8 M Na. The measured shear strength of the 8 M Na melter feed was 79 Pa at 40°C. However, after a one-week mixing period, the settled solids shear strength of the 8 M Na melter feed dramatically increased to approximately 610 Pa at 40°C. The shear strength increased further at ambient temperature (approximately 23°C) to 2600 Pa.

Acronyms

BNI	Bechtel National Inc.
EDS	Energy Dispersive X-Ray Spectroscopy
GFC	Glass Former Chemicals
IR	Infrared Spectroscopy
JCPDS	Joint Center for Powder Diffraction
LAW	Low-Activity Waste
NIST	National Institute of Standards and Technology
NMR	Nuclear Magnetic Resonance
PNWD	Battelle – Pacific Northwest Division
QA	Quality Assurance
QAPjP	Quality Assurance Project Plan
PLM	Polarized Light Microscopy
PSD	Particle Size Distribution
RPP	River Protection Project
R&T	Research and Technology
SE	Secondary Electrons
SEM	Scanning Electron Microscopy
VSL	Vitreous State Laboratory
UPA	Ultrafine Particle Size Analyzer
WTP	Waste Treatment Plant
XRD	X-Ray Diffraction

Definitions

Apparent Viscosity – The measured shear stress divided by the measured shear rate.

Density – The mass per unit volume.

Interstitial Solution – The solution contained between the suspended solid particles of a sludge sample.

Newtonian Fluid – A fluid whose apparent viscosity is independent of shear rate.

Non-Newtonian Fluid – A fluid whose apparent viscosity varies with shear rate.

Rheogram/Flow Curve – A plot of shear stress versus shear rate.

Shear Strength – The minimum stress required to initiate fluid movement as determined by the vane method. This definition is different from “yield stress” which is defined below.

Sludge – Wet solids having little or no standing liquid, (i.e., mud-like).

Slurry – A mixture of solids and solution.

Solution – A liquid phase possibly containing dissolved material.

Supernatant Liquid – A liquid phase overlying material deposited by settling, precipitation, or centrifugation.

Solids Settling Rate – The rate at which solids in a homogenized sample settle. This is typically the change in the settled solids interface height as a function of time.

Vol% Settled Solids – The percentage of the volume of the slurry sample that the settled solids occupy after settling for 72 hours under one gravity. These settled solids will contain interstitial solution.

Vol% Centrifuged Solids – The volume of the solids layer that separates from the bulk slurry after 1 hour of centrifugation at 1000 gravities divided by the total sample volume on a percentage basis. These centrifuged solids will contain interstitial solution.

Wt% Total Oxides – The percentage of the mass of the bulk sample that remains after converting all non-volatile elements to oxides. Some volatile elements such as cesium might be lost in this process.

Wt% Dissolved Solids – The mass of dissolved species in the supernatant liquid divided by the total mass of the supernatant liquid on a percentage basis. This definition is the same as “Wt% Dissolved Solids” from Table 4-2 (a) from the R&T plan, document number 24590-WTP-PL-RT-01-002, latest revision, for waste sample slurries. This is also the same as “Wt% Oven Dried Solids” from Table 4-2 (b) from the R&T plan, document number 24590-WTP-PL-RT-01-002, latest revision, for the liquid fraction analysis. This is also the same as the “Wt% Soluble Solids” from Table 4-2 (c) from the R&T plan, document number 24590-WTP-PL-RT-01-002, latest revision, for the HLW solids analyses.

Wt% Total Dried Solids – The percentage of the mass of the sample that remains after removing volatiles including free water by drying at $105 \pm 5^\circ\text{C}$ for 24 h. This definition is the same as “Wt% Total Dried Solids” from Table 4-2 (a) from the R&T plan, document number 24590-WTP-PL-RT-01-002, latest revision, for waste sample slurries.

Wt% Undissolved Solids – A calculated value reflecting to the mass (on a percent basis) of solids remaining if all the supernatant liquid and interstitial solution could be removed from the bulk slurry.

Yield Stress – The minimum stress required to initiate fluid movement as determined by a flow curve using a rheological model. This definition is different from “shear strength” which is defined above. [Note: this is the same value as “Yield Strength” delineated in Table 4.2a of the WTP R&T Plan, document number 24590-WTP-PL-RT-01-002, latest revision.]

Contents

Summary	iii
Acronyms	x
Definitions	xi
1.0 Introduction.....	1.1
2.0 Sample Preparation Details	2.1
2.1 Pretreated Feed	2.1
2.2 Melter Feed.....	2.3
3.0 Physical Properties Testing.....	3.1
3.1 Physical Properties Methodology	3.1
3.2 Physical Properties Results	3.3
3.2.1 Density and Solids Content.....	3.4
3.2.2 pH Measurements.....	3.10
3.2.3 Settling Behavior	3.10
4.0 Rheology.....	4.1
4.1 Equipment Details	4.2
4.2 Pretreated Waste	4.4
4.3 Melter Feed.....	4.13
4.4 Mixing/Aging	4.18
4.5 Settled Solids Rheology	4.25
5.0 Shear Strength.....	5.1
5.1 Measurement Equipment and Theory.....	5.1
5.2 System Validation and Calibration.....	5.3
5.3 Results from Shear Strength Measurements.....	5.4
6.0 Particle Size Distribution	6.1
6.1 Instrument Description	6.1
6.2 Particle Size Distribution Data Reporting Details.....	6.1
6.3 Calibration Checks	6.4
6.4 Operating Conditions	6.4

6.5	Suspending Medium.....	6.5
6.6	Results.....	6.6
7.0	Identification of Solids	7.1
7.1	Introduction	7.1
7.2	Experimental.....	7.1
7.2.1	Microstructural Analysis of Sub-Samples	7.1
7.3	Characterization Results of AP-101 Precipitated Solids	7.2
7.3.1	Scanning Electron Microscopy of the Solids	7.2
7.3.2	Infrared Spectroscopy of the Solids	7.8
7.3.3	Raman Data of the Washed Solids	7.10
7.3.4	Multinuclear NMR of Supernatant.....	7.12
7.3.5	X-ray Diffraction of the Solids	7.14
7.4	Discussion	7.19
7.4.1	Nitrate-Cancrinite	7.19
7.4.2	Nitrates	7.19
7.4.3	Carbonates	7.19
7.5	Conclusion.....	7.20
8.0	Conclusions	8.1
9.0	References.....	9.1
	Appendix A – Guideline Rheology Reporting.....	A.1

Figures

Figure S.1. Summary of AP-101 6 M Na LAW Melter Feed and LAWA-126 Glass Former Mix Particle Size Distribution	viii
Figure 2.1. Evaporated Pretreated Wastes.....	2.2
Figure 2.2. 10 M Na AP-101 Pretreated LAW Precipitated Solids Dissolution	2.3
Figure 2.3. AP-101 Melter Feed Samples Following Glass Former Chemical Additions	2.5
Figure 3.1. Settling Data for 6 M Na Pretreated AP-101 Waste at 25°C and 40°C	3.11
Figure 3.2. Settling Data for 8 M Na Pretreated AP-101 at 25°C and 40°C	3.11
Figure 3.3. Settling Data for 6 M Na Melter Feed at 25°C and 40°C.....	3.12
Figure 3.4. Settling Data for 8 M Na Melter Feed at 25°C and 40°C.....	3.12
Figure 4.1. Haake RS300 98 cP Viscosity Standard Calibration Check at 25°C	4.3
Figure 4.2. Flow Curve of 4.9 M Na AP-101 Pretreated Waste (Without Glass Formers) at 25°C.....	4.5
Figure 4.3. Flow Curve of 4.9 M Na AP-101 Pretreated Waste (Without Glass Formers) at 40°C.....	4.6
Figure 4.4. Flow Curve of 6 M Na AP-101 Pretreated Waste (Without Glass Formers) at 25°C	4.7
Figure 4.5. Flow Curve of 6 M Na AP-101 Pretreated Waste (Without Glass Formers) at 40°C	4.8
Figure 4.6. Flow Curve of 8 M Na AP-101 Pretreated Waste (Without Glass Formers) at 25°C	4.9
Figure 4.7. Flow Curve of 8 M Na AP-101 Pretreated Waste (Without Glass Formers) at 40°C	4.10
Figure 4.8. Flow Curve of 10 M Na AP-101 Pretreated Waste (Without Glass Formers) at 25°C.....	4.11
Figure 4.9. Flow Curve of 10 M Na AP-101 Pretreated Waste (Without Glass Formers) at 40°C.....	4.12
Figure 4.10. Flow Curve of 6 M Na AP-101 Melter Feed (With Glass Formers) at 25°C	4.14
Figure 4.11. Flow Curve of 6 M Na AP-101 Melter Feed (With Glass Formers) at 40°C	4.15
Figure 4.12. Flow Curve of 8 M Na AP-101 Melter Feed (With Glass Formers) at 25°C	4.16
Figure 4.13. Flow Curve of 8 M Na AP-101 Melter Feed (With Glass Formers) at 40°C	4.17
Figure 4.14. Flow Curve of 8 M Na AP-101 Melter Feed (one hour mixing with Glass Formers Chemicals) at 25°C	4.19
Figure 4.15. Flow Curve of 8 M Na AP-101 Melter Feed (one hour mixing with Glass Formers Chemicals) at 40°C	4.20
Figure 4.16. Flow Curve of 8 M Na AP-101 Melter Feed (one day mixing with Glass Formers Chemicals) at 25°C	4.21
Figure 4.17. Flow Curve of 8 M Na AP-101 Melter Feed (one day mixing with Glass Formers Chemicals) at 40°C	4.22
Figure 4.18. Flow Curve of 8 M Na AP-101 Melter Feed (one week mixing with Glass Formers Chemicals) at 25°C	4.23
Figure 4.19. Flow Curve of 8 M Na AP-101 Melter Feed (one week mixing with Glass Formers Chemicals) at 40°C	4.24
Figure 4.20. Flow Curve of 8 M Na AP-101 Melter Feed Settled Solids at 25°C	4.26
Figure 4.21. Flow Curve of 8 M Na AP-101 Melter Feed Settled Solids at 40°C	4.27

Figure 5.1. Geometrical Requirements of a Shear Vane.....	5.2
Figure 5.2. Typical Response of a Shear Vane.....	5.3
Figure 5.3. Viscometer Calibration Check With 98.0 cP Viscosity Standard at 25°C.....	5.4
Figure 5.4. Shear Strength Response of 6M and 8M Na AP-101 Melter Feed Settled Solids.....	5.6
Figure 5.5. Shear Strength Response of 1-Week Aged 8 M Na AP-101 Melter Feed Settled Solids	5.7
Figure 6.1. Particle Size Distribution on a Volume Basis.....	6.8
Figure 6.2. Cumulative Particle Size Distribution on a Volume Basis.....	6.9
Figure 6.3. Particle Size Distribution on an Area Basis.....	6.10
Figure 6.4. Cumulative Particle Size Distribution on an Area Basis.....	6.11
Figure 6.5. Particle Size Distribution on a Number Basis.....	6.12
Figure 6.6. Cumulative Particle Size Distribution on a Number Basis.....	6.13
Figure 7.1. Scanning Electron Micrographs of Sodium- and Potassium-Bearing Phases in AP-101-A (6 M Na) and AP-101-B (8 M Na).....	7.3
Figure 7.2. Sodium and Potassium Phase in AP-101-C (10 M Na).....	7.4
Figure 7.3. X-ray Analysis of Sodium and Potassium Phase in AP-101-C (10 M Na).....	7.4
Figure 7.4. An Alumino-Silicate Phase was Observed in AP-101-B (8 M Na).....	7.5
Figure 7.5a. Polarized Light Microscopy Image of Particles of Washed Solids	7.6
Figure 7.5b. Low magnification SEM Image of particles	7.6
Figure 7.6a. Backscattered SEM Image of Particles at 20keV	7.6
Figure 7.6b. Secondary SEM Image of the Same Particles at 10keV.....	7.6
Figure 7.7. SE Higher Magnification Image of “twine-like” material shown in Figure 7.6b. The image was obtained at 10keV to enhance the particle morphology	7.7
Figure 7.8. X-ray Energy Dispersive Spectrum of “Twine-Like” Particles	7.8
Figure 7.9. Infrared Spectra of AP-101 Dried Solids A, B, and C (6 M, 8 M, 10 M Na, respectively)	7.9
Figure 7.10. Infrared Spectra of AP-101 Solids A (6 M Na), B (8 M Na), C (10 M Na), and C (10 M Na) Washed Twice.....	7.10
Figure 7.11. The Raman Spectra of AP-101 Solids: 1 st and 2 nd Wash of Solids C (10 M Na).....	7.11
Figure 7.12. ²⁷ Al Spectrum of Native AP101 Tank Supernatant	7.13
Figure 7.13. X-ray Diffraction Scan of the Sodium and Potassium Phases in AP-101-C (10M Na).....	7.15
Figure 7.14. X-ray Diffraction Scan of the Alumino-Silicate Phase in AP-101-C (10M Na) with a match to Hydroxy-Cancrinite	7.18

Tables

Table S.1. Summary of AP-101 Pretreated LAW Measurements ^a	iv
Table S.2. Summary of AP-101 LAW Melter Feed Measurements.....	vi
Table S.3. Summary of 8 M Na AP-101 LAW Melter Feed Mixing/Aging Measurements.....	vii
Table 2.1. Glass Formers Added to the AP-101 Samples	2.4
Table 2.2. Guideline Reporting Format Mixing Details	2.5
Table 3.1. Physical Properties of 6 M Na AP-101 Pretreated Waste	3.5
Table 3.2. Physical Properties of 8 M Na AP-101 Pretreated Waste	3.6
Table 3.3. Physical Properties of 10 M Na AP-101 Pretreated Waste.....	3.7
Table 3.4. Physical Properties of 6 M Na AP-101 Melter Feed.....	3.8
Table 3.5. Physical Properties of 8 M Na AP-101 Melter Feed.....	3.9
Table 3.6. pH of the AP-101 Melter Feed.....	3.10
Table 4.1. Apparent Viscosity of the AP-101 Pretreated Waste Based on Newtonian Behavior	4.4
Table 4.2. Viscosity of the AP-101 Melter Feed Based on Newtonian Behavior	4.13
Table 4.3. Viscosity of Mixed/Aged 8 M Na AP-101 Melter Feed Based on Newtonian Behavior.....	4.18
Table 4.4. pH of Mixed/Aged 8 M Na AP-101 Melter Feed.....	4.18
Table 4.5. Bingham Plastic Parameters of AP-101 LAW 8 M Na Melter Feed Settled Solids One Week after Glass Former Chemical Addition.....	4.25
Table 5.1. Summary of Shear Strength Data	5.6
Table 6.1. Particle Size Analyzer Calibration Data	6.4
Table 6.2. Approximate Shear Conditions of Microtrac X100 for Various Suspending Mediums and Flowrates.....	6.5
Table 6.3. Summary of Volume Particle Size Distribution Data (Provided by Microtrac Software).....	6.7
Table 7.1. EDS Compositional Analysis.....	7.8
Table 7.2. Compounds Used For Interpreting Raman Data	7.12
Table 7.3. Major Peaks in AP-101-C in the XRD Scan of the Alumino-Silicate	7.16
Table A.1. AP-101 4.9 M Na Pretreated Waste Rheology Data at 25°C (File Name: 061902a).....	A.1
Table A.2. AP-101 4.9 M Na Pretreated Waste Rheology Data at 40°C (File Name: 061902e).....	A.2
Table A.3. AP-101 6 M Na Pretreated Waste Rheology Data at 25°C (File Name: 062002a)	A.3
Table A.4. AP-101 6 M Na Pretreated Waste Rheology Data at 40°C (File Name: 062002e)	A.4
Table A.5. AP-101 8 M Na Pretreated Waste Rheology Data at 25°C (File Name: 062002i)	A.5
Table A.6. AP-101 8 M Na Pretreated Waste Rheology Data at 40°C (File Name: 062002m)	A.6
Table A.7. AP-101 10 M Na Pretreated Waste Rheology Data at 25°C (File Name: 062002u)	A.7
Table A.8. AP-101 10 M Na Pretreated Waste Rheology Data at 40°C (File Name: 062002r)	A.8
Table A.9. AP-101 6 M Na Melter Feed Rheology Data at 25°C (File Name: 073002c).....	A.9
Table A.10. AP-101 6 M Na Melter Feed Rheology Data at 40°C (File Name: 073002h)	A.10

Table A.11. AP-101 8 M Na Melter Feed Rheology Data at 25°C (File Name: 073102c).....	A.11
Table A.12. AP-101 8 M Na Melter Feed Rheology Data at 40°C (File Name: 073102k)	A.12
Table A.13. AP-101 8 M Na Melter Feed Rheology Data at 25°C one hour after Glass Former Chemical Addition (File Name: 082202a)	A.13
Table A.14. AP-101 8 M Na Melter Feed Rheology Data at 40°C one hour after Glass Former Chemical Addition (File Name: 082202e)	A.14
Table A.15. AP-101 8 M Na Melter Feed Rheology Data at 25°C one day after Glass Former Chemical Addition (File Name: 082302a)	A.15
Table A.16. AP-101 8 M Na Melter Feed Rheology Data at 40°C one day after Glass Former Chemical Addition (File Name: 082302e)	A.16
Table A.17. AP-101 8 M Na Melter Feed Rheology Data at 25°C one week after Glass Former Chemical Addition (File Name: 082902a)	A.17
Table A.18. AP-101 8 M Na Melter Feed Rheology Data at 40°C one week after Glass Former Chemical Addition (File Name: 090302c)	A.18
Table A.19. AP-101 8 M Na Melter Feed Settled Solids Rheology Data at 25°C one week after Glass Former Chemical Addition (File Name: 092502f)	A.19
Table A.20. AP-101 8 M Na Melter Feed Settled Solids Rheology Data at 40°C one week after Glass Former Chemical Addition (File Name: 092502g)	A.20

1.0 Introduction

The objectives of this work were to obtain accurate measurement of solids concentration, densities, and rheological properties (TP-RPP-WTP-104 Rev 0) on actual AP-101 pretreated low activity waste samples and corresponding melter feed samples. The physical and rheological properties of these process streams are important considerations in the selection of flowsheet and processing equipment such as mixers, pumps, piping and tanks. Measurements on actual waste are also required to verify and validate results obtained with simulants.

Actual samples from tank AP-101 were used in this testing. Multiple AP-101 samples were received from Hanford's 222-S laboratory. These samples were composited and diluted to approximately 5 M Na. The diluted AP-101 sample was characterized by Goheen et al. (2002). Next, the diluted AP-101 material was processed through cesium and technetium ion exchange columns as described by Fiskum et al. (2002) and Burgeson et al. (2002), respectively. This pretreated AP-101 Low-Activity Waste (LAW) is the focus of this document.

The 4.9 M Na AP-101 pretreated LAW was evaporated to various Na concentrations (6 M , 8 M , and 10 M) for physical and rheological property measurements. The physical and rheological properties were measured in accordance with the Waste Treatment Plan (WTP) project approved guidelines developed by Smith and Prindiville (2002). Rheological testing was conducted at 25°C and 40°C. Settling and physical properties testing was conducted at ambient (nominally 23°C to 25°C) and 40°C. For this work, ambient is reported as 25°C. Solids were observed to precipitate during evaporation of the pretreated LAW to 6 M, 8 M, and 10 M Na concentrations. An effort to characterize these precipitated solids is discussed in this document.

Project approved glass former chemicals (CFG; Schumacher and Hansen, 2002) were added to the 6 M and 8 M Na samples to produce LAW melter feed material. Physical and rheological properties of these melter feed samples were measured. Mixing and aging studies were also conducted on the 8 M Na melter feed sample. An 8 M Na sample was placed in a mixing vessel at a power to volume ratio consistent with that expected in the WTP. Glass formers were added and the mixing continued for 1 week. During this week, shear stress versus shear rate analyses were conducted after 1 hour, 1 day, and 1 week. Shear strength (by vane method) and shear stress versus shear rate analyses were conducted on the settled solids layer taken from the 1 week mixed sample.

This report describes the experimental approach and results of the testing. Specifications for this work were provided in Test Specification Number 24590-LAW-TSP-RT-01-001. This report also provides the means of communicating results of testing conducted under test plan (TP-RPP-WTP-104).

2.0 Sample Preparation Details

This section details preparation of the actual AP-101 samples used for testing. The first section (Section 2.1) describes the history of the material and evaporation steps used to adjust the Na concentration to replicate the feed that will be supplied to the vitrification plant from the final evaporator in the pretreatment unit. After evaporation to adjust the Na concentration, this material is referred to as pretreated feed. Section 2.2 describes the addition of glass former chemicals to the pretreated feed to form the melter feed; this material is hereafter referred to as melter feed. Unless otherwise stated, all temperatures in this work are reported to $\pm 2^{\circ}\text{C}$.

2.1 Pretreated Feed

The actual AP-101 waste samples used in this testing were prepared under conditions similar to those planned in the River Protection Project Waste Treatment Plant (RPP-WTP) Flow sheet. Liquid samples from Hanford tank 241-AP-101 were received by PNWD for process testing. The liquid samples were composited in April of 2000. The composite was then Cs ion exchanged (Fiskum et al., 2002) then Tc ion exchanged (Burgeson et al., 2002). The resulting pretreated waste (with Cs and Tc removed) was used for testing described in this report.

Following Tc ion exchange, the pretreated waste sample had a Na concentration of 4.9 M. The density of the waste was measured at ambient ($\sim 23^{\circ}\text{C}$). This measurement was conducted in duplicate by placing subsamples in 25-mL volumetric flasks of known mass. The density was then calculated by dividing the mass by the volume. The measured densities of the two subsamples were 1.261 and 1.257 g/mL with an average value of 1.259 g/mL.

The sample was divided into four fractions and concentrated by evaporation to target Na concentrations of 6, 8, and 10 M. Evaporations were conducted in a vacuum oven at $\sim 50^{\circ}\text{C}$ under approximately 23 inches of Hg vacuum. One of the fractions was concentrated to a calculated Na concentration of 6 M. Two of these fractions were concentrated to a calculated Na concentration of 8 M, and the fourth sample was concentrated to a calculated Na concentration of 10 M.

During the evaporation step, precipitation was observed in the 6 M, 8 M, and 10 M Na samples. These samples are shown in a photograph (Figure 2.1) along with a sample of the original pretreated waste (i.e., 4.9 M Na). As described in Section 3.0, the 6 M Na sample contained visible solids (< 1 wt%), the 8 M and 10 M Na samples contained 1.2 and 6.7 wt% undissolved solids respectively at 25°C . Characterization at 10 M Na was limited because the 6.7 wt% undissolved solids present after evaporation exceeds the 2 wt% undissolved solids is the current limit for pretreated feed to the LAW vitrification plant.

4.9 M Na

6 M Na

8 M Na

10 M Na

8 M Na



Figure 2.1. Evaporated Pretreated Wastes

A 5-mL aliquot of homogenized 10 M Na evaporated AP-101 pretreated LAW was drawn to qualitatively investigate the solubility of the precipitated solids. A small quantity (approximately 1 mL) of deionized water was added incrementally to the aliquot. The aliquot was then shaken and allowed to equilibrate at ambient temperature (approximately 23°C) for approximately one hour prior to observation. After the first addition of deionized water, the samples were centrifuged to minimize the amount of suspended solids. The results from these observations are shown in Figure 2.2. It was concluded that a fraction of these solids do not readily redissolve with the addition of deionized water after 1 hr. This is probably due to slow dissolution rates. An effort to identify the species that compose these solids is discussed in Section 7.

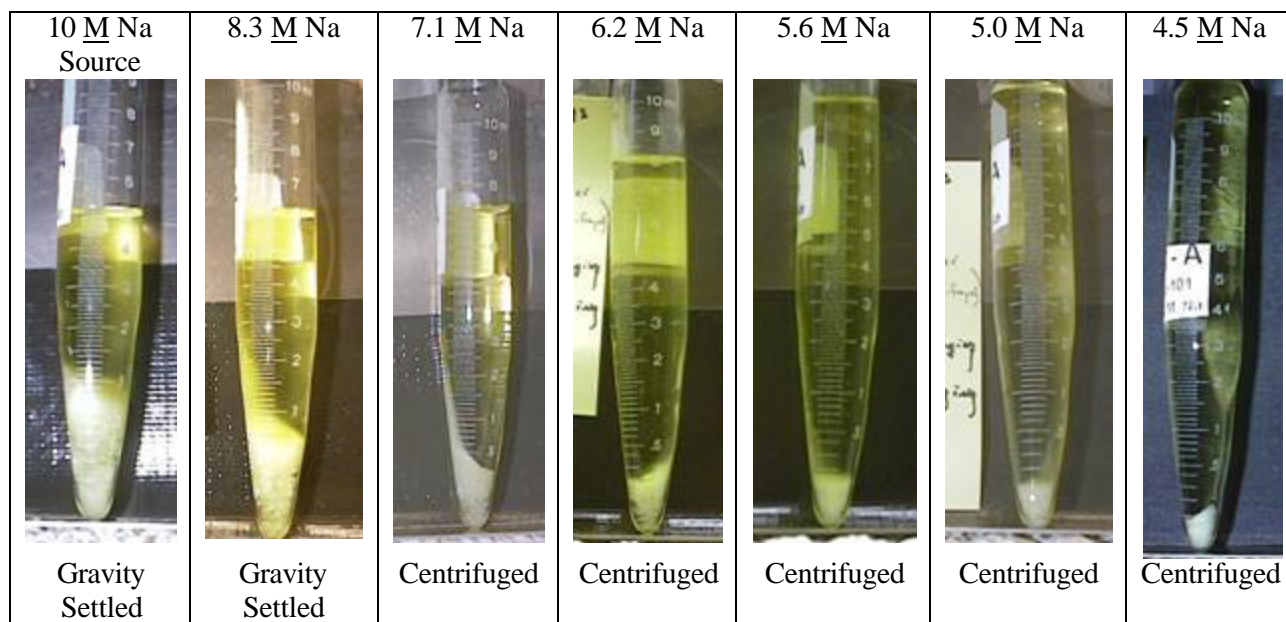


Figure 2.2. 10 M Na AP-101 Pretreated LAW Precipitated Solids Dissolution

2.2 Melter Feed

After physical and rheological characterization of the pretreated feed, glass former chemicals were added to the 6 M Na sample and one of the 8 M Na samples. A second 8 M Na sample was prepared as a melter feed for a mixing/aging study that is discussed in Section 4.4. Glass former quantities were based on the formulation provided by the Vitreous State Laboratory (VSL) (LAWA-126). The VSL formulation was based on a 4.85M Na feed on a mass per liter basis. The quantities of glass formers were first adjusted on a per liter basis to the target Na concentrations (6 M and 8 M). The masses to be added to the 6 M Na samples were calculated using an adjustment factor of 1.24 (6 M Na/4.85M Na=1.237). The adjustment factor for the 8 M Na sample was 1.649 (8 M Na/4.85M Na=1.649). These adjusted masses on a liter basis were then multiplied by the volume of sample to calculate how much glass formers to add to each sample. Table 2.1 lists the quantity and type of glass formers added to each of the two AP-101 pretreated feed samples.

Prior to addition, the individual dry glass former constituents were weighed into a vessel and mixed together at the formulation ratio. The appropriate mass for addition to each of the samples was then weighed into a unique container. The glass former mixtures were then slowly added to the samples while the samples were stirred using an overhead mixer. Following the glass former addition, the samples were stirred for an additional hour. Table 2.2 provides mixing information formatted to meet guidelines developed by Smith and Prindiville (2002).

For all samples in this work, a 1 inch (2.54 cm) diameter impeller was used. A cylindrical bottle with a 2.2 inch (5.5 cm) diameter was used during initial glass former addition. For the mixing/aging testing a spherical container was used to minimize evaporation. The spherical bottle had a diameter of 3.4 inch (8.6 cm). The agitator rotational rate was chosen based on a relationship (see Equation 2.1) designed to keep the level of power input to the mixture per unit volume constant between WTP mixer designs and the lab-scale mixer. The following equation was used:

$$N^3 = \left(1.96 \times 10^9 \frac{\text{rpm}^3 \cdot \text{cm}^5}{\text{ml}} \right) \cdot \frac{V}{D_i^5} \quad (2.1)$$

Where, N = impeller speed (rpm)
 V = Sample volume (ml)
 D_i = impeller diameter (cm)

After stirring for one hour, samples were removed for physical and rheological testing. The resulting melter feed material is shown in Figure 2.3. Physical properties and rheology measurements are described in Sections 3 and 4 respectively.

Table 2.1. Glass Formers Added to the AP-101 Samples

		VSL LAWA-126 Glass Formulation Recipe g/L			Mass Added (g)		
					Starting Vol 57.6 mL	Starting Vol 57.9 mL	Starting Vol 100.8 mL
Additive	Comment	4.9 M	6 M	8 M	6 M	8 M	8 M Mixing/ Aging
Kyanite (Al ₂ SiO ₅)	Raw Kyanite, 325 Mesh	57.66	71.733	95.11	4.104	5.033	9.611
Orthoboric Acid (H ₃ BO ₃)	Technical Grade	141.69	175.29	233.72	10.085	12.367	23.617
Wollastonite (CaSiO ₃)	Powder untreated, NYAN 325 Mesh	34.21	42.32	56.43	2.435	2.986	5.702
Hemetite –Red Iron Oxide (Fe ₂ O ₃)	Red Iron Oxide, 325 Mesh (5001)	43.97	54.40	72.53	3.130	3.838	7.329
Olivine (Mg ₂ SiO ₄ with some Fe ₂ SiO ₄)	325 Mesh (#180)	25.05	30.99	41.32	1.783	2.186	4.175
Ground Silica Sand (SiO ₂)	Sil-co-Sil 75, 200 Mesh	296.87	367.26	489.68	21.130	25.912	49.483
Rutile (TiO ₂)	Premium Grade, Airfloated	16.99	21.02	28.02	1.209	1.483	2.832
Zincite –Zinc Oxide (ZnO)	KADOX-920	24.24	29.99	39.98	1.725	2.116	4.040
Zircon Sand (ZrSiO ₄)	Flour 325 Mesh	36.66	45.35	60.47	2.609	3.200	6.111

Table 2.2. Guideline Reporting Format Mixing Details

Mixing Operation Data Needed to Compare Mixing of the Melter Feed	
Melter Feed ID: LAWA-126	
Processing Scale (lab/bench, pilot, or full): lab	
Activity/Property	Data or Explanation
Order of Chemical Additions	Dry glass formers combined then added to waste in mixing vessel
Mixing Time	1 hr
Impeller Speed	~400 RPM for initial GFC addition ~490 RPM for mixing/aging
Impeller Diameter	1 inch (2.54 cm)
Tank Diameter	~2.2 inch (5.5 cm) for initial GFC addition ~3.4 inch (8.6 cm) for mixing/aging
Number of Baffles	0
Size of Baffles	NA
Depth of Impeller	Approximately midpoint of sample



Figure 2.3. AP-101 Melter Feed Samples Following Glass Former Chemical Additions

3.0 Physical Properties Testing

Samples of the AP-101 pretreated feed and melter feed described in Section 2 were characterized for selected physical properties according to the methodology defined in Section 4 of 24590-WTP-GPG-RTD-001, *Guidelines for Performing Chemical, Physical, and Rheological Properties Measurements*. Section 3.1 of this report provides the general protocol, nomenclature, equations, and definitions from the guidelines document. The following physical properties were all measured at 25°C with selected properties measured at 40°C as noted and required by the Test Plan (TP-RPP-WTP-104 Rev 0):

- Density of the bulk slurries, settled solids, centrifuged solids, and centrifuged supernatant.
- The weight percent (wt%) and volume percent (vol%) settled solids, wt% and vol% centrifuged solids, wt% total solids, wt% total dried solids, and wt% undissolved solids.

Under the guideline methodology, settled solids are defined as the solids layer that separates from the bulk slurry after 3 days of gravity settling. Centrifuged solids are defined as the solids layer that separates from the bulk slurry after 1 hour of centrifugation at 1000 gravities. Weight percent oven dried solids is defined as the percent of solids remaining after oven drying the centrifuged solids fraction at 105°C. Weight percent total dried solids is defined as the percent of solids remaining after drying the bulk sample (solid and liquid fractions) at 105°C.

3.1 Physical Properties Measurement Methodology

For this testing, a known mass of each slurry was placed in triplicate in volume graduated centrifuge cones. The samples were then allowed to settle for 3 days. The total mass (M_B) and volume (V_B) of the settled solids were recorded, and the density of the bulk slurry calculated ($\rho_B = M_B/V_B$). These results can be biased low due to entrained gas as well as an inability to clearly measure the total sample volume due to material smeared on the sides of the centrifuge tubes. Therefore, the bulk slurry densities were recalculated later in the work using volumes recorded following centrifugation. Following settling, the volume of the settled solids (V_{SS}) and volume of the bulk sample (V_B) were recorded. The vol% settled solids was then calculated ($P_{VSS} = V_{SS}/V_B \times 100\%$).

The settled slurries were then centrifuged at approximately 1,000 times the force of gravity for 1 hour. Note that for the 40°C set of measurements, the aliquots were removed from a temperature controlled oven at 40°C prior to the centrifugation process which occurred at ambient temperature (~23°C). After centrifugation, the aliquots were returned to the oven where the 40°C testing temperature was restored. All of the centrifuged supernatant was then transferred to a graduated cylinder, its mass (M_S) and volume (V_S) recorded, and the density calculated ($\rho_{CL} = M_{CL}/V_{CL}$). The mass (M_{CS}) and volume (V_{CS}) of the centrifuged solids were also recorded. In addition, the vol% centrifuged solids ($P_{VCS} = V_{CS}/V_B \times 100\%$) was calculated.

In many cases, centrifugation can result in the release of gas in the form of bubbles or foams. Therefore, comparison of the bulk density measurements before and after centrifugation is very important in understanding the rheology of some samples. In addition, it is possible that not all of the gas is released from the slurry by centrifugation, so the density results following centrifugation may be biased low.

The centrifuged solids and supernatant aliquots were dried separately at 105°C for 24 hours. The mass of the dried centrifuged supernatant (M_{DCL}) and dried centrifuged solids (M_{DCS}) were then measured. Assuming all mass lost during the drying process is water and not another volatile component, the wt% total dried solids in the bulk slurry was calculated ($P_{MTS} = \{[(M_{DCL} \times M_S)/(M_{VL} \times M_B)] + [M_{DCS}/M_B]\} \times 100 \%$), where M_{VL} is the mass of centrifuged liquid prior to drying. Waters of hydration or volatile organics can lead to low bias in M_{DCS}/M_{CS} . The wt% oven dried solids calculated from $P_{ODS} = M_{DCS} / M_{CS} \times 100\%$.

A calculation was then performed to determine the wt% solids in the samples excluding all interstitial liquid. This is referred to as P_{MUDES} . The following equation was used:

$$P_{MUDES} = \left(1 - \frac{1 - \frac{M_{DCS}}{M_{CS}}}{1 - \frac{M_{DCL}}{M_{VL}}} \right) \times \frac{M_{CS}}{M_B} \times 100 \% \quad (3.1)$$

This calculation assumes that: 1) the supernatant and the interstitial liquid had the same composition, and 2) all mass loss during the drying of the centrifuged solids was water loss from interstitial liquid.

The mass percent of undissolved solids (P_{MUSS}) in the settled solids layer can be calculated from Equation 3.2.

$$P_{MUSS} = \frac{(P_{MUDES}/100) \cdot M_B}{M_B - (V_B - V_{SS})\rho_{CL}} \times 100 \% \quad (3.2)$$

The mass percent of undissolved solids (P_{MUCS}) in the centrifuged solids layer can be calculated from Equation 3.3.

$$P_{MUCS} = \frac{(P_{MUDES}/100) \cdot M_B}{M_B - (V_B - V_{CS})\rho_{CL}} \times 100 \% \quad (3.3)$$

The average particle density (ρ_p) of the undissolved solids can be calculated from Equation 3.4.

$$\rho_p = \frac{(P_{MUDES}/100)}{\frac{1}{\rho_B} - \frac{1 - (P_{MUDES}/100)}{\rho_{CL}}} \quad (3.4)$$

The density of the settled solids (ρ_{SS}) can be calculated from Equation 3.5.

$$\rho_{SS} = \frac{1}{\frac{(P_{MUSS}/100)}{\rho_p} + \frac{1 - (P_{MUSS}/100)}{\rho_{CL}}} \quad (3.5)$$

The density of the centrifuged solids (ρ_{CS}) can be calculated from Equation 3.6.

$$\%_{CS} = \frac{1}{\frac{(P_{MUCS}/100)}{\%_p} + \frac{1 - (P_{MUCS}/100)}{\%_{CL}}} \quad (3.6)$$

The mass percent of settled solids (P_{MSS}) in the sample can be calculated from Equation 3.7.

$$P_{MSS} = \frac{r_{SS} \cdot V_{SS}}{M_B} \times 100 \% \quad (3.7)$$

The mass percent of centrifuged solids (P_{MCS}) in the sample can be calculated from Equation 3.8.

$$P_{MCS} = \frac{r_{CS} \cdot V_{CS}}{M_B} \times 100 \% \quad (3.8)$$

The vol% of undissolved solids (P_{VUDS}) in the sample can be calculated from Equation 3.8.

$$P_{VUDS} = \frac{(P_{MUCS}/100) \cdot \%_B}{\%_p} \times 100 \% \quad (3.8)$$

The vol% of undissolved solids (P_{VUSS}) in the settled solids can be calculated from Equation 3.9.

$$P_{VUSS} = \frac{(P_{MUCS}/100) \cdot \%_{SS}}{\%_p} \times 100 \% \quad (3.9)$$

The vol% of undissolved solids (P_{VUCS}) in the centrifuged solids can be calculated from Equation 3.10.

$$P_{VUCS} = \frac{(P_{MUCS}/100) \cdot \%_{CS}}{\%_p} \times 100 \% \quad (3.10)$$

3.2 Physical Properties of AP-101 Pretreated LAW and LAW Melter Feed

Physical properties results for each sample of the pretreated wastes and melter feed materials along with average values can be found in Tables 3.1-3.5. Given that undissolved solids content of the 6 M Na pretreated waste at 25°C was too low for accurate quantification (< 1 wt%), scope of the undissolved solids testing on the 6 M Na pretreated waste at 40°C was limited to conserve actual waste quantity. Tests on the 8 M Na pretreated waste, 6 M Na melter feed, and 8 M Na melter feed were conducted at 25°C and 40°C. Since the 10 M Na sample was removed from the scope of this work, selected testing on the 10 M Na pretreated waste was only conducted at 25°C.

3.2.1 Density and Solids Content

The 25°C pretreated waste contained <1, 1.2 and 6.7 wt% undissolved solids at 6 M, 8 M and 10 M Na, respectively. The 10 M Na sample exceeds the WTP bounding criteria of 2 wt% undissolved solids in the pretreated LAW stream. Based on the increase in solids from 6 M Na to 10 M Na in the pretreated feed, this solution appears to be saturated and precipitates as the evaporation operations proceed. These precipitated solids appear to dissolve at higher temperatures (i.e. 40°C). This was observed in the wt% undissolved solids for the 8 M Na sample, which decreased from 1.2 wt% at 25°C to 0.81 wt% at 40°C. Analyses discussed in Section 7.0 were performed to characterize the chemical composition and crystal structure of the precipitate.

When glass former chemicals were added to the pretreated waste, the resulting melter feed had approximately 50 vol% settled solids at 6 M Na and 60 vol% settled solids at 8 M Na at 25°C as shown in Tables 3.4 and 3.5. This is consistent with the ratio of glass former chemicals added to each of the samples. This was associated with a bulk density increase from 1.64 to 1.74 g/mL and an increase in wt% undissolved solids from 32.9 to 37.7 wt% between the 6 M Na and 8 M Na melter feed samples, respectively at 25°C. This is not unexpected since most of the glass former chemicals are insoluble. At 40°C, the solids packing appears to change, as evident by the vol% settled solids increasing by approximately 10% for the 6 M Na melter feed sample and 20% for the 8 M Na melter feed sample while the undissolved solids content remains relatively constant across both temperatures.

Table 3.1. Physical Properties of 6M Na AP-101 Pretreated Waste

Physical Property^a	A-1	A-2	A-3	Average
Density – Bulk slurry (g/mL)	1.325 @ 25°C 1.292 @ 40°C	1.335 @ 25°C 1.289 @ 40°C	1.315 @ 25°C 1.298 @ 40°C	1.325 @ 25°C 1.293 @ 40°C
Density – settled solids (g/mL)	b	b	b	b
Density – centrifuged solids (g/mL)	b	b	b	b
Density - supernatant liquid (g/mL)	1.34	1.33	1.34	1.33
Density – average particle (g/mL)	b	b	b	b
Vol. % settled solids after 72 hours	3.8 @ 25°C 2.2 @ 40°C	3.8 @ 25°C 2.4 @ 40°C	3.8 @ 25°C 2.4 @ 40°C	3.8 @ 25°C 2.3 @ 40°C
Vol% centrifuged solids	1.9	2.0	1.9	1.9
Vol% undissolved solids	b	b	b	b
Vol% undissolved solids in settled solids	b	b	b	b
Vol% undissolved solids in centrifuged solids	b	b	b	b
Wt% settled solids	b	b	b	b
Wt% centrifuged solids	b	b	b	b
Wt% total dried solids	35.1	36.7	35.6	35.8
Wt% dissolved solids	35.2	36.7	35.6	35.8
Wt% undissolved solids	b	b	b	b
Wt% undissolved solids in settled solids	b	b	b	b
Wt% undissolved solids in centrifuged solids	b	b	b	b
<p>a Unless otherwise stated measurements were taken a 25°C. b too little solids to quantify.</p>				

Table 3.2. Physical Properties of 8M Na AP-101 Pretreated Waste

Physical Property^a	Temperature	B-1	B-2	B-3	Average
Density – Bulk slurry (g/mL)	25°C: 40°C:	1.407 1.364	1.389 1.365	1.402 1.352	1.399 1.360
Density – settled solids (g/mL)	25°C: 40°C:	a	a	a	a
Density – centrifuged solids (g/mL)	25°C: 40°C:	a	a	a	a
Density - supernatant liquid (g/mL)	25°C: 40°C:	1.41	1.40	1.41	1.40
Density – average particle (g/mL)	25°C: 40°C:	a	a	a	a
Vol. % settled solids after 72 hours	25°C: 40°C:	9.4 8.0	10.2 8.2	10.0 9.0	9.9 8.4
Vol% centrifuged solids	25°C: 40°C:	6.7	6.5	7.1	6.8
Vol% undissolved solids	25°C: 40°C:	a	a	a	a
Vol% undissolved solids in settled solids	25°C: 40°C:	a	a	a	a
Vol% undissolved solids in centrifuged solids	25°C: 40°C:	a	a	a	a
Wt% settled solids	25°C: 40°C:	a	a	a	a
Wt% centrifuged solids	25°C: 40°C:	a	a	a	a
Wt% total dried solids	25°C: 40°C:	42.9 42.9	43.0 42.9	43.1 43.1	43.0 43.0
Wt% dissolved solids	25°C: 40°C:	42.3 42.4	42.3 42.4	42.2 42.7	42.3 42.5
Wt% undissolved solids	25°C: 40°C:	1.0 0.86	1.2 0.78	1.5 0.80	1.2 0.81
Wt% undissolved solids in settled solids	25°C: 40°C:	a	a	a	a
Wt% undissolved solids in centrifuged solids	25°C: 40°C:	a	a	a	a
a too little solids to quantify.					

Table 3.3. Physical Properties of 10 M Na AP-101 Pretreated Waste at 25°C

Physical Property	C-1	C-2	C-3	Average
Density – Bulk slurry (g/mL)	1.441	1.473	1.468	1.461
Density – supernatant liquid (g/mL)	1.44	1.45	1.45	1.45
Wt% total dried solids	49.6	51.3	46.2	49.0
Wt% dissolved solids	46.0	48.1	41.7	45.3
Wt% undissolved solids	6.6	5.9	7.7	6.7

Table 3.4. Physical Properties of 6M Na AP-101 Melter Feed

Physical Property	Temperature	Melt-A-1	Melt-A-2	Melt-A-3	Average
Density – Bulk slurry (g/mL)	25°C:	1.645	1.646	1.643	1.645
	40°C:	1.590	1.586	1.586	1.587
Density – settled solids (g/mL)	25°C:	1.95	1.95	1.94	1.95
	40°C:	1.77	1.78	1.79	1.78
Density – centrifuged solids (g/mL)	25°C:	2.12	2.12	2.08	2.11
	40°C:	1.97	2.00	2.01	1.99
Density – supernatant liquid (g/mL)	25°C:	1.33	1.34	1.34	1.34
	40°C:	1.31	1.30	1.29	1.30
Density – average particle (g/mL)	25°C:	3.22	3.10	2.99	3.10
	40°C:	2.25 ^a	3.11	3.15	3.13
Vol. % settled solids after 72 hours	25°C:	50.6	49.7	49.4	49.9
	40°C:	60.4	60.7	59.1	60.1
Vol. % centrifuged solids	25°C:	40.2	39.2	40.4	39.9
	40°C:	42.3	41.1	40.9	41.4
Vol% undissolved solids	25°C:	16.8	17.5	18.2	17.5
	40°C:	29.8 ^a	16.0	15.9	15.9
Vol% undissolved solids in settled solids	25°C:	33.0	34.9	36.5	34.8
	40°C:	49.3 ^a	26.7	26.8	26.8
Vol% undissolved solids in centrifuged solids	25°C:	41.8	44.6	45.0	43.8
	40°C:	70.4 ^a	38.9	38.8	38.9
Wt% settled solids	25°C:	60.4	59.3	58.8	59.5
	40°C:	67.4	67.3	66.7	67.1
Wt% centrifuged solids	25°C:	51.8	50.6	51.2	51.2
	40°C:	52.5	51.9	51.8	52.1
Wt% total dried solids	25°C:	58.2	57.9	58.0	58.0
	40°C:	62.8	55.7	55.7	58.1
Wt% dissolved solids	25°C:	37.4	37.2	37.3	37.3
	40°C:	35.2	35.2	35.4	35.3
Wt% undissolved solids	25°C:	32.9	32.9	33.0	32.9
	40°C:	42.1 ^a	31.4	31.5	31.4
Wt% undissolved solids in settled solids	25°C:	54.4	55.4	56.1	55.3
	40°C:	62.5 ^a	46.0	47.2	46.6
Wt% undissolved solids in centrifuged solids	25°C:	63.5	65.1	64.5	64.3
	40°C:	80.3 ^a	60.4	60.7	60.6
^a not included in average					

Table 3.5. Physical Properties of 8M Na AP-101 Melter Feed

Physical Property	Temperature	Melt-B-1	Melt-B-2	Melt-B-3	Average
Density – Bulk slurry (g/mL)	25°C:	1.730	1.748	1.746	1.742
	40°C:	1.740	1.736	1.728	1.734
Density – settled solids (g/mL)	25°C:	1.96	1.98	1.98	1.97
	40°C:	1.82	1.82	1.81	1.81
Density – centrifuged solids (g/mL)	25°C:	2.08	2.13	2.11	2.11
	40°C:	2.05	2.05	2.01	2.04
Density – supernatant liquid (g/mL)	25°C:	1.38	1.38	1.40	1.39
	40°C:	1.38	1.37	1.38	1.38
Density – average particle (g/mL)	25°C:	3.01	3.09	2.95	3.01
	40°C:	3.15	2.40 ^a	3.18	3.17
Vol. % settled solids after 72 hours	25°C:	60.5	60.6	59.7	60.3
	40°C:	82.4	81.7	80.9	81.7
Vol. % centrifuged solids	25°C:	50.0	48.9	49.1	49.3
	40°C:	53.5	54.3	55.1	54.3
Vol% undissolved solids	25°C:	21.6	21.4	22.4	21.8
	40°C:	20.3	35.7 ^a	19.2	19.7
Vol% undissolved solids in settled solids	25°C:	35.4	35.0	37.4	36.0
	40°C:	24.6	43.7 ^a	23.7	24.2
Vol% undissolved solids in centrifuged solids	25°C:	43.2	43.8	45.6	44.2
	40°C:	37.9	65.8 ^a	34.8	36.4
Wt% settled solids	25°C:	68.9	69.2	67.7	68.6
	40°C:	86.0	85.6	84.7	85.4
Wt% centrifuged solids	25°C:	60.2	59.5	59.2	59.6
	40°C:	63.1	64.0	64.0	63.7
Wt% total dried solids	25°C:	65.3	65.3	65.3	65.3
	40°C:	64.5	71.9 ^a	65.8	65.2
Wt% dissolved solids	25°C:	44.0	44.1	44.2	44.1
	40°C:	43.6	43.9	46.8	44.8
Wt% undissolved solids	25°C:	37.5	37.7	37.8	37.7
	40°C:	36.8	49.4 ^a	35.3	36.0
Wt% undissolved solids in settled solids	25°C:	54.5	54.6	55.8	54.9
	40°C:	42.7	57.7	41.7	47.4
Wt% undissolved solids in centrifuged solids	25°C:	62.4	63.4	63.8	63.2
	40°C:	58.2	77.2	55.1	56.7

^a not included in average

3.2.2 pH Measurements

The pH of the AP-101 pretreated waste and melter feeds were measured with a pH probe. Previous analysis of the AP-101 supernate indicates a hydroxide concentration of approximately 2 M at a concentration of 5 M Na (Russell et al. 2002). Consequently, the expected sample pH should be approximately 14.3 for the 4.9 M Na sample. Unfortunately, pH measurement (with a pH probe) for samples above pH 14 is typically considered unreliable. The pH for the pretreated waste was measured at above pH 14 at three Na concentrations, 6 M, 8 M, and 10 M. Since the glass former chemicals (see Table 2.1) contain acidic species such as boric acid, the pH of the resulting melter feed interstitial liquid dropped significantly. The pH measurement results for the melter feed material can be found in Table 3.6. Additional solids precipitation is possible due to this pH change (e.g. aluminum hydroxide).

Table 3.6. pH of the AP-101 Melter Feed

[Na], <u>M</u>	pH (at ambient)
6	12.3
8	12.5

3.2.3 Settling Behavior

Data from the settling portion of the study can be found in Figures 3.1-3.4. This data consists of settling measurements performed on ~5 mL samples in centrifuge cones as specified by Smith and Prindiville (2002). One representative data run is shown as the vol% settled solids as a function of time following initial agitation. Settling measurements were performed on two sets of samples. The first set of settling measurements involves the solids that precipitated during evaporation of the pretreated material. These samples consist of pretreated waste at Na concentrations of 6 M and 8 M. Settling measurements on the 10 M Na sample were not performed. Two temperatures were examined, 25°C and 40°C.

This settling study indicates that the precipitated solids from the pretreated feed settle relatively quickly in the “particulate” settling regime defined by Perry and Green (1997). In this settling regime, the solid particles fall freely to the bottom of the vessel, and a solids layer builds from the bottom of the vessel upwards.

The data indicates that the majority of the particles in the pretreated waste settle within the first hour after agitation stopped. However, a significant fraction of fine particles continue to settle over the next several hours. Ten minutes after agitation stops, the settled solids vol% was measured at approximately 2% for the 6 M Na 25°C sample. However, 2% of the sample appeared to settle in 30 seconds when measured at 40°C. The same behavior was observed in the 8 M Na sample, at 25°C approximately 5% of the sample was settled after 10 minutes. At 40°C after 5 minutes, approximately 6% of the sample had settled. Faster settling at higher temperatures is expected due to a lower fluid viscosity.

As shown in Figure 3.1 and 3.2, the 6 M Na pretreated LAW samples reached a 72-hour settled solids value of approximately 3.8% at both 25°C and 40°C. The 8 M Na samples had 72-hour settled solids values of 9.9 % at both 25°C and 40°C. Note that a difference is seen in the 6 M and 8 M Na pretreated waste samples settled solids percent at 40°C as reported in Tables 3.1 and 3.2 and shown in Figures 3.1 and 3.2. This is due to the fact that the settling study results shown in Figures 3.1 and 3.2 were performed at both 25°C and 40°C on subsamples that were used for the 25°C settled solids values shown in Tables 3.1 and 3.2. Separate subsamples were obtained for the 40°C settled solids values shown in Tables 3.1 and 3.2. These 40°C physical properties subsamples shown in Tables 3.1 and 3.2 indicate 2.3 and 8.4

vol% settled solids at 6 M and 8 M Na respectively. For conservatism, the settled solids values in Tables 3.1 and 3.2 should be used for process design issues, while the settling behavior can be derived from Figures 3.1 and 3.2.

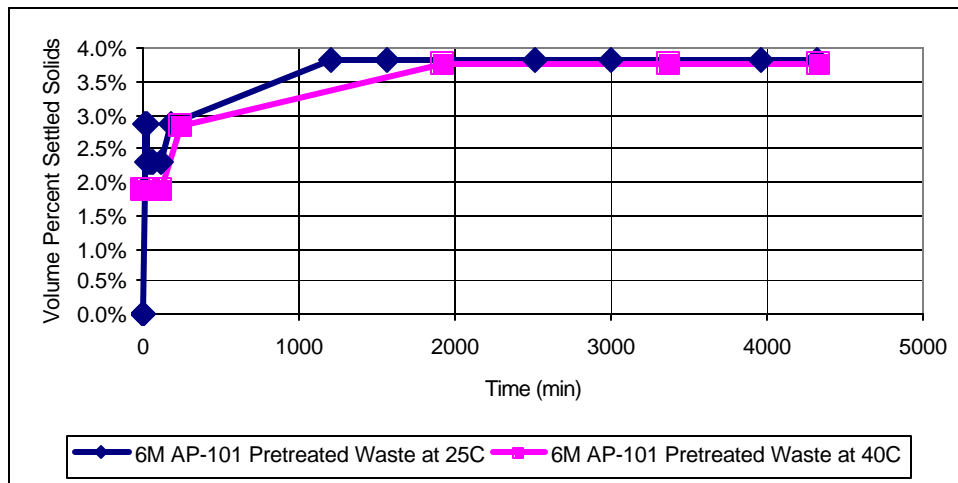


Figure 3.1. Settling Data for 6 M Na Pretreated AP-101 Waste at 25°C and 40°C

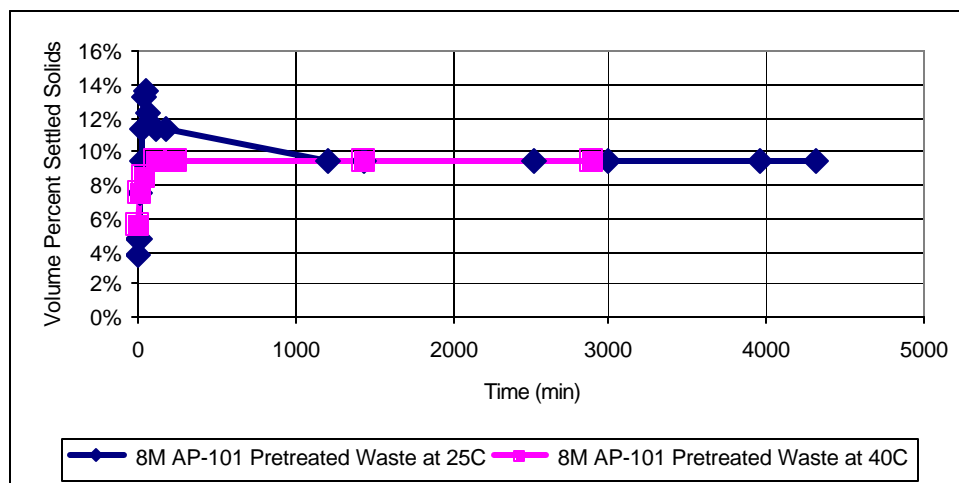


Figure 3.2. Settling Data for 8 M Na Pretreated AP-101 at 25°C and 40°C

As shown in Figures 3.3 and 3.4, the melter feed materials settled in the “zone” or “hindered” settling regime. This regime occurs due to the particles interacting and settling as a mass. This behavior is characterized by the settled solids layer height decreasing from the fully suspended volume to a final settled solids volume.

As one can see, this zone settling behavior was relatively slow and several hundred minutes passed before the majority of the sample had settled. The 6 M Na sample appears to have settled faster than the 8 M Na sample. This is likely due to the higher viscosity of the interstitial liquid and undissolved solids

concentration in the 8 M Na sample. The 72-hour settled solid vol% value for the 6 M Na sample was approximately 50% while the 8 M Na 72-hour value was approximately 60% at 25°C. This increase in settled solids volume is expected since the glass formulation is scaled based on Na content. That is to say, on a volume basis, 33% ($8/6 \approx 1.33$) more glass former chemicals were added to prepare the 8 M Na melter feed compared to the 6 M melter feed. It should be noted that quantitative prediction of vol% settle solids based on Na concentration is complicated by several factors including dissolution, precipitation, and compaction.

At 40°C the settling rate slows and the packing efficiency of both the 6 M Na and 8 M Na melter feed samples decreases. This is demonstrated by the observed increase in vol% settled solids at elevated temperatures while the wt% undissolved solids remains relatively constant. This results in approximately a 10% volume increase in settled solids vol% between 25°C and 40°C for the 6 M Na melter feed sample and a 20% volume increase in settled solids vol% between 25°C and 40°C for the 8 M Na melter feed sample. Over a larger time span, the 40°C vol% settled solids may approach the 25°C values.

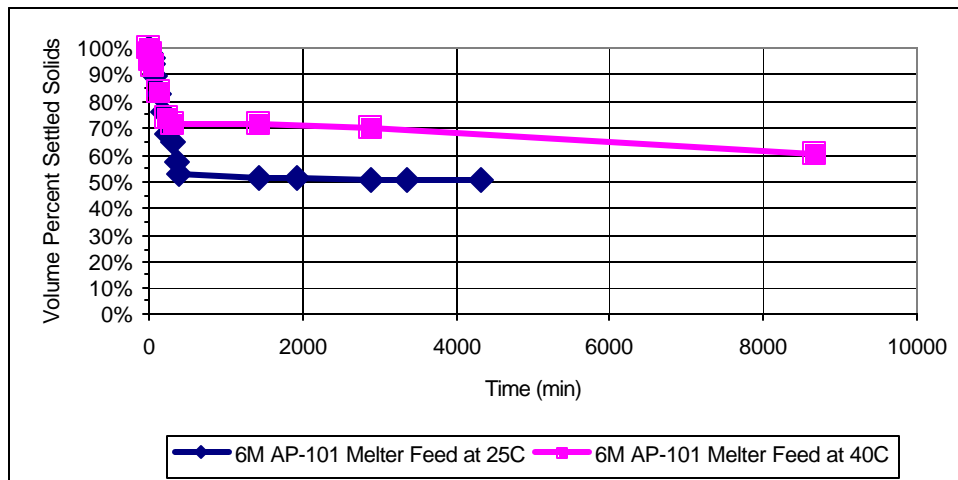


Figure 3.3. Settling Data for 6 M Na Melter Feed at 25° C and 40° C

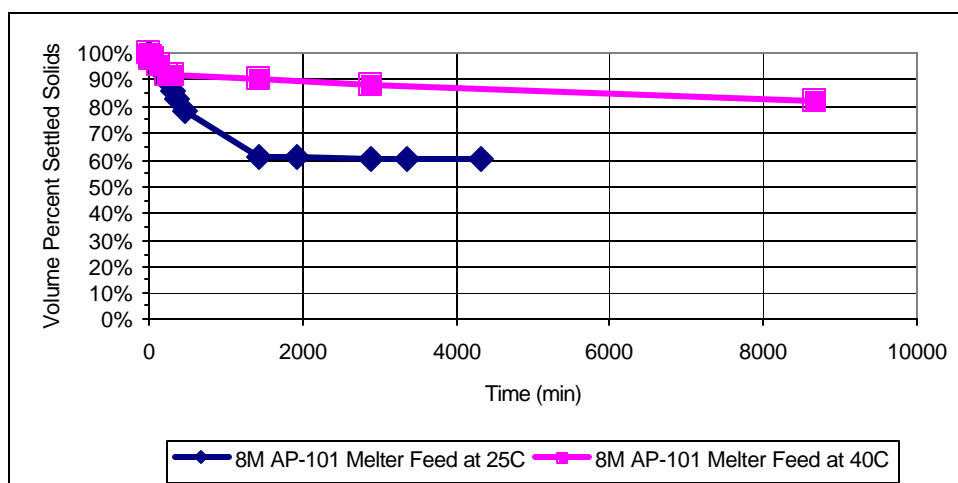


Figure 3.4. Settling Data for 8 M Na Melter Feed at 25° C and 40° C

4.0 Rheology

Viscosity is the internal resistance to flow of a fluid against external forces. Mathematically, viscosity is defined as the ratio of shear stress to shear rate. For a Newtonian fluid, this value is constant. For non-Newtonian fluids, this ratio can change based on flow conditions and shear history. The rheological data is most often presented as a rheogram. Rheograms provide flow data over a range of shear rates rather than at one shear rate. A rheometer changes the shear rate to a chosen value while measuring and recording the resulting shear stress. This is the primary difference between a rheometer and a viscometer. In this study, a rheometer was used. From a rheogram, viscosity data, yield stress data, and flow curve information are obtained. Viscosity is usually reported in units of centipoise (cP). One cP is equal to a millipascal second (mPa·s). There are several types of flow curves that have been well studied and have defined mathematical curve fits assigned to them. These curve fits are usually used to describe and predict flow behaviors of fluids. Some materials have a yield point, a minimal external force that must be applied before any flow is obtained. The four curve fits that best describe most slurries and consequently tank waste are as follows:

1. Newtonian

$$\mathbf{t} = \mathbf{h}\mathbf{g} \quad (4.1)$$

Where, \mathbf{t} is the shear stress.
 \mathbf{h} is the Newtonian viscosity.
 \mathbf{g} is the shear rate.

2. Ostwald (or Power Law)

$$\mathbf{t} = m\mathbf{g}^n \quad (4.2)$$

Where, m is the power law consistency index.
 n is the power law index.
 \mathbf{g} is the shear rate.

If $n < 1$, then the material is referred to as pseudoplastic (shear thinning). If $n > 1$, that material is referred to as dilatant (shear thickening). Since dilatant flow behavior is rare, dilatant behavior is an indication of possible Taylor Vortices or other measurement errors.

3. Bingham Plastic

$$\mathbf{t} = \mathbf{t}_O^B + k_B\mathbf{g} \quad (4.3)$$

Where, \mathbf{t}_O^B is the Bingham yield index.
 k_B is the Bingham consistency index.
 \mathbf{g} is the shear rate.

4. Herschel-Bulkley

$$\mathbf{t} = \mathbf{t}_O^H + k\mathbf{g}^b \quad (4.4)$$

Where, \mathbf{t}_O^H is the Herschel-Bulkley yield index.
 k is the Herschel-Bulkley consistency index.
 b is the Herschel-Bulkley power law index.
 \mathbf{g} is the shear rate.

Examples of Newtonian fluids include water and honey. For these fluids, the viscosity is constant over all shear conditions. A Bingham plastic is a fluid that contains a yield point, but once enough force has been applied to exceed the yield point, the material behaves in a Newtonian fashion over the rest of the shear rate range. A pseudoplastic, or power law fluid, has a viscosity that varies with stress in a non-linear fashion. It is modeled by the Ostwald equation. A yield pseudoplastic is a power law fluid with a yield index and is modeled with the Herschel-Bulkley equation.

4.1 Equipment Details

A Haake RS300 rheometer was used for the work described in this section. The RS300 system has been configured with a temperature controlled concentric cylinder rotational system. The sensor system consists of an inner cylinder that is placed inside an outer cylinder with a known annulus. When the inner cylinder rotates, the resulting fluid resistance to the flow is measured electronically. When this signal is combined with the rotational rate, it can be mathematically transformed into shear stress and shear rate data. For the samples analyzed in this report, Haake DG41 (pretreated waste) and Z41 (melter feed) sensor systems were utilized. The DG41 sensor has a large available surface area to increase the instrument sensitivity for relatively low viscosity samples. The Z41 sensor possesses a relatively large annular region to allow measurement of fairly concentrated slurries with larger particles.

The testing was conducted as follows. The samples were loaded into the sample container, and the shear rate was increased from 0-1000 s^{-1} in 5 minutes. The sample was held at a shear rate of 1000 s^{-1} for 1 minute. Lastly, the shear rate was decreased from 1000-0 s^{-1} in 5 minutes. The test was then immediately repeated with the same sample. If the subsequent data was in close agreement with the previous run, the testing for that sample was considered complete. If there was noticeable variation in the data, the sample was ramped through this cycle again until two consecutive similar data sets were obtained. The purpose of this repetition was to qualitatively determine if rheological changes occur while under the influence of shear. Shear history is often an important part of determining expected rheological behaviors. Once the previous sample was tested to the point of obtaining consistent data, it was removed, and a new sample was loaded for the next run.

The purpose of this set of testing parameters was to identify the rheological behavior and shear sensitivity of the materials. The first ramp cycle shows newly loaded or fresh sample behavior including breakdown of sample structure through hysteresis, if present. Hysteresis is when the ramp down curve is different from the ramp up curve. An immediate repeat allows little or no time for the sample to recover. The complete cycle repeat with the used sample shows the effects of a shear history with a short time of recovery for the sample.

A 98 cP (at 25°C) viscosity standard oil was used to validate the calibration of the machine. A value of 98.8 cP was measured at 25°C. This plot is shown in Figure 4.1.

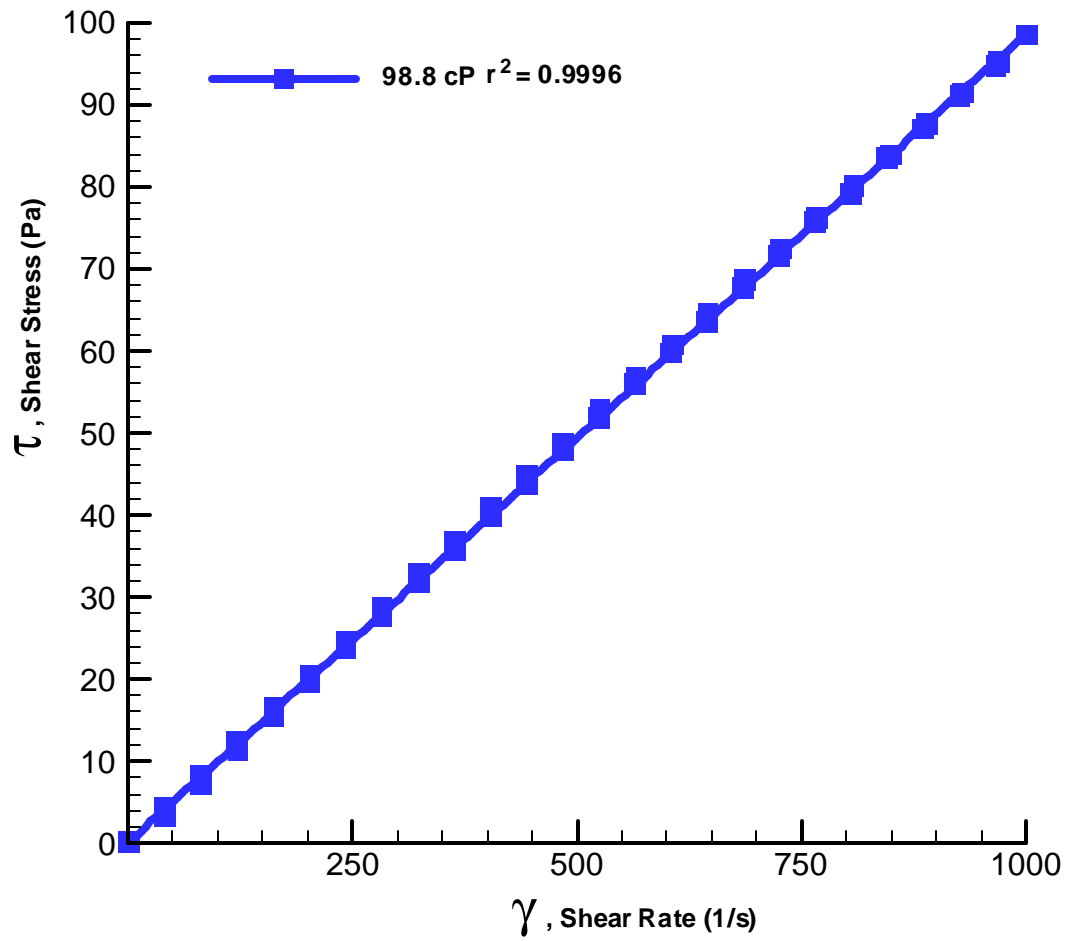


Figure 4.1. Haake RS300 98 cP Viscosity Standard Calibration Check at 25°C

4.2 Pretreated Waste

Rheograms from pretreated waste at various Na concentrations are shown in Figures 4.2-4.9. Each figure provides a least squares rheological model fit (see Section 4.0) for each increasing shear rate analysis. Data points are also provided for the decreasing shear rate analysis. These wastes did not contain glass former chemicals. However, these wastes did contain various amounts of solid precipitates that formed during evaporation. The solids caused spurious data points (i.e. noisy data) when they interacted with the surfaces of the sensors (see Figures 4.4-4.9) with a 500 μm annular region distance. As expected, data from the 10 M Na pretreated waste showed the greatest number of spurious points (see Figures 4.8-4.9). Due to these spurious points, the correlation coefficients are extremely small (see Appendix A) and are not presented in Figures 4.8 and 4.9. However, Newtonian behavior can still be recognized by filtering the spurious data and considering the values obtained over multiple runs. Results are summarized in Table 4.1. As expected, the viscosity of the waste increases with increasing Na concentration and decreasing temperature. The higher concentration wastes appear to behave as a power-law fluid. However, these wastes can be adequately modeled as a Newtonian fluid. Newtonian model least squares fits are presented in the rheograms.

Table 4.1. Newtonian Viscosity of the AP-101 Pretreated Waste

[Na], M	Viscosity, cP (mPa·s)	
	25°C	40°C
4.9	3.5	2.5
6	5.2	3.6
8	8.0	5.4
10	11.8	7.2

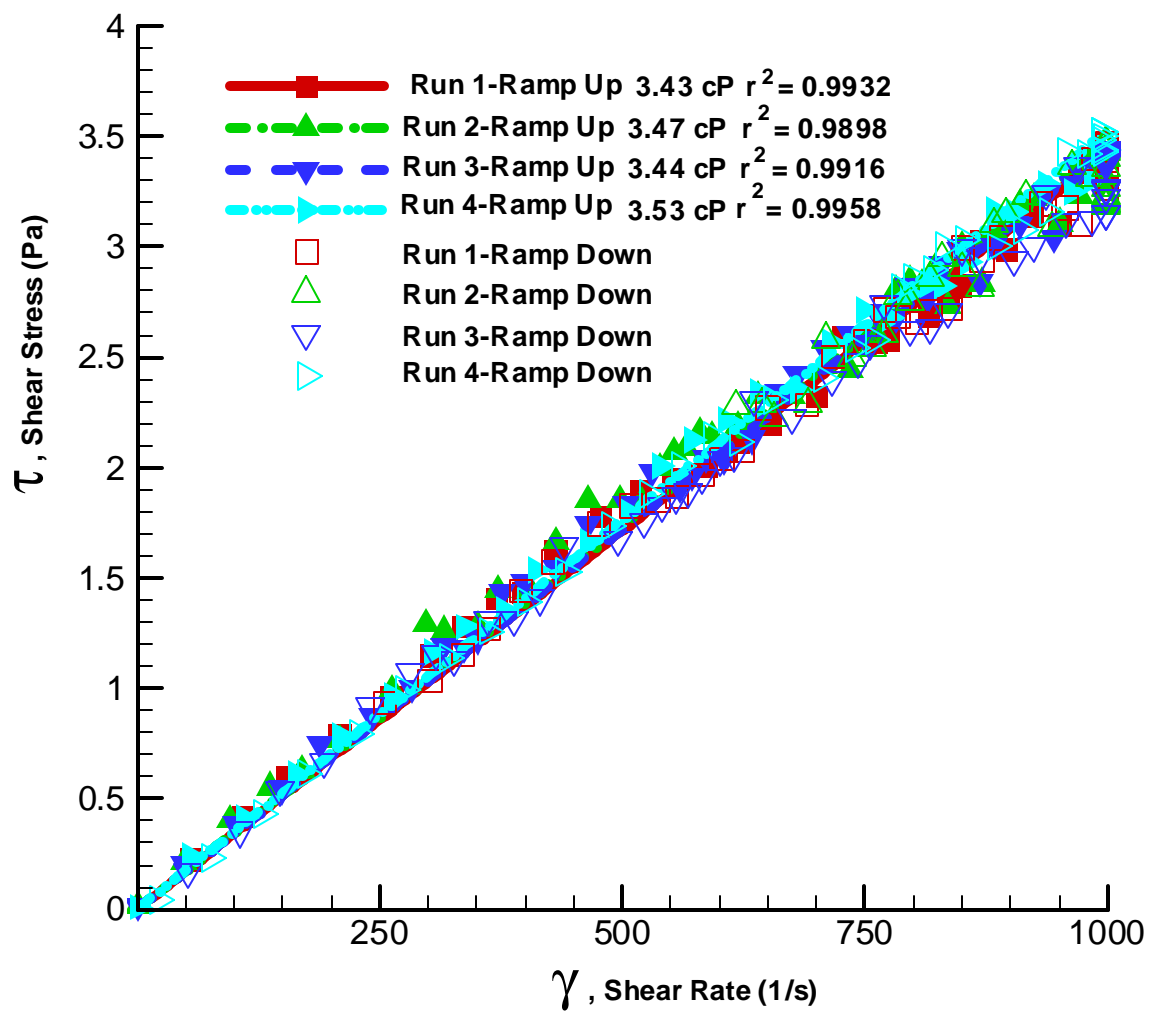


Figure 4.2. Flow Curve of 4.9 M Na AP-101 Pretreated Waste (Without Glass Formers) at 25°C

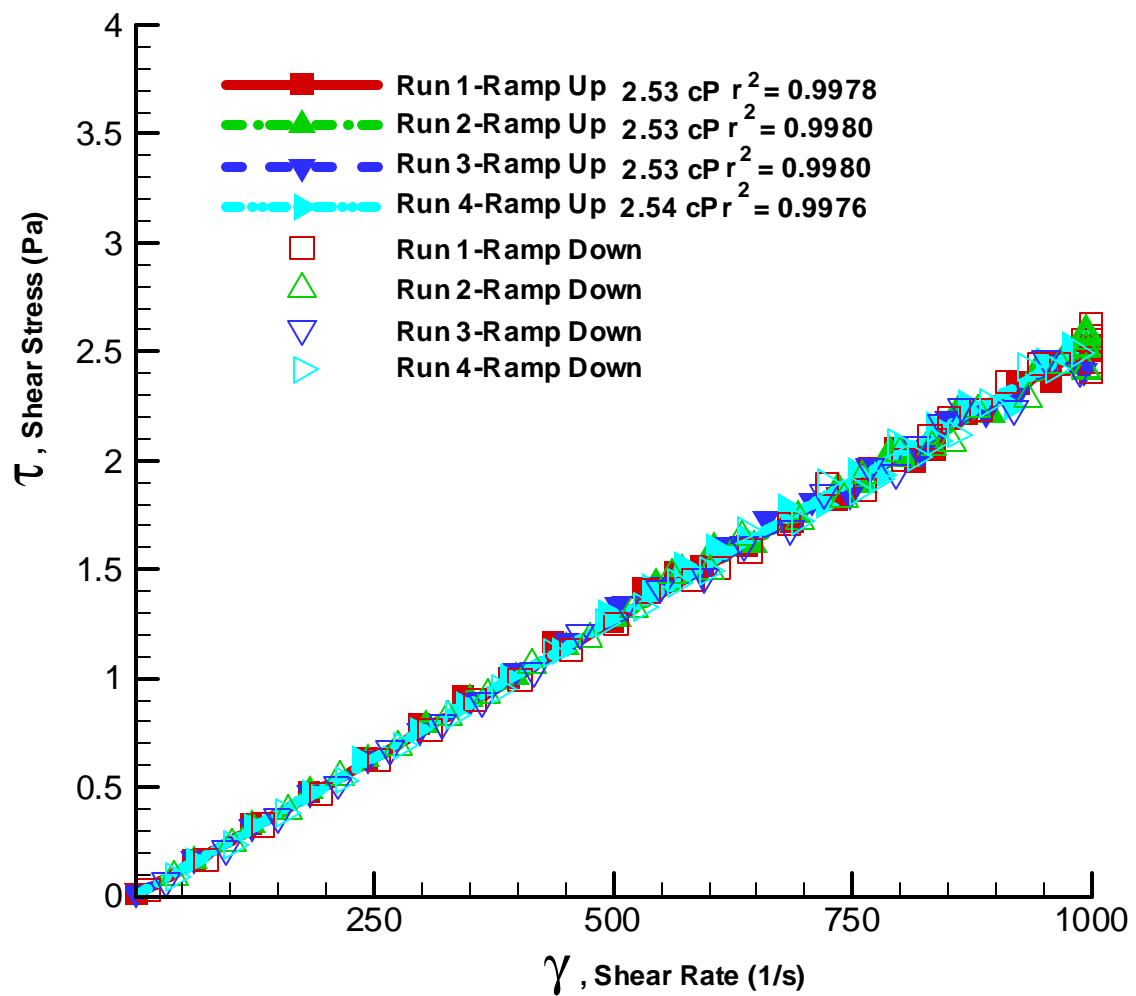


Figure 4.3. Flow Curve of 4.9 M Na AP-101 Pretreated Waste (Without Glass Formers) at 40°C

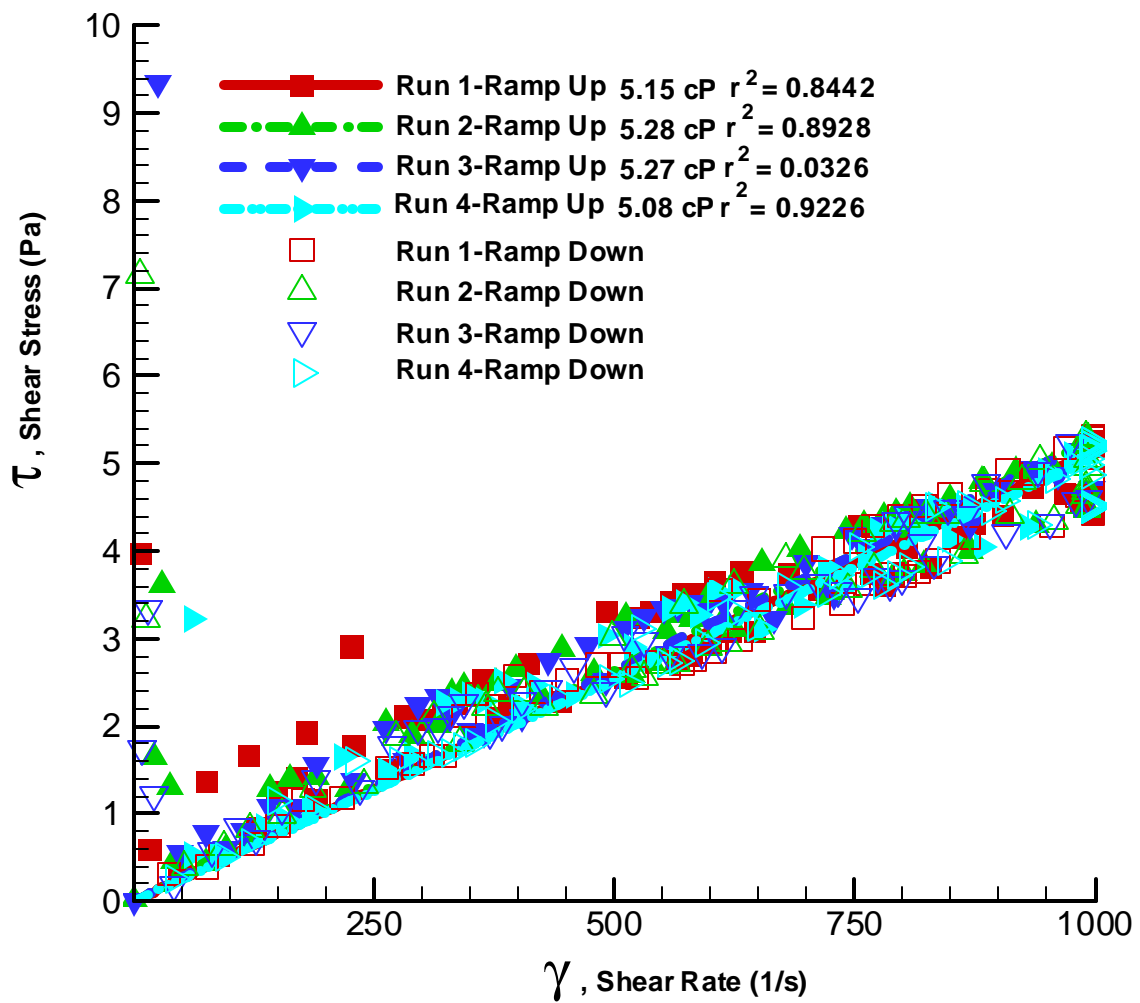


Figure 4.4. Flow Curve of 6 M Na AP-101 Pretreated Waste (Without Glass Formers) at 25°C

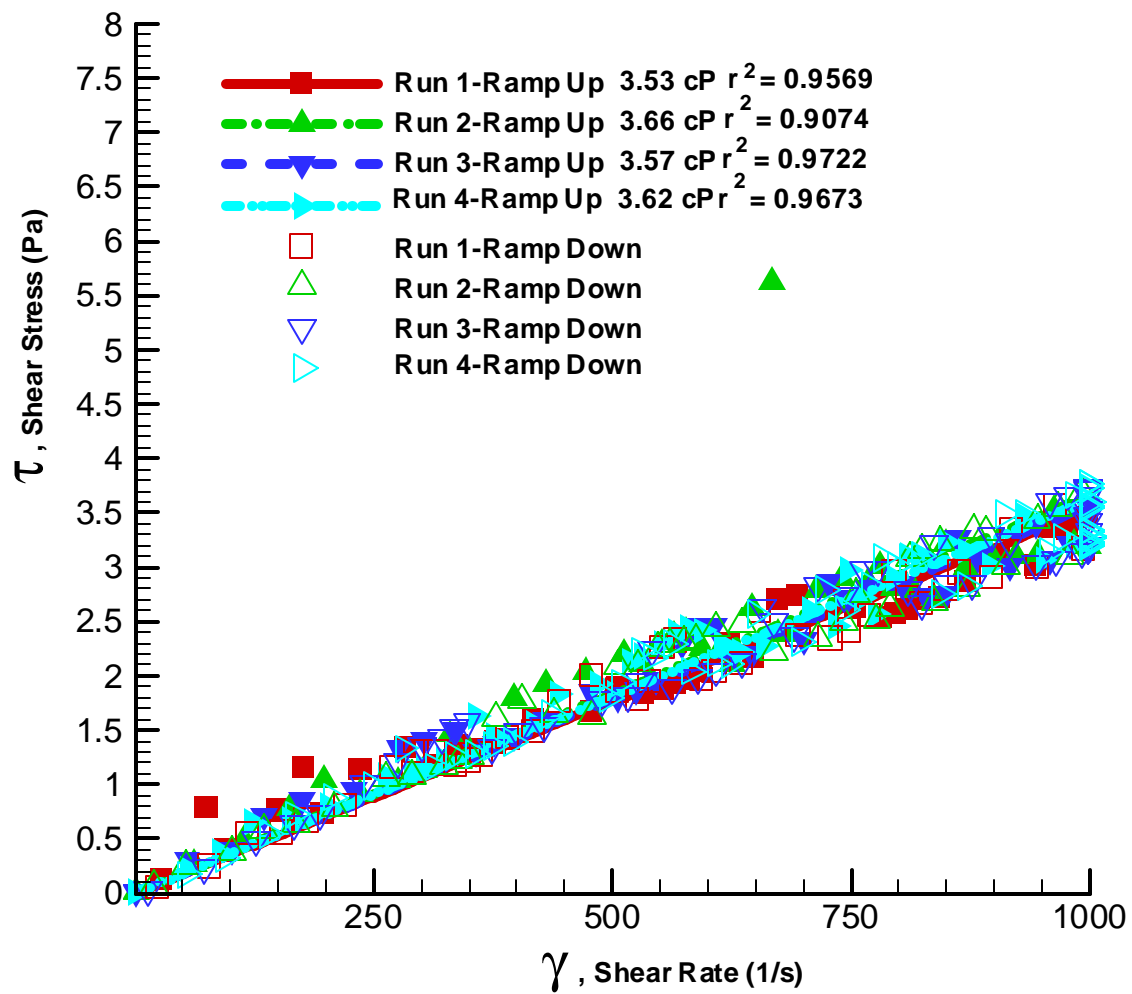


Figure 4.5. Flow Curve of 6 M Na AP-101 Pretreated Waste (Without Glass Formers) at 40°C

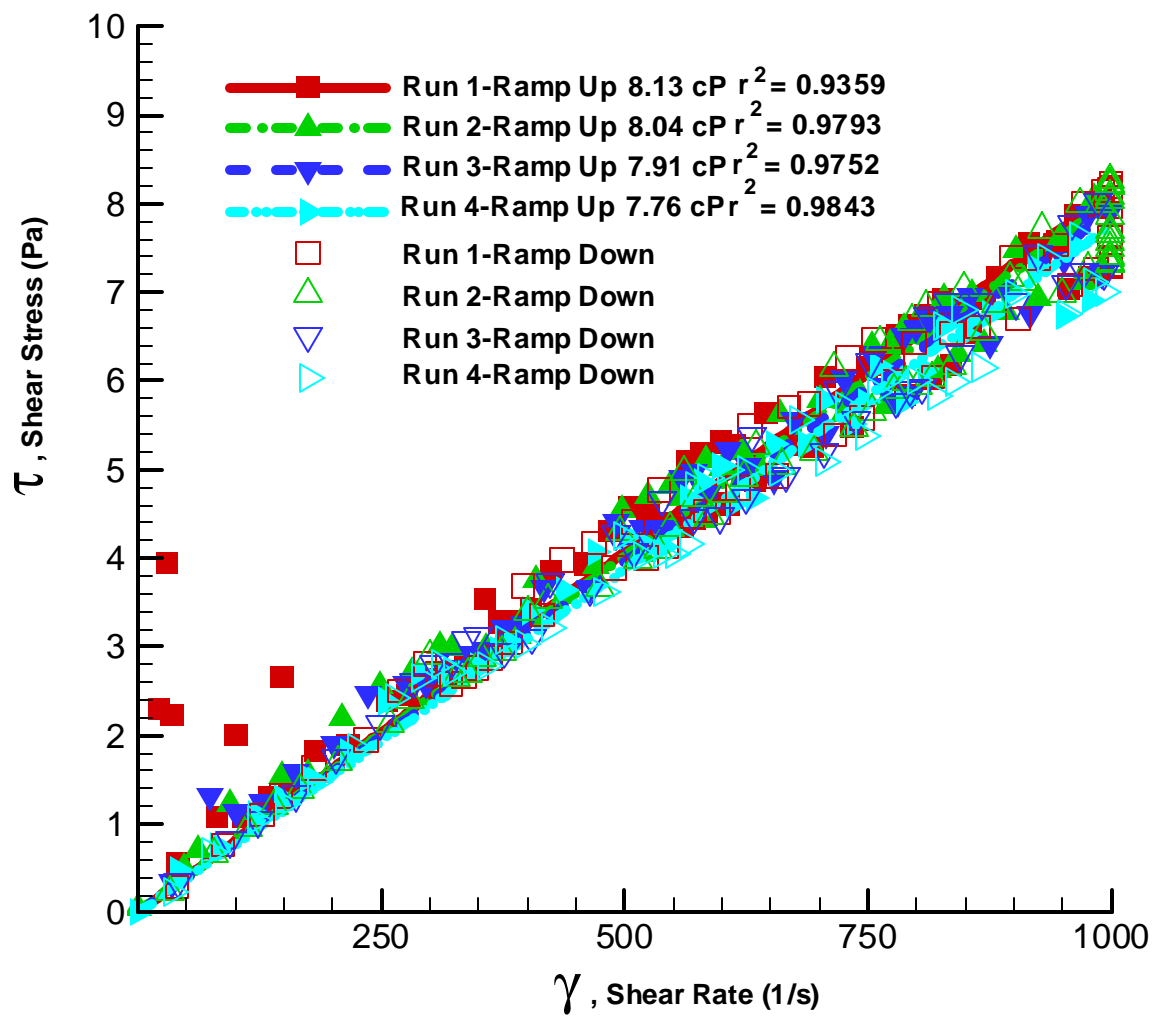


Figure 4.6. Flow Curve of 8 M Na AP-101 Pretreated Waste (Without Glass Formers) at 25°C

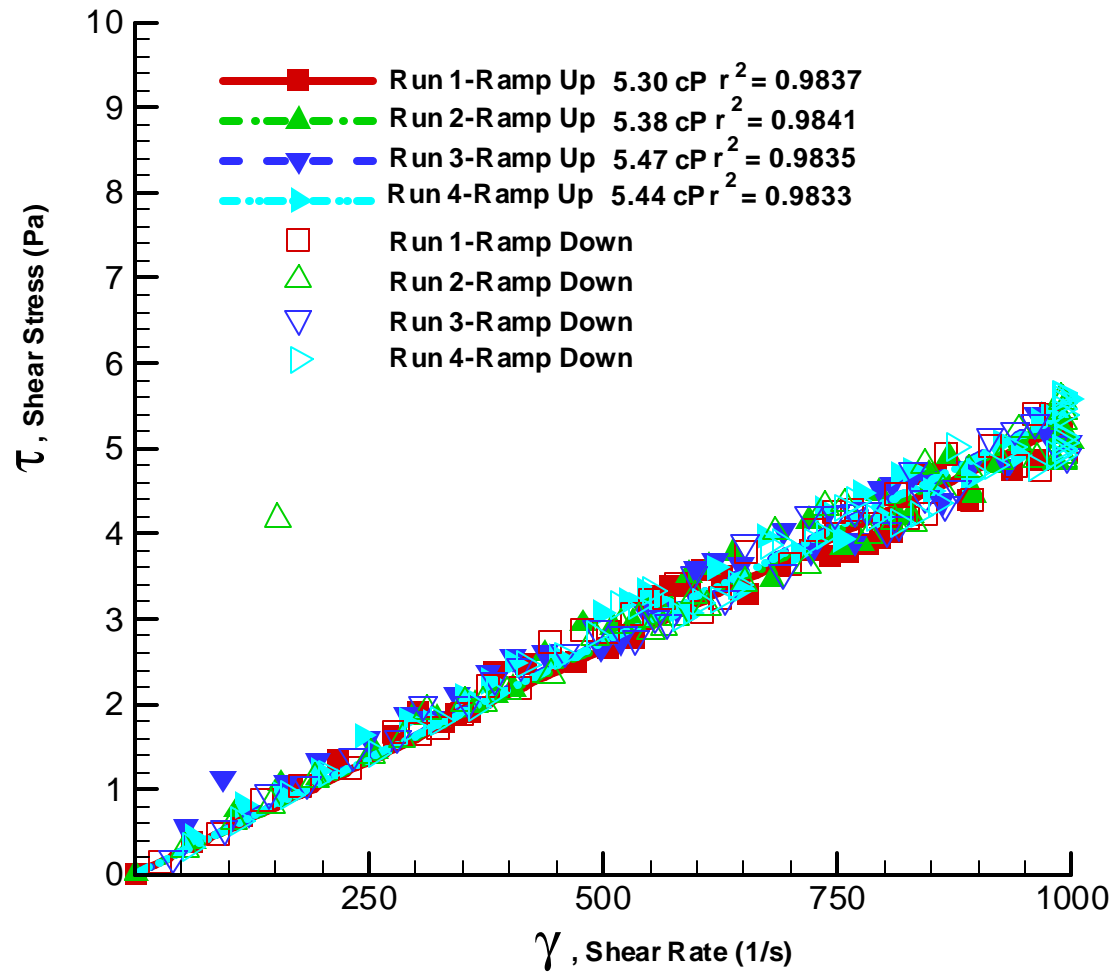


Figure 4.7. Flow Curve of 8 M Na AP-101 Pretreated Waste (Without Glass Formers) at 40°C

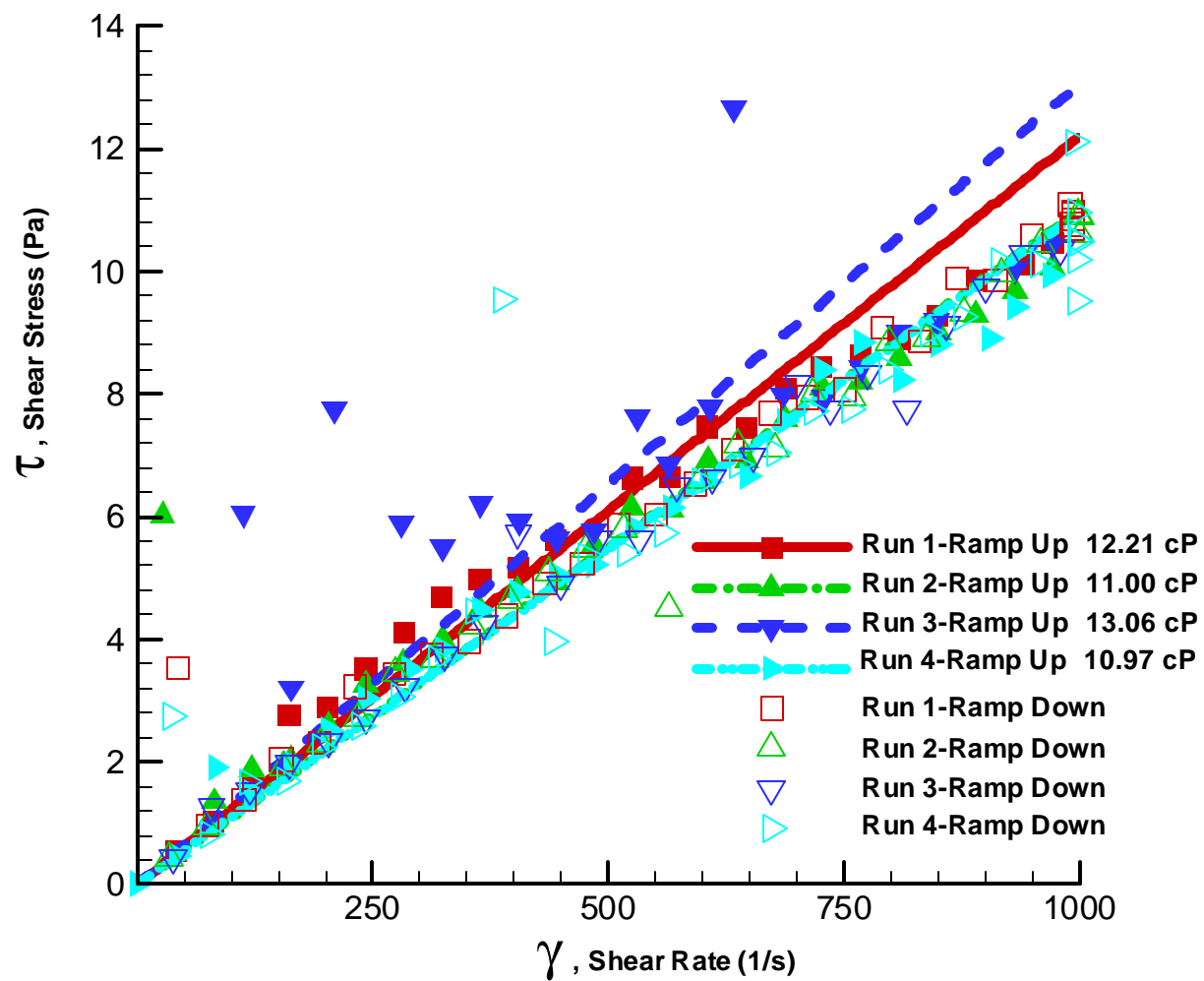


Figure 4.8. Flow Curve of 10 M Na AP-101 Pretreated Waste (Without Glass Formers) at 25°C

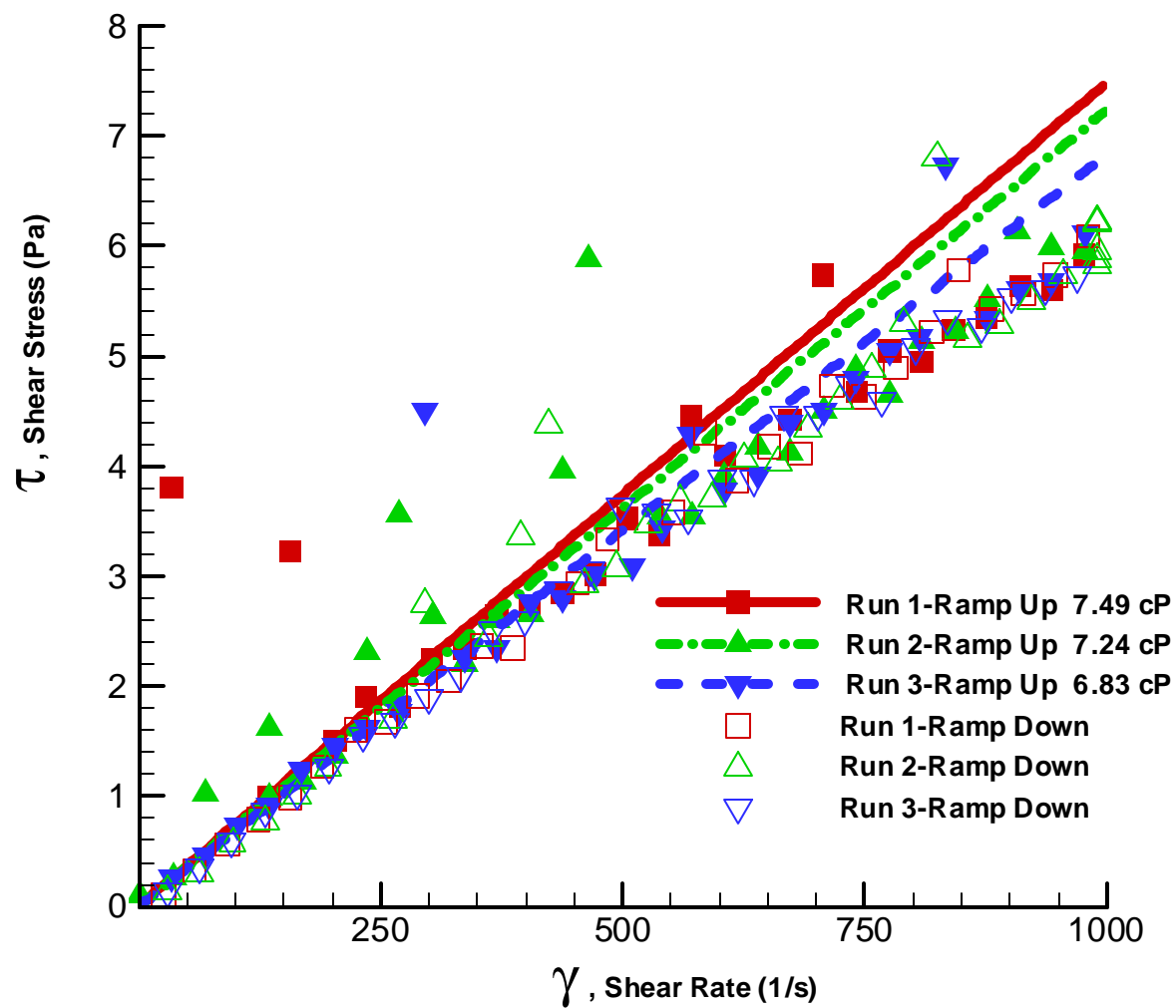


Figure 4.9. Flow Curve of 10 M Na AP-101 Pretreated Waste (Without Glass Formers) at 40° C

4.3 Melter Feed

Rheograms for each of the AP-101 melter feed samples show strong Newtonian behavior at both temperatures and concentrations (see Figures 4.10-4.13). Results are summarized in Table 4.2. As expected, the viscosity of the 6 M Na suspension is significantly less than the viscosity of the 8 M Na suspension. This is due to the higher concentration of glass former chemicals added to the 8 M Na sample and the higher viscosity of the 8 M Na pretreated waste. In addition, both suspensions showed strong temperature dependence. As seen in Figures 4.10-4.13, there is a minor increase in the sample viscosity between the first and last analysis of each sample. This apparent hysteresis is most likely due to a combination of evaporation of the interstitial fluid and settling of the solids particles during the run. Settling during the rheology measurements typically result in rheograms that can be modeled most accurately as yield power-law fluids with an exponent greater than unity. Fortunately, the settling rate during the analysis was sufficiently slow and these melter feeds can be adequately modeled as a Newtonian fluid. Newtonian model least squares fits are presented in the rheograms. The first segment of each run (i.e., ramp-up) was used to determine flow characteristics. However, a combination of sample evaporation and solids settling is suspected as the reason for the observed shear thickening hysteresis seen in the ramp-up and ramp-down portions of some rheograms.

Table 4.2. Newtonian Viscosity of the AP-101 Melter Feed

[Na], M	Viscosity, cP (mPa·s)	
	25°C	40°C
6	13.2	9.7
8	39.9	27.0

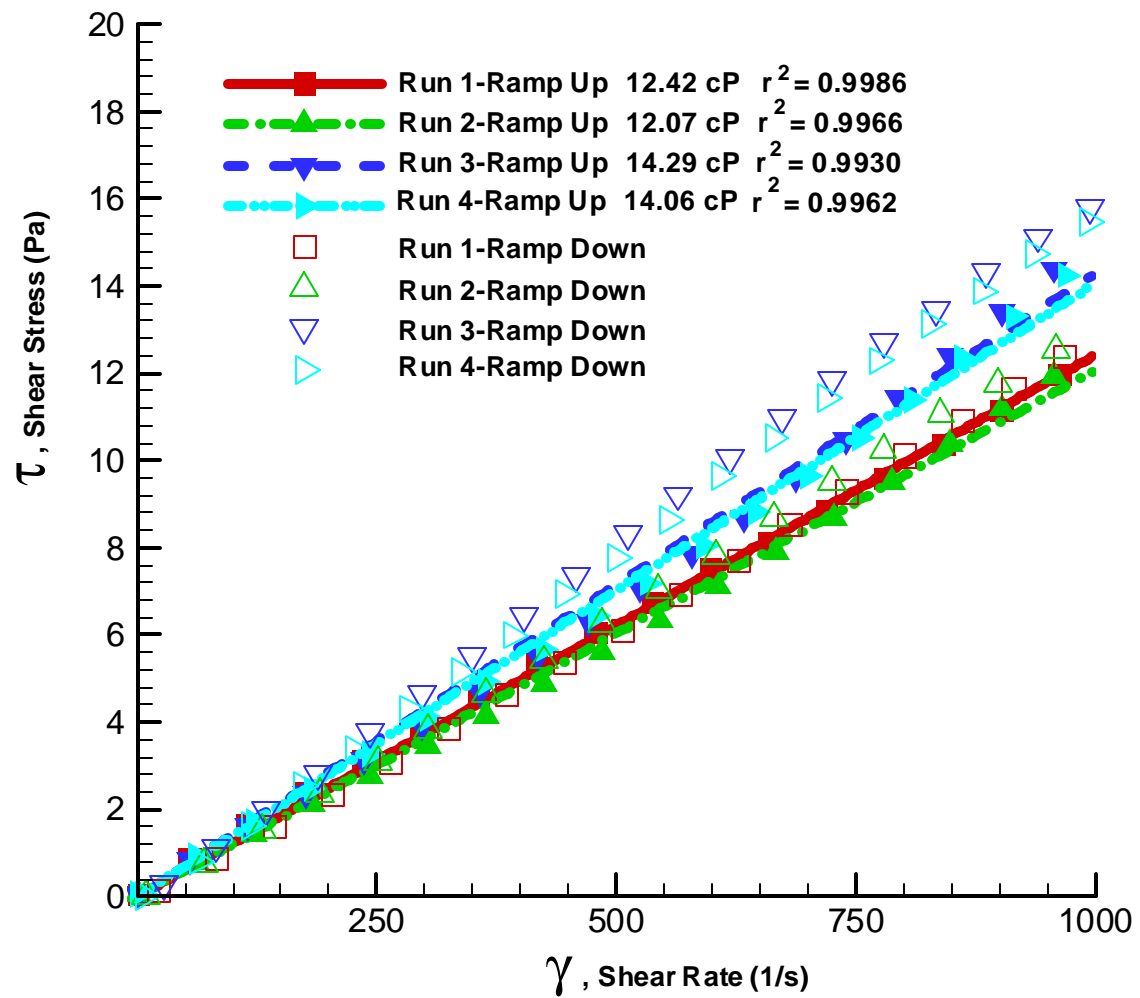


Figure 4.10. Flow Curve of 6 M Na AP-101 Melter Feed (With Glass Formers) at 25°C

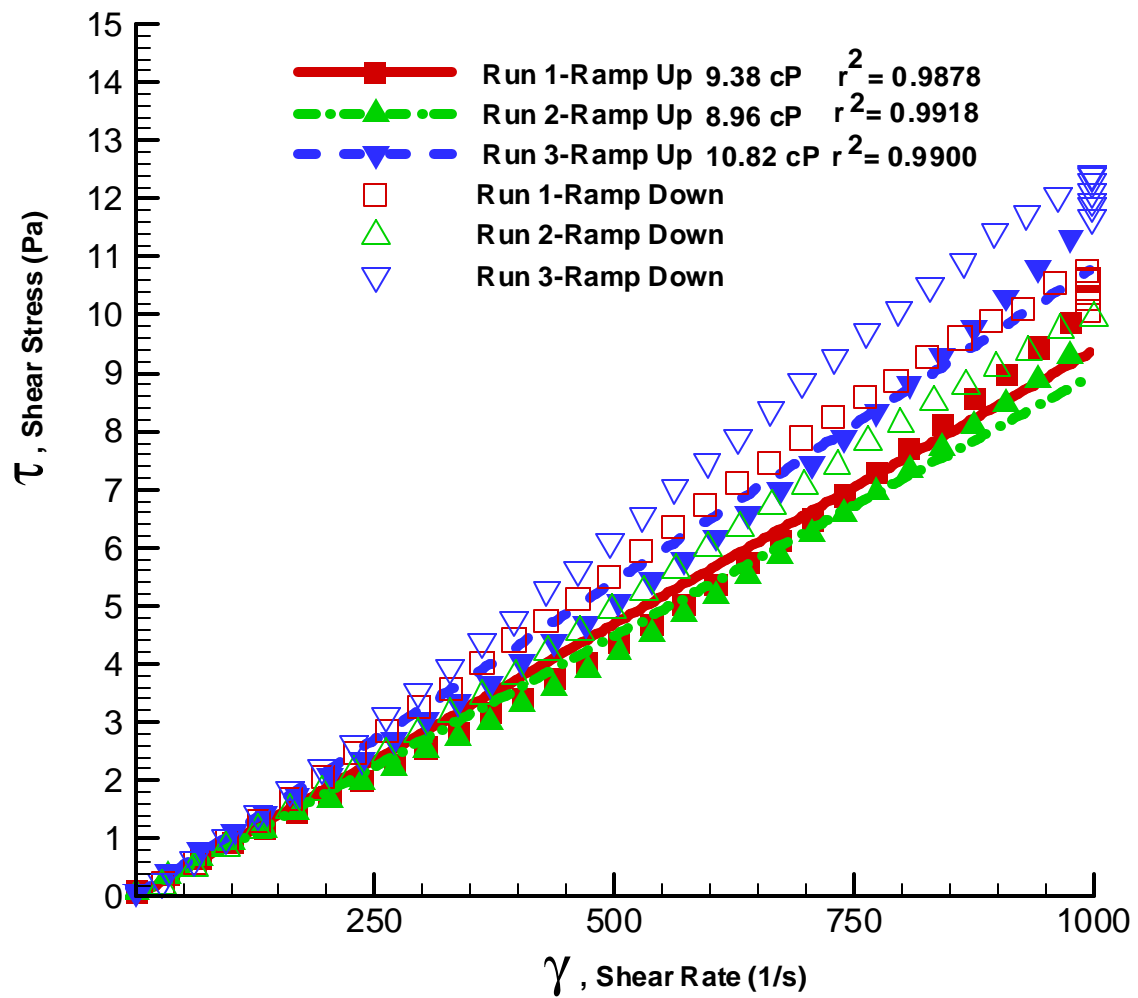


Figure 4.11. Flow Curve of 6 M Na AP-101 Melter Feed (With Glass Formers) at 40°C

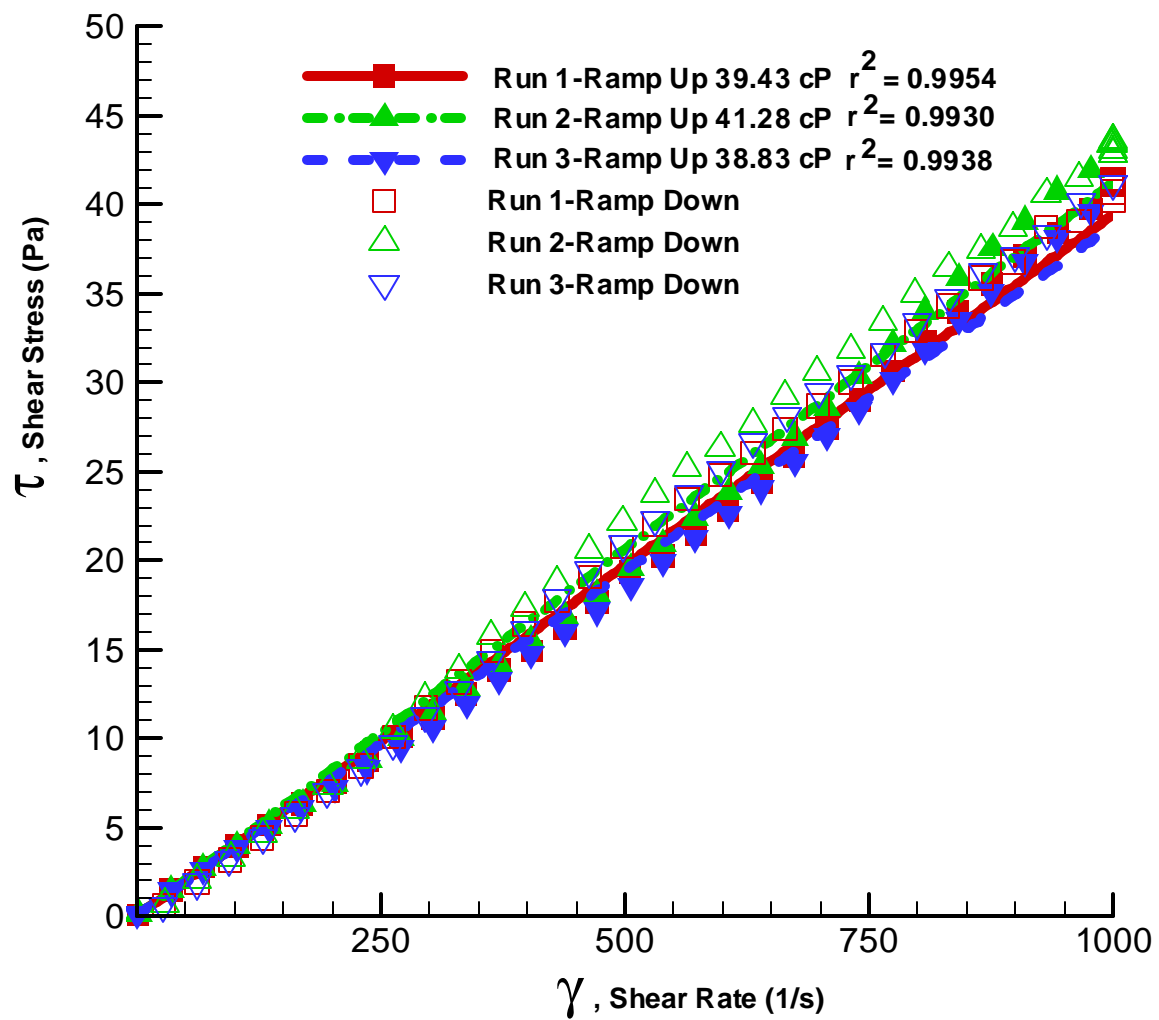


Figure 4.12. Flow Curve of 8 M Na AP-101 Melter Feed (With Glass Formers) at 25°C

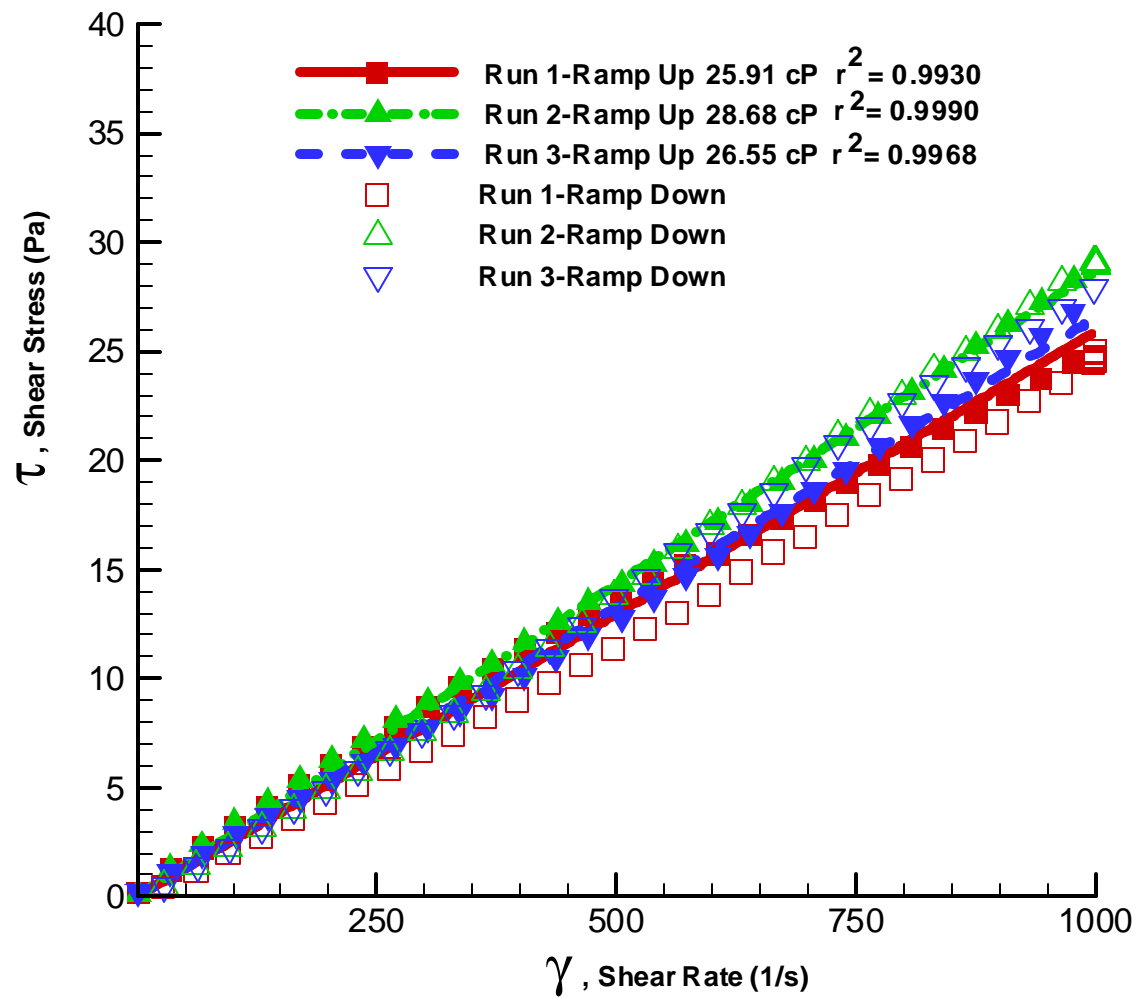


Figure 4.13. Flow Curve of 8 M Na AP-101 Melter Feed (With Glass Formers) at 40°C

4.4 Mixing/Aging

This section describes rheological measurements performed on 8 M AP-101 melter feed material that was mixed for a week with selected measurements performed after one hour, one day, and one week of mixing. Glass former chemicals (GFC), as formulation LAWA-126, were added to an 8 M Na AP-101 pretreated LAW sample with target quantities consistent with Table 2.1. The sample was then mixed with the impeller system discussed in Section 2.2 for a period of one hour at ambient temperature (~23°C). Rheological measurements on this sample at 25°C and 40°C were then performed. The sample was returned to the mixing vessel and mixed for a period of one day. A second set of rheological measurements at 25°C and 40°C was then performed. Finally, the sample was returned to the mixing vessel and mixed for a period of six more days (total of one week). A third set of rheological measurements was then performed. Figures 4.14-4.19 present the mixing/aging rheograms at 25°C and 40°C over one hour, one day, and one week intervals. Deionized water was added to these samples to keep a constant volume while mixing thus minimizing error due to evaporation.

A summary of the rheological measurements from the mixing/aging phase of the AP-101 melter feed characterization can be found in Table 4.3. As expected, at higher temperatures the viscosity of the melter feed drops. At 25°C, the mixing/aging viscosity measurements significantly increase after one day of mixing but do not reach the viscosity measured in Table 4.2 (39.9 cP). At 40°C, the mixing/aging viscosity measurements significantly increase after one week of mixing and are comparable to the viscosity measured in Table 4.2 (27.0 cP). The material used in the measurements discussed in Table 4.2 has a mixing/aging history of the being mixed for one hour and aged for approximately one month. Based on these measurements, the viscosity range of the AP-101 LAW melter feed processed through the WTP is expected to be within approximately 25 cP to 40 cP at 25°C and 20 cP to 30 cP at 40°C depending on mixing/aging history.

Table 4.3. Newtonian Viscosity of Mixed/Aged 8 M Na AP-101 Melter Feed

Temperature	Viscosity, cP (mPa·s)		
	1-hour after GFC addition	1-day after GFC addition	1-week after GFC addition
25°C	24.7	30.6	31.0
40°C	19.8	21.6	28.7

The pH of the melter feed was also measured during the mixing/aging portion of the study. Results of these measurements are shown in Table 4.4. The pH of the sample remains identical to the reported value of 12.5 (see Section 3.2.2) throughout the mixing/aging process. Therefore, the observed changes in the rheological behavior of the slurry were not associated with changing pH.

Table 4.4. pH of Mixed/Aged 8 M Na AP-101 Melter Feed

pH at ambient		
1-hour after GFC addition	1-day after GFC addition	1-week after GFC addition
12.5	12.5	12.5

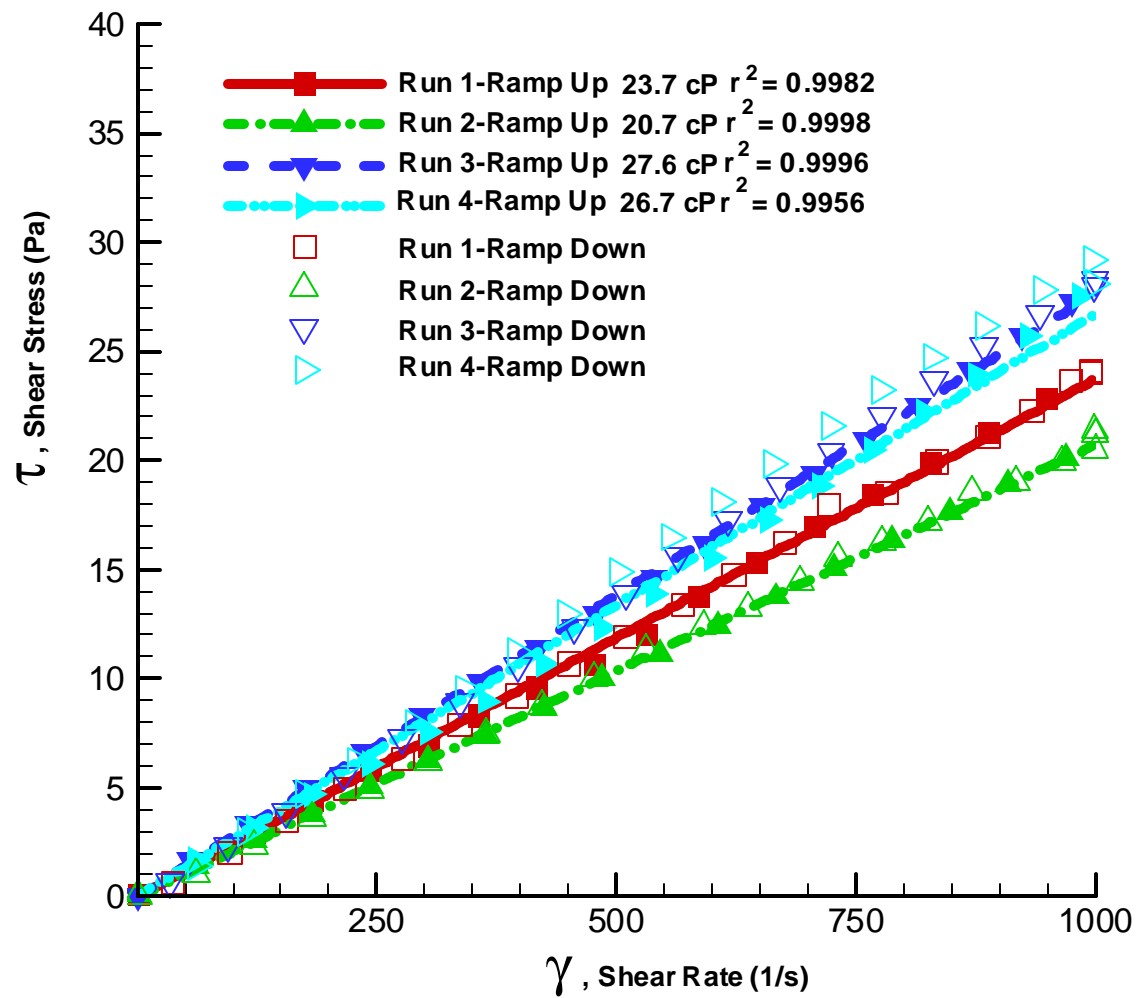


Figure 4.14. Flow Curve of 8 M Na AP-101 Melter Feed (one hour mixing with Glass Formers Chemicals) at 25° C

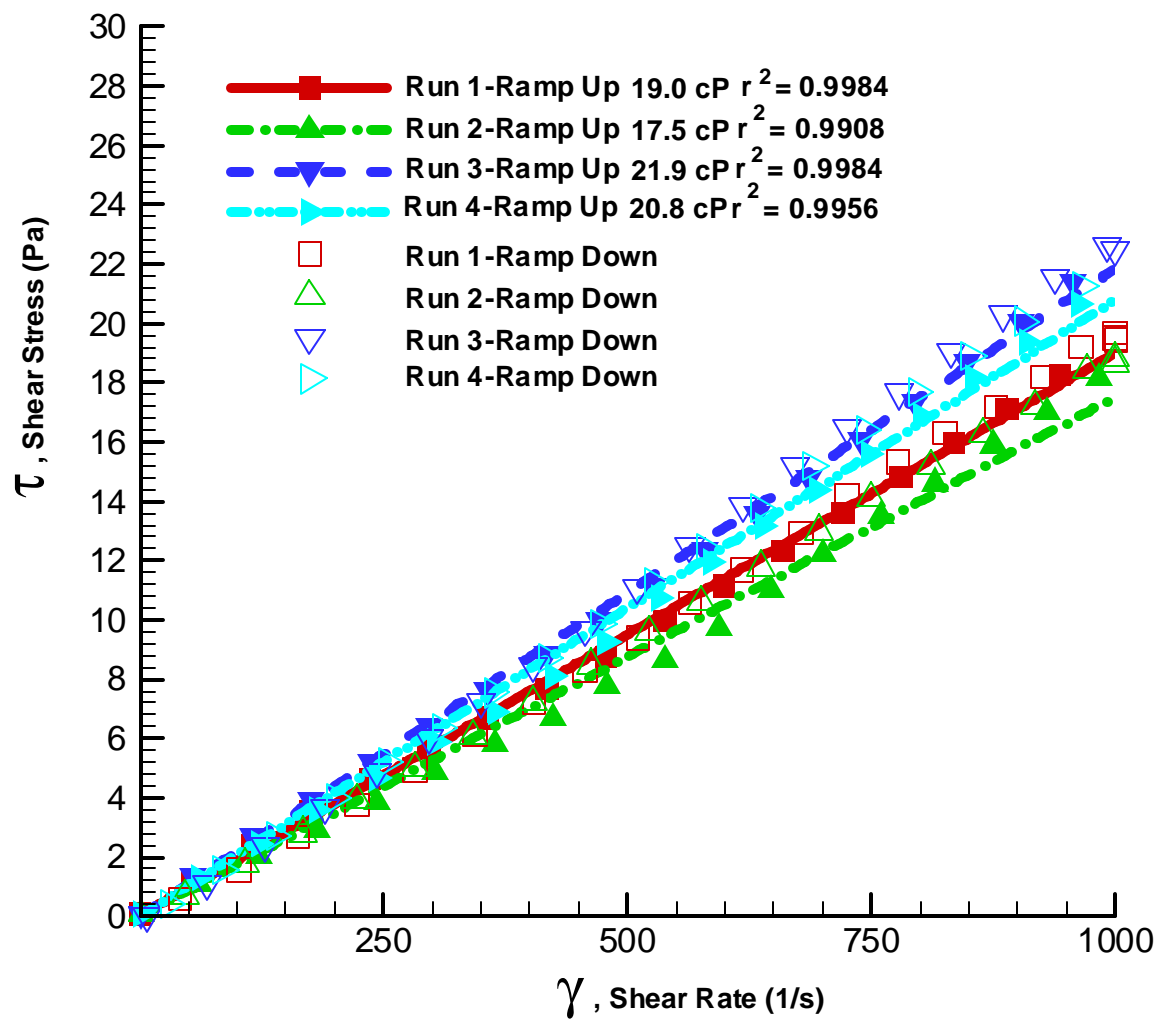


Figure 4.15. Flow Curve of 8 M Na AP-101 Melter Feed (one hour mixing with Glass Formers Chemicals) at 40°C

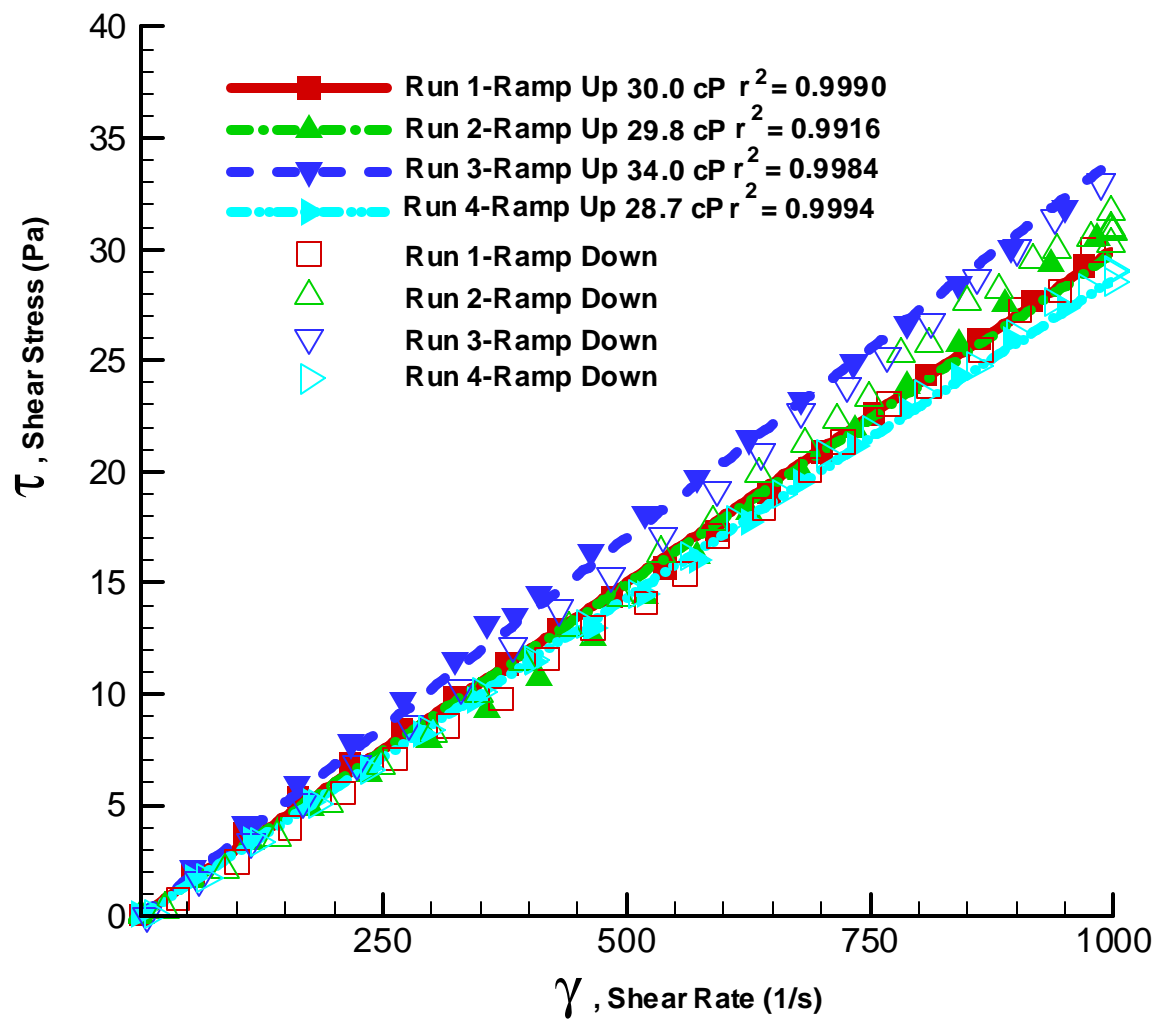


Figure 4.16. Flow Curve of 8 M Na AP-101 Melter Feed (one day mixing with Glass Formers Chemicals) at 25°C

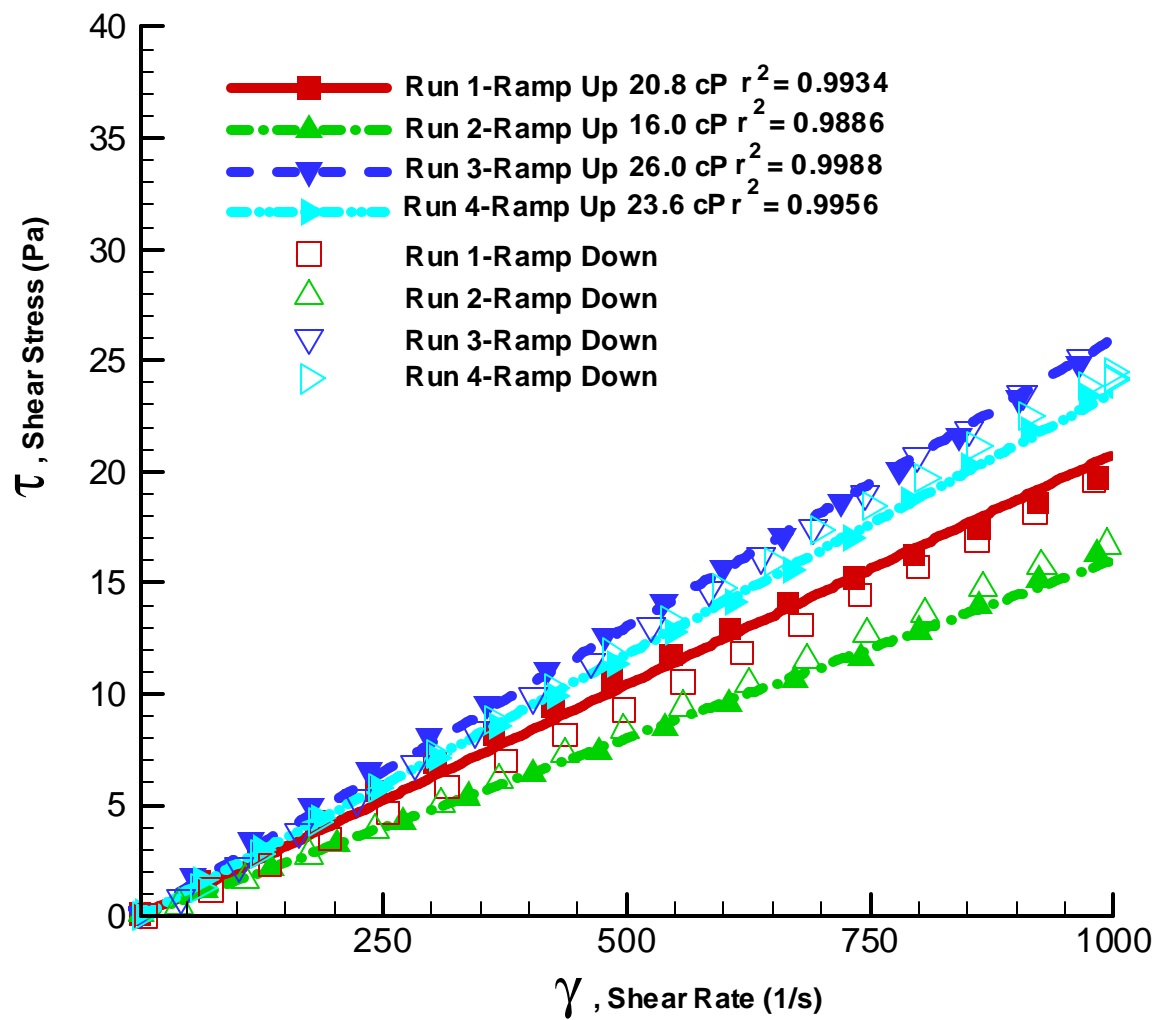


Figure 4.17. Flow Curve of 8 M Na AP-101 Melter Feed (one day mixing with Glass Formers Chemicals) at 40°C

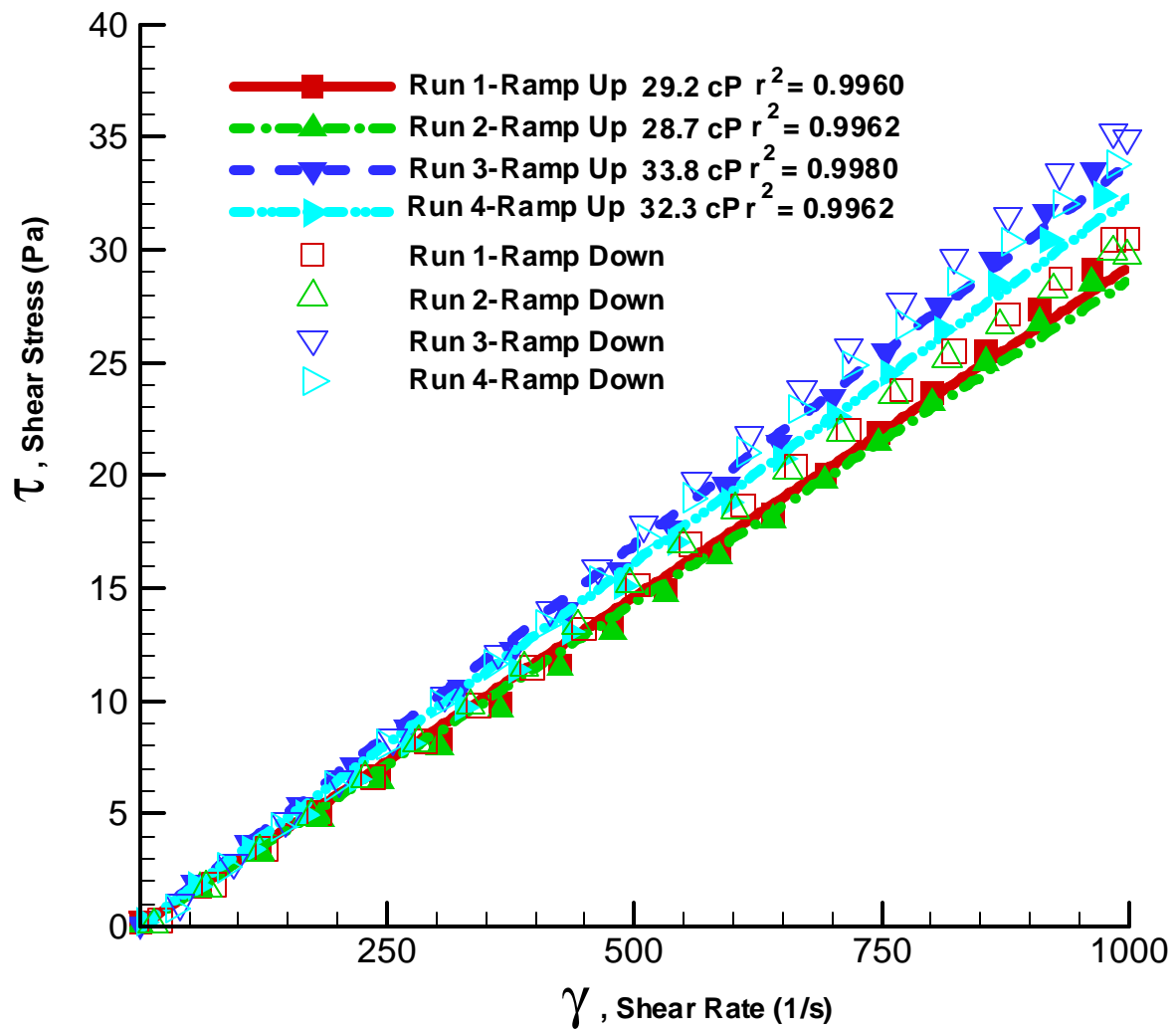


Figure 4.18. Flow Curve of 8 M Na AP-101 Melter Feed (one week mixing with Glass Formers Chemicals) at 25° C

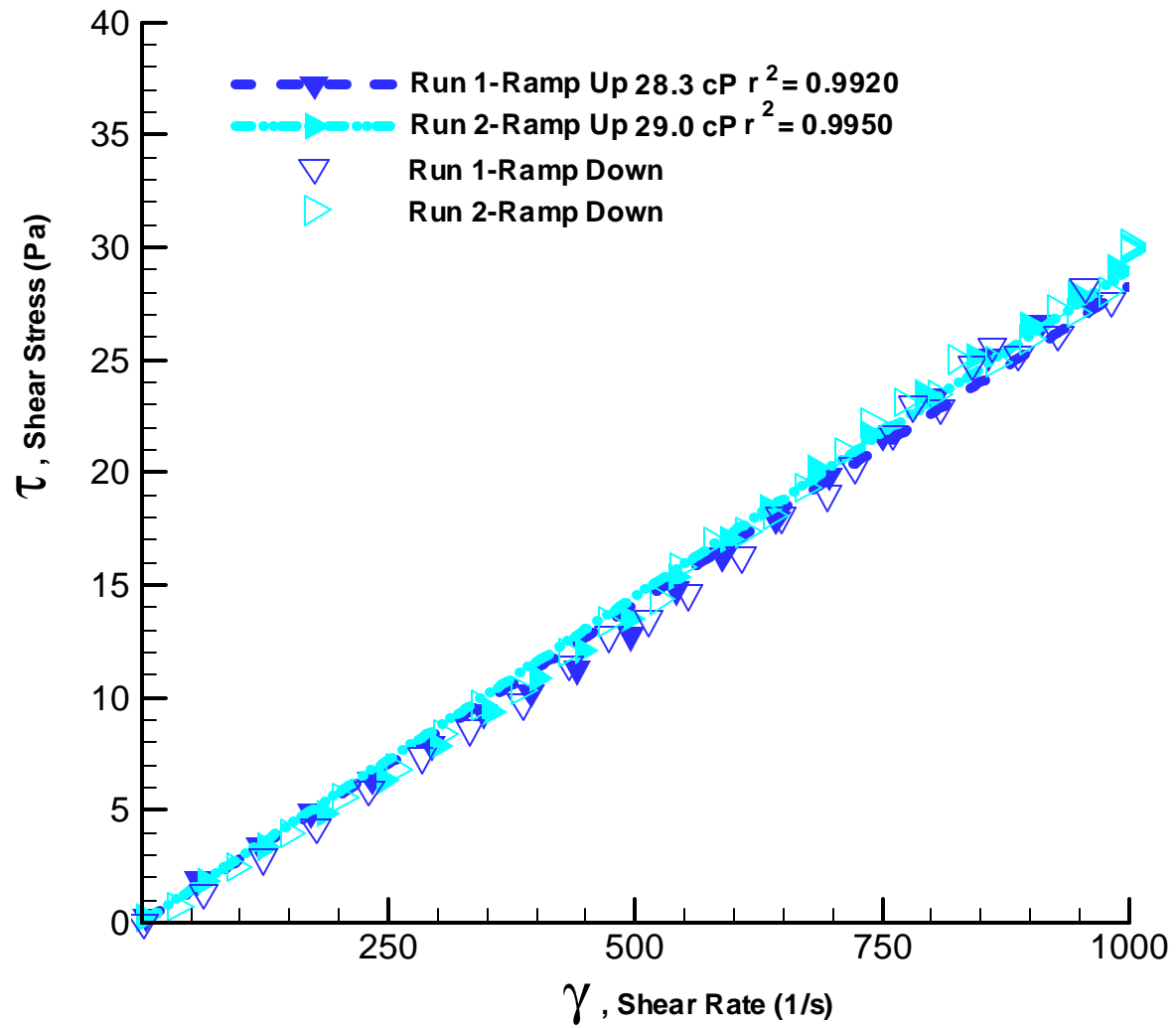


Figure 4.19. Flow Curve of 8 M Na AP-101 Melter Feed (one week mixing with Glass Formers Chemicals) at 40°C

4.5 Settled Solids Rheology

Following the mixing tests described in Section 4.4, the 8 M Na Melter Feed sample was left undisturbed for one week. After this time, the supernatant liquid was decanted and the shear strength of the settled solids layer was measured as described later in Section 5.0 of this report. After the shear strength measurement, the rheology of the settled solids fraction of the melter feed was then measured in the Haake RS-300 with the Z-41 sensor. Wall slip^c was observed during the shear rate ramp-up portion of these runs from 0 to 1000 s⁻¹. For this reason, the ramp-up phase of the rheogram was discarded and only the ramp down phase of the rheogram was used for a model fit. Figures 4.20 and 4.21 present the resulting rheograms at 25°C and 40°C, respectively.

The settled solids exhibit Bingham Plastic behavior at both 25°C and 40°C. Both the Bingham consistency and yield indices (see Equation 4.3) appear to decrease with increasing temperature. Significant scatter was observed between the data runs at each temperature. This scatter is most likely due to sub-sampling differences between each run. At high solids concentrations, the Bingham plastic parameters can be modeled as an asymptotic function of solids concentration (Dabak and Yucel 1987). This can result in small sub-sampling differences translating to large rheological differences. The highest measured Bingham Plastic parameters for these runs at each temperature are shown in Table 4.5. The highest value was selected because this is a conservative basis for process design engineering purposes.

Table 4.5. Bingham Plastic Parameters of AP-101 LAW 8 M Na Melter Feed Settled Solids One Week after Glass Former Chemical Addition

Temperature	Consistency Index (cP)	Yield Index (Pa)
25°C	207.3	26.4
40°C	167.7	7.6

^c Wall slip occurs when a thin layer of fluid forms between the suspension and the rheometer measuring surface. The measurement surface can then rotate with a lesser amount of torque resulting in measurement errors.

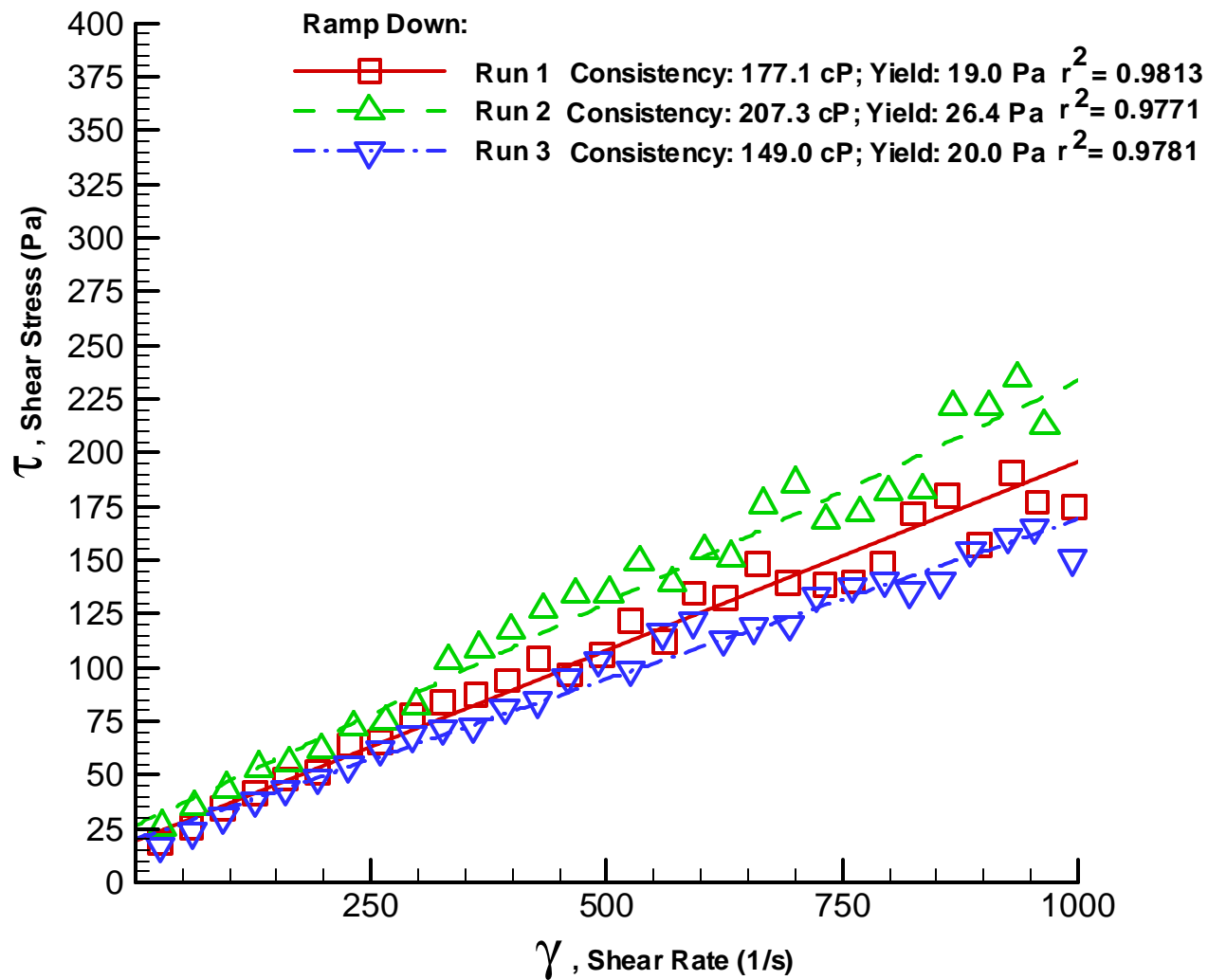


Figure 4.20. Flow Curve of 8 M Na AP-101 Melter Feed Settled Solids at 25°C

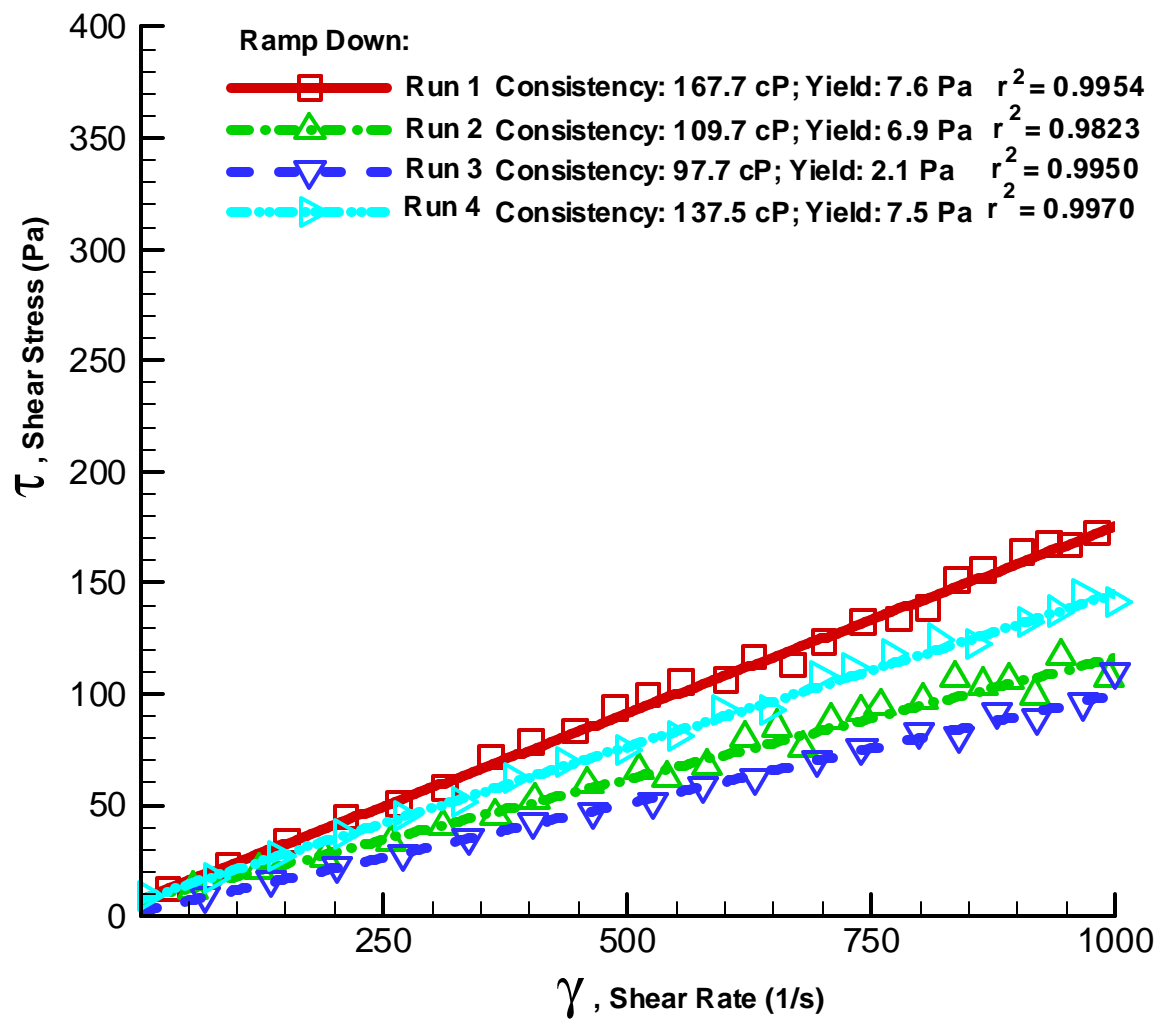


Figure 4.21. Flow Curve of 8 M Na AP-101 Melter Feed Settled Solids at 40°C

5.0 Shear Strength

According to *Guidelines for Performing Chemical, Physical, and Rheological Properties Measurements* (24590-WTP-GPG-RTD-001 Rev 0), the shear strength is defined as the minimum stress required to initiate fluid movement as determined by the vane method. Materials that possess a shear strength exhibit solid-like behavior at low stresses and fluid-like behavior at high stresses. During the solid-like behavior, the material behaves elastically, where a material will strain to a point at a given stress. When the stress is removed in the elastic regime, the material will return to its initial state. The shear strength is regarded as the transition between the elastic behavior and viscous flow.

Materials that exhibit shear strength are typically solid/liquid multiphase systems. In these systems, the solid particles are usually attracted to each other through electrostatic forces. This creates a network of attracted particles (e.g., a flocculated structure) that can impede viscous flow at low stresses. Viscous flow is achieved when the applied stress is high enough to break apart the structure. Examples of materials that exhibit shear strength include cements, soils, paints, pastes, and various food products (Liddell and Boger 1996).

Many techniques have been devised to measure shear strength. The most common technique involves extrapolating data from a conventional rheogram (i.e., shear stress/shear rate) to zero shear rate. The extrapolation can be made through the use of rheological models such as the Bingham, Herschel-Bulkley, or the Casson model. This technique requires accurate experimental data at low shear rates. Due to slip flow, inertial effects, etc, this is often difficult with conventional viscometers. Consequently, direct measurement of shear strength using a shear vane has been developed.

5.1 Measurement Equipment and Theory

Direct measurement of shear strength can be made by slowly rotating a vane immersed in the sample material and measuring the resulting torque as a function of time. The torque can be converted to a shear stress by making several assumptions (Liddell and Boger 1996). Firstly, the material is assumed to be sheared only along the cylinder defined by the dimensions of the vane. This assumption has been shown to be only a slight oversimplification. The actual diameter of the sheared surface may be up to 5% larger than the vane dimensions (Bowles 1977, Keentok 1982, Keentok et al. 1985). Secondly, it is assumed that the stress is distributed uniformly over the cylindrical sheared surface. Although the stress actually peaks sharply at the vane tips (Barnes and Carnali 1985, Keentok et al. 1985), it has been shown that the error due to this assumption is minimal (Alderman et al. 1991, Avramidis and Turain. 1991, James et al. 1987, Nguyen and Boger 1985a, Nguyen and Boger 1985b, Nguyen and Boger 1983). Therefore, a good approximation of the measured stress can be calculated from equation (5.1). Where K is the vane constant defined in equation (5.2).

$$\tau = T / K \quad (5.1)$$

$$K = \frac{\rho D^3}{2} \left(\frac{H}{D} + \frac{1}{3} \right) \quad (5.2)$$

Where, τ is the calculated shear strength (Pa).
 T is the measured torque (Nm).

K is the shear vane constant (m^3).
 D is the shear vane diameter (m).
 H is the shear vane height (m).

In addition, the shear vane must be immersed in the test material such that wall and end effects are negligible. Figure 5.1 shows an accepted material testing geometry to minimized wall and end effects (Dzuy and Boger 1985). These geometry requirements were confirmed prior to material testing.

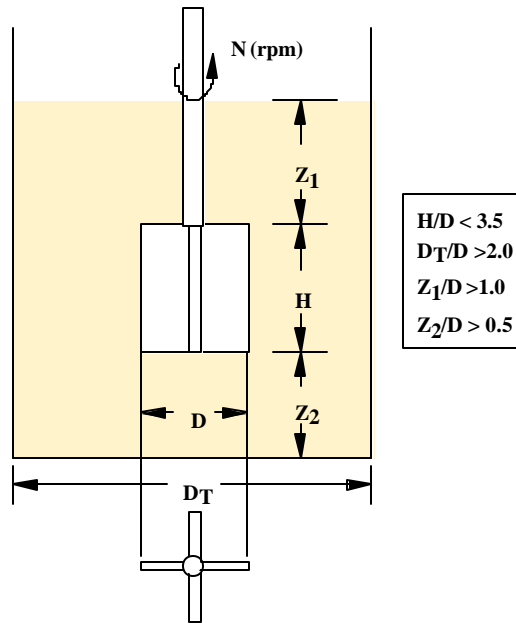


Figure 5.1. Geometrical Requirements of a Shear Vane

A typical stress-time profile is shown in Figure 5.2. The profile shows an initial linear region, followed by a non-linear region, a stress maximum, and a stress decay region. The shape of the stress time profile can be explained from a consideration of the network bonds within the material. The initial linear region represents the elastic deformation of the network bonds. The non-linear region represents visco-elastic flow (also called creep flow), where the network bonds are stretched beyond their elastic limit and some of the bonds begin to break. The linear and non-linear regions are separated by point τ_y . At the maximum stress, τ_s , the majority of the bonds are broken and the material begins to flow as a fully viscous fluid. The network typically collapses and stress decay is observed.

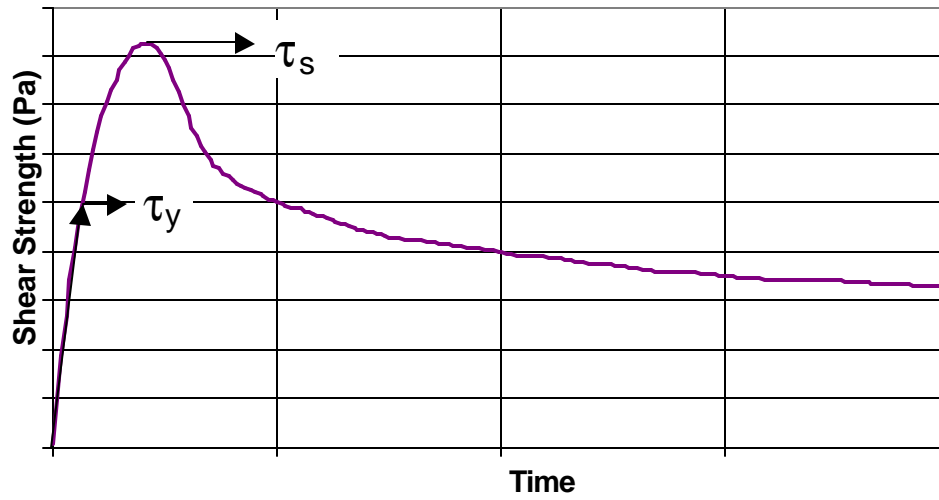


Figure 5.2. Typical Response of a Shear Vane

From this response, two shear strengths can be defined. One corresponding to the transition between elastics and visco-elastic flow, τ_y , and the other corresponding to the transition between visco-elastic and fully viscous flow, τ_s . Most researchers regard the transition between visco-elastic and fully viscous flow as the definitive shear strength of the material. In this report, shear strength will be defined by the transition between visco-elastic and fully viscous flow, τ_s .

5.2 System Validation and Calibration

Initially, a viscosity standard was measured with the cup/cylinder geometry on the Haake RS300 rheometer. While this does not implicitly test the vane geometry, it ensures that the torque detection system used by the viscometer is functioning and calibrated properly. The results of this test are shown in Figure 5.3. As expected, Newtonian behavior of the standard was observed with a measured viscosity of 97.1 cP at 25°C. This viscosity was measured over a shear rate range of 0 s⁻¹ to 1000 s⁻¹. This measured viscosity results in approximately 1% error from the documented viscosity of 98 cP at 25°C. This error is within the allowable 10% value specified in PNWD Test Instruction TI-RPP-WTP-168, “AP-101 Melter Feed Rheology Testing” and is typical of this particular viscometer model.

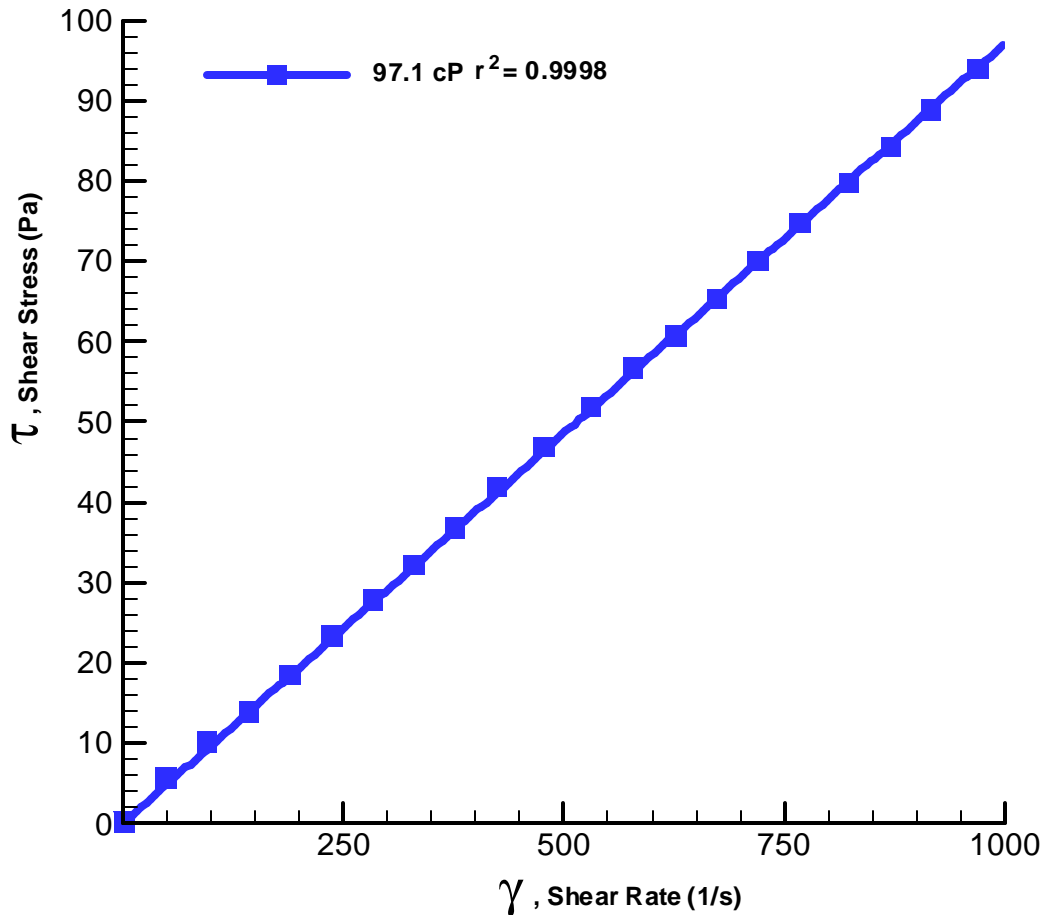


Figure 5.3. Viscometer Calibration Check With 98.0 cP Viscosity Standard at 25°C

5.3 Results from Shear Strength Measurements

With the calibration of the Haake RS300 rheometer established, shear strength measurements were taken on the settled solids from the 6 M Na and 8 M Na melter feed samples. The shear vanes were immersed in the settled solids according to the geometrical requirements outlined in Figure 5.1. Two shear vanes were used for this report, one with dimensions of D=1.6 cm H=1.6 cm; and the other having dimensions of D=1.6 cm H=0.8 cm. The rotational speed of the viscometer was set at a constant 0.3 RPM (0.0314 rad/s). The resulting shear stress/time curves are shown in Figure 5.4.

For the 6 M and 8 M Na melter feed samples, three data runs were obtained (see Table 5.1). The first set of data (Run 1) indicated that the shear strength of the 6 M Na sample was an order of magnitude greater than the 8 M Na sample. However, these samples were disturbed during the transfer into the glovebox with the RS300 rheometer, and the first set of measurements was discarded. In order to obtain data on undisturbed samples, a second set of data (Run 2 in Table 5.1) was acquired with care being taken not to disturb the samples when transferring the material. The results from this set of data indicate a significantly higher shear strength indicating that the samples remained undisturbed prior to testing.

Again, the 6 M Na sample possessed a shear strength an order of magnitude greater than the 8 M Na sample. Lastly, the samples were immediately mixed and measured for shear strength a third time (Run 3 in Table 5.1). The purpose of this set of tests was to validate the large increase in shear strength in the second set of data. Results from these tests show a shear strength comparable to the first set of data indicating that runs 1 and 3 represent recently settled (i.e. disturbed) solids, and run 2 data represents material valid for aged samples (undisturbed for 48 hours).

One possible explanation for the order of magnitude difference between the recently settled and aged samples could be ionic strength differences in the 6 M and 8 M Na samples resulting in particle surface charge differences. Changes in particle surface charge can then alter the attractive and repulsive dynamics of the slurry particles thus changing the overall network strength of the settled solids layer. Another more likely explanation is the effect of a higher precipitated solids concentration in the 8 M Na sample compared to the 6 M Na sample. These precipitated solids could disrupt the settled solids “network” resulting in a lower shear strength in the 8 M Na sample. A last possible explanation of this behavior involves the vane being immersed in varying levels of the “compression” zone of the settled solids layer. This zone consists of the large/dense fraction of material that settles quickly to the bottom of the vessel. Since the 6 M Na material contains a lesser percentage of undissolved solids compared to the 8 M Na sample, the “compression” zone of the 6 M Na sample should be less than the 8 M Na sample. This would lead to lower shear strength measurements on the 6 M Na sample. Since the opposite behavior is observed this last explanation has been discounted.

The 8 M Na melter feed sample was mixed for one week as part of the mixing/aging study prior to being analyzed for shear strength (see Figure 5.5 and Table 5.1). After one week of continuous mixing, the agitator was shutdown and the sample was allowed to settle in the mixing vessel for one week at ambient temperature. The supernatant was then removed and the remaining settled solids were transferred from the mixing vessel to a shear strength measurement vessel and placed in an oven at 40°C. The sample was left in the oven undisturbed for approximately 48 hours. After this time, the shear vane measurement was performed. The results of this test indicate a shear strength of 610 Pa.

Next, this same sample was remixed and left undisturbed at ambient temperature for five days. After this time, another shear vane measurement was performed. The results of this test indicate a shear strength of approximately 2600 Pa.

The large difference between the two shear strength measurements (at ambient temperature and at 40°C) indicates that the shear strength of the sample is significantly sensitive to temperature. To verify the results of the 25°C analysis, the technician remixed the solids and immediately inserted the shear vane into the sample and repeated the shear strength measurement at ambient temperature. This sample was not allowed to remain undisturbed prior to the measurement. The results of this test indicated a relatively high shear strength of approximately 1100 Pa confirming the high temperature sensitivity.

All three of these shear strength values for the mixed/aged 8 M Na sample are significantly higher than the 79 Pa value on the sample that was not part of the mixing/aging study. The lower shear strength sample was only mixed for one hour. This indicates that the shear strength of the 8M Na melter feed material significantly increases due to mixing and/or aging. One possible explanation for this increase in shear strength due to mixing and aging is particle attrition during long term mixing. Particle attrition will shift the particle size to smaller particles with a higher surface area. The increased surface area increases the network bond strength resulting in higher shear strength values. Another possible explanation is chemical changes during aging. As the slurry ages, species may be absorbed on the surface of the particles changing the network bond strength and resulting shear strength over time. As well, it is possible for aging to result in changes to the crystalline structure of the waste solids and/or glass former chemicals also impacting shear strength.

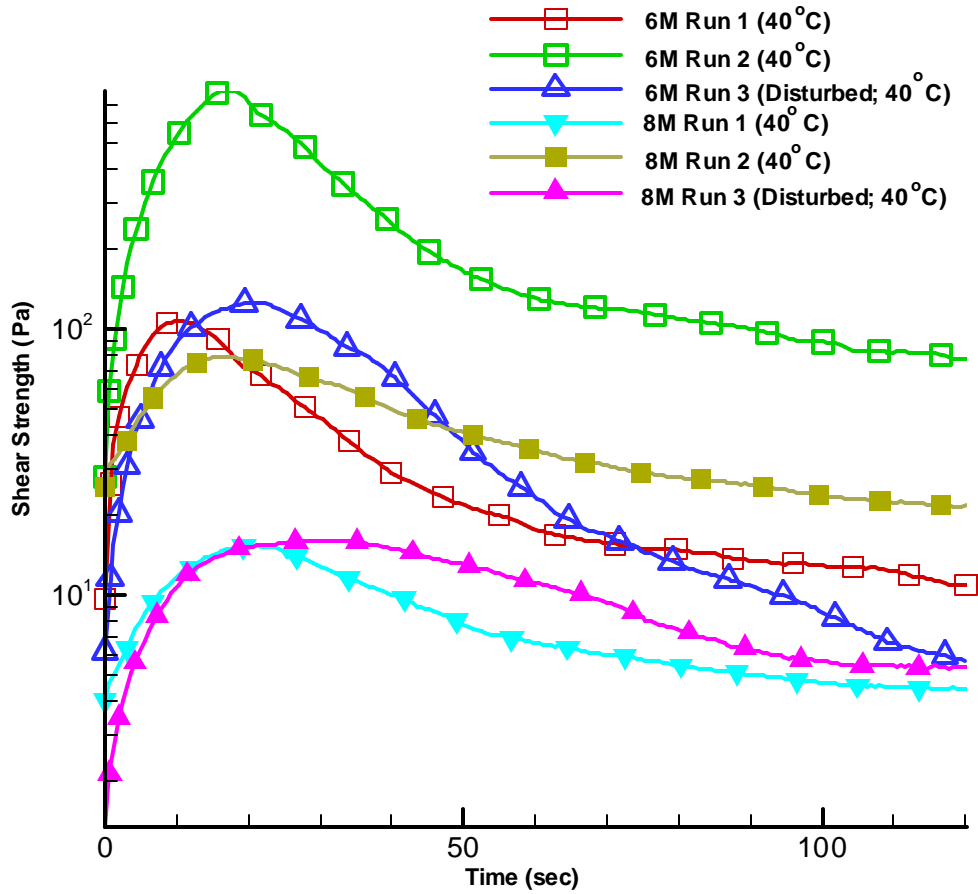


Figure 5.4. Shear Strength Response of 6 M and 8 M Na AP-101 Melter Feed Settled Solids

Table 5.1. Summary of Shear Strength Data

Sample	Temp.	Shear Strength (Pa)		
		Run 1	Run 2	Run 3
6 M Na	40°C	110	790	130
8 M Na	40°C	15	79	16
8 M Na (mixed 1 week)	40°C	610	n/a	n/a
	Ambient (~23°C)	2600	1100	n/a
Shaded Data Rejected Due to Disturbed Sample				
n/a – not applicable				

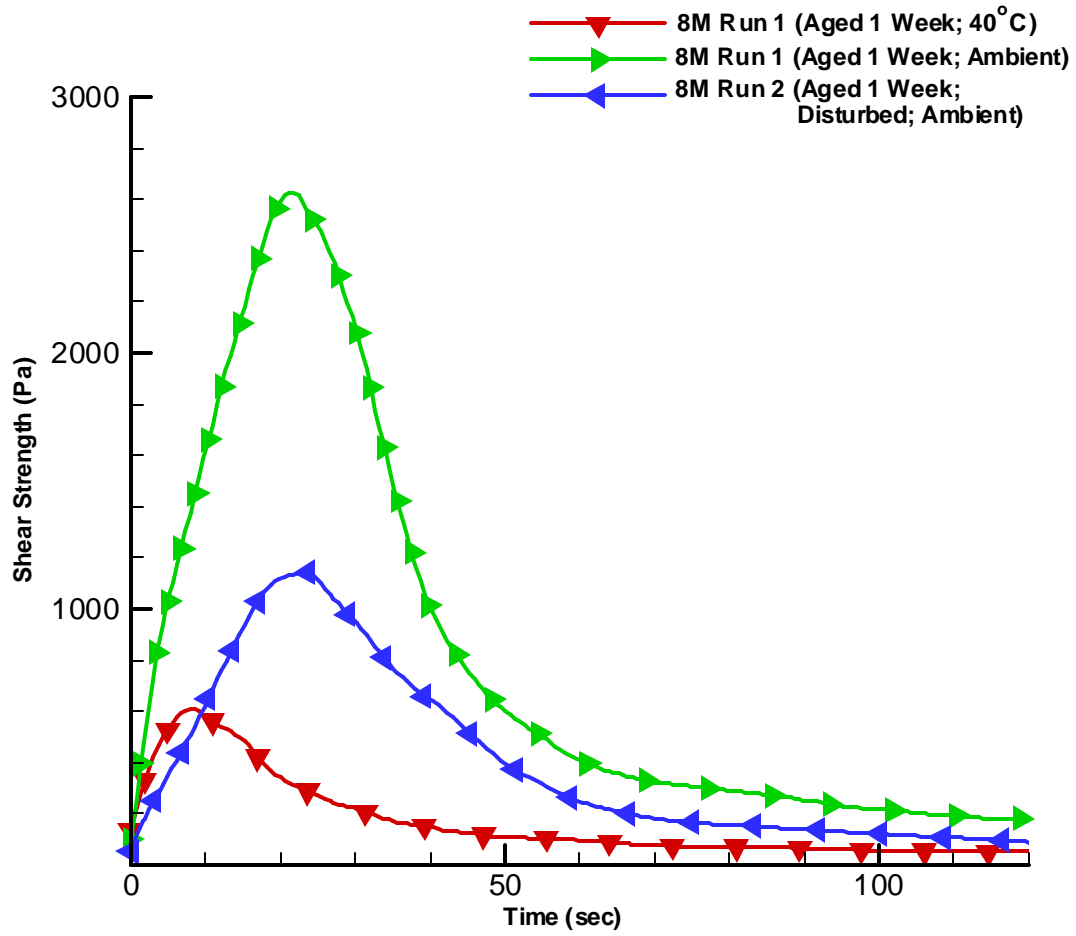


Figure 5.5. Shear Strength Response of 1-Week Aged 8 M Na AP-101 Melter Feed Settled Solids

6.0 Particle Size Distribution

The particle size distributions of 6 M Na melter feed sample that was mixed for 30 minutes after glass former chemicals addition and aged for 5 days is described in this section. A Microtrac X-100 particle size analyzer and a Microtrac ultrafine particle size analyzer (UPA) were both used to measure the particle size distribution of this sample.

6.1 Instrument Description

The Microtrac X-100 Particle Analyzer measures particle diameter by scattered light from a laser beam projected through a stream of the sample particles diluted in a suspending medium. The amount and direction of light scattered by the particles is measured by an optical detector array and then analyzed to determine the size distribution of the particles. This measurement is limited to particles with diameters between 0.12 and 704 μm . The other instrument used, the Microtrac UPA, measures particle diameter by Doppler shifted scattered light. This method is limited to particles with diameters between 0.003 nm and 6.5 μm .

6.2 Particle Size Distribution Data Reporting Details

The particle size results are saved in the form of a histogram with varying bin sizes. The upper range of each bin is determined by a geometric sequence (see Equation 6.1):

$$\hat{d}_{i+1} = \frac{\hat{d}_i}{\sqrt[4]{2}} \quad (6.1)$$

Where,

$$\hat{d}_1 = 704.0 \text{ mm for the X100}$$

$$\forall i = 1 \dots 50 \text{ for the X100}$$

$$\hat{d}_1 = 6.541 \text{ mm for the UPA}$$

$$\forall i = 1 \dots 44 \text{ for the UPA}$$

The lower range for each bin is determined as follows (see Equation 6.2):

$$\check{d}_i = \hat{d}_{i+1} \quad (6.2)$$

Where,

$$\check{d}_{50} = \frac{\hat{d}_{50}}{\sqrt[4]{2}} = 0.122 \text{ mm for the X100}$$

$$\check{d}_{44} = \frac{\hat{d}_{44}}{\sqrt[4]{2}} = 0.0032 \text{ mm for the UPA}$$

The bin centered values for this bin set is determined by Equation 6.3:

$$\bar{d}_i = \frac{\hat{d}_i + \check{d}_i}{2} \quad (6.3)$$

The particle size distribution stored by the Microtrac instruments represents the volume percent of particles attributed to a particular bin. This is usually called the “differential” volume distribution. For example, a value of 5 in the first bin of a volume distribution for the X100 indicates that 5% of the volume of the particles measured by the instrument are between $\widehat{d}_1 = 704.0 \text{ mm}$ and $\widetilde{d}_1 = 592.0 \text{ mm}$. The bin centered value, $\bar{d}_1 = 648.0 \text{ mm}$, would be used to display this data point on a graph. The volume distribution data will be denoted as, V_i . These data can be represented as a “cumulative” distribution through Equation 6.4 shown below. If the differential distribution is properly normalized to 100%, the range of the cumulative distribution will be between 0% and 100%. When displayed on a graph, the cumulative distribution uses the upper range of the bins such that a data point is represented by (\widehat{d}_i, V_i^C) . The resulting graph should be interpreted as V_i^C percent of volume of the sample has particles smaller than \widehat{d}_i .

$$V_{i+1}^C = 100\% - \sum_{j=1}^i V_j \quad (6.4)$$

$$V_1^C = 100\%$$

If one assumes that the particles are spherical with an equivalent diameter of \bar{d}_i , the differential distribution can be transformed from a volume basis to a number basis. The number basis represents the percent number or percent of the population of particles in a certain size range. For example, a value of 5 in the first bin of a number distribution for the X100 indicates that 5% of the population of the particles measured by instrument are between $\widehat{d}_1 = 704.0 \text{ mm}$ and $\widetilde{d}_1 = 592.0 \text{ mm}$. The bin centered value, $\bar{d}_1 = 648.0 \text{ mm}$, would be used to display this data point on a graph. The percent number distribution, N_i , can be calculated through Equation 6.5:

$$n_i = \left(\frac{6 \cdot V_i}{\rho \bar{d}_i^3} \right) \quad (6.5)$$

$$N_i = 100\% \times \frac{n_i}{\sum_i n_i}$$

These data can be represented as a “cumulative” distribution through Equation 6.6 shown below. If the differential distribution is properly normalized to 100%, the range of the cumulative distribution will be between 0% and 100%. When displayed on a graph the cumulative distribution uses the upper range of the bins such that a data point is represented by (\widehat{d}_i, N_i^C) . The resulting graph should be interpreted as N_i^C percent of the population of particles in the sample is smaller than \widehat{d}_i .

$$N_{i+1}^C = 100\% - \sum_{j=1}^i N_j \quad (6.6)$$

$$N_1^C = 100\%$$

When comparing the volume and number distributions, note that the volume distribution is weighted cubically towards larger particles. For example, 1–10 μm particle has the same volume as 1,000–1 μm particles.

Lastly, the data can be displayed on a surface area basis. If one assumes that the particles are spherical, the surface area of the resulting sphere and the number distribution can be used to calculate the area distribution. As an example, a value of 5 in the first bin of an area distribution for the X100 indicates that 5% of the surface area of the particles in the slurry are between $\bar{d}_1 = 704.0 \mu\text{m}$ and $\bar{d}_1 = 592.0 \mu\text{m}$. The bin centered value, $\bar{d}_1 = 648.0 \mu\text{m}$, would be used to display this data point on a graph. The percent area distribution, A_i , can be calculated through Equation 6.7:

$$a_i = \rho \bar{d}_i^2 N_i$$

$$A_i = 100\% \times \frac{a_i}{\sum_i a_i} \quad (6.7)$$

When comparing the area and number distributions, note that the area distribution is weighted to the second power towards larger particles. For example, 1–10 μm particle has the same surface area as 100–1 μm particles.

These area data can be represented as a “cumulative” distribution through Equation 6.8 shown below. If the differential distribution is properly normalized to 100%, the range of the cumulative distribution will be between 0% and 100%. When displayed on a graph, the cumulative distribution uses the upper range of the bins such that a data point is represented by (\bar{d}_i, A_i^C) . The resulting graph should be interpreted as A_i^C percent of the surface area of particles in the sample is smaller than \bar{d}_i .

$$A_{i+1}^C = 100\% - \sum_{j=1}^i A_j$$

$$A_1^C = 100\% \quad (6.8)$$

The mean value for the differential form of these distributions can be calculated by Equations 6.9 shown below. This value represents the centroid of the distribution.

$$d_V = \frac{\sum_i V_i \bar{d}_i}{\sum_i V_i}$$

$$d_N = \frac{\sum_i N_i \bar{d}_i}{\sum_i N_i} \quad (6.9)$$

$$d_A = \frac{\sum_i A_i \bar{d}_i}{\sum_i A_i}$$

The median value of the cumulative form of these distributions is shown by Equation 6.10. This value represents the diameter where 50% of the particles have a smaller volume, population, or surface area; and 50% of the particles have a larger volume, population, or surface area. Since this diameter rarely falls directly on the 50% value, the lever rule is used to calculate this point.

$$\begin{aligned}
 D_V &= V_i^C \Big|_{50\%} \\
 D_N &= N_i^C \Big|_{50\%} \\
 D_A &= A_i^C \Big|_{50\%}
 \end{aligned}
 \tag{6.10}$$

6.3 Calibration Checks

Both instruments performances were checked against a range of NIST traceable standards from Duke Scientific Corporation. These standards are polystyrene microspheres dispersed in a 1 mM KCl solution. These standards were run prior to analysis of the sample. Results from these standard tests are presented in Table 6.1. The mean diameter of the number distribution represents the centroid of the distribution. To check the functionality of the instrument, a close fit of the number basis mean data is typically required (approximately 10%). Due to deterioration of the particle size instrument, a 10% difference between the number basis mean results and NIST traceable values of the Duke Scientific particle size standards could not be reached. However, the number basis mean results were within approximately 15% of the NIST traceable values.

Table 6.1. Particle Size Analyzer Calibration Data

NIST Traceable Particle Size Standard		Measured Mean Diameter on a Number Basis (mm)
X-100	0.895 μm Duke Scientific Standard (Lot #15924)	0.776
	2.0 μm Duke Scientific Standard (Lot# 15992)	1.696
	50.4 μm Duke Scientific Standard (Lot# 19213)	42.14
UPA	0.096 μm Duke Scientific Standard (Lot #15976)	0.0976
	0.895 μm Duke Scientific Standard Lot #15924)	0.9391
	2.0 μm Duke Scientific Standard (Lot #15992)	2.218

6.4 Operating Conditions

The particle size distribution (PSD) of the 6 M Na melter feed sample was measured in the Microtrac X-100 at a flow rate of 60 mL/s. The samples were then sonicated with two intervals of 40W ultrasonic waves for 30 sec while flowing at a rate of 60 mL/sec. The PSD after sonication was then measured. The ultrasonic energy input is used to determine the shear sensitivity of the slurry in order to investigate whether flocculation/deagglomeration is occurring. Analyses were performed in triplicate on each sample under all flow/sonication conditions. The averages of these triplicate measurements are provided in Section 6.5. No sonication or flow options are available for the UPA. Therefore, the sample is placed in the instrument, and the measurements are performed on the as-received, stationary material.

6.5 Suspending Medium

The suspending medium for the AP-101 analyses was an AP-101 simulant tank supernatant discussed in WTP-RPT-057, Rev. A (Russell et al., 2002). The simulant was fabricated at 4.9 M Na and evaporated to a concentration of 6 M Na. In order to mimic the composition of the melter feed supernate, boric acid (the only glass former chemical that has a significant solubility) was added to the simulant in a quantity consistent with Table 2.1. White solids were observed to precipitate after the addition of the boric acid. The filtered simulant was then used as a suspending medium in the particle size instrument. Some tests were also performed using deionized water as a suspending medium.

Based on suspending medium and flow rate through the particle size analyzer, a wide range of shear conditions occur. Since these suspending mediums are Newtonian, the shear rate profile in the particle size analyzer tubing is linear with a shear rate value of zero at the pipe centerline. The approximate shear rate at the pipe wall and at the position where average pipe velocity occurs is shown in Table 6.2. Due to the presence of low shear conditions in the center of the pipe, flocculation and agglomeration of particles is possible when the sample is not sonicated.

Table 6.2. Approximate Unsonicated Shear Conditions of Microtrac X100 for Various Suspending Mediums and Flowrates

Suspending Medium	Pipe Diameter (mm)	Suspending Medium Density (g/mL)	Suspending Medium Viscosity (cP)	Flow Rate (mL/sec)	Reynolds Number	Shear Rate at centerline (s ⁻¹)	Average Shear Rate (s ⁻¹)	Shear Rate at Wall (s ⁻¹)
Deionized Water	6.3	1.0	1.0	40	8,100	0	5,200	6,900
Deionized Water	6.3	1.0	1.0	60	12,000	0	11,000	14,000
6 <u>M</u> Na AP-101 Simulant	6.3	1.3*	5.2*	40	2,000	0	1,200	1,600
6 <u>M</u> Na AP-101 Simulant	6.3	1.3*	5.2*	60	3,000	0	3,700	4,900

* Used properties for 6 M AP-101 pretreated LAW (see Tables 3.1 & 4.1)

6.6 Results

The particle size distributions on a volume basis are shown in Figures 6.1 and 6.2. The 6 M Na melter feed appears to consist of particles in the 1 to 30 μm range. As the shear of the sample increases due to sonication, slight changes to the PSD are observed. Particles in the 6 to 20 μm range appear to deagglomerate and the volume of particles in the 1 to 6 μm range slightly increases.

The summary data in Table 6.3 are provided by the Microtrac software which resolves the particle size distribution into multiple Gaussian distribution fits. This algorithm indicates that the 6 M Na melter feed samples in AP-101 simulant contain two distributions of particles, one peak at approximately 5 μm and the other at 15 μm . The volume contribution of the 5 μm peak increases after sonication indicating deagglomeration. The resulting mean particle size on a volume basis for the sonicated 6 M Na melter feed sample in simulant is 9.2 μm . Approximately 10 vol% of the particles are below 2.6 μm , 50 vol% (i.e., median value) below 7.6 μm , 90 vol% below 18.2 μm , and 95 vol% below 20.2 μm . The 6 M Na melter feed samples in deionized water also contain two peaks, one at 5 μm and the other at 20 μm . The increase in particle size for the second peak from 15 to 20 μm can be attributed to solubility differences between the two suspending mediums. The glass former chemicals in deionized water also exhibit bimodal particle size distributions with one peak at approximately 1 μm particle size and the other at 23 μm with particles as large as 40 μm present. This change in distribution can be explained by dissolution of the larger glass former chemicals in the AP-101 pretreated waste. Precipitation of solids may also occur due to the addition of the glass former chemicals. This precipitation would be consistent with the formation of white solids when boric acid was added to the AP-101 simulant (see Section 6.4).

The X100 instrument indicated a “high background” flag when using the AP-101 simulant as the suspending medium. For this reason, deionized water was used as a suspending medium on a second set of data. This data set did not have a “high background” flag. This set of data produced a distribution similar to data generated with the AP-101 simulant suspending medium. This appears to corroborate the first set of data. Changes in the particle size distribution are expected due to solubility and flocculation differences when using deionized water as a suspending medium. Some limited flocculation was observed in the deionized water runs as particles in the 3 to 15 μm range appear to deagglomerate into particles in the 0.3 to 3 μm range after sonication.

Lastly, a set of particle size analysis runs were performed on the dry glass former chemicals used in this melter feed formulation (LAWA-126) suspended in deionized water. This sample shows a significant increase in larger particles compared to the 6 M Na melter feed sample. This can be explained by dissolution of the glass former chemicals. Alternatively, if the precipitates from the LAW pretreated waste are smaller than the glass former chemicals, then this could also explain the observed shift in the distribution to smaller particles. The particle size distribution of the precipitates in the LAW pretreated waste was not measured. Only a small change in particle size distribution was observed after the sonication of the glass former chemical material. The particle size distribution exhibits two major peaks, one at approximately 1 μm and the other at approximately 23 μm . The resulting mean particle size on a volume basis is 19.9 μm . Approximately 10 vol% of the particles are below 1.1 μm , 50 vol% (i.e., median value) below 17.2 μm , 90 vol% below 43.8 μm , and 95 vol% below 50.8 μm .

Table 6.3. Summary of Volume Particle Size Distribution Data (Provided by Microtrac Software)

Description	Peak 1 (mm)				Peak 2 (mm)			
	Low (16%)	Peak (50%)	High (84%)	Contribution	Low (16%)	Peak (50%)	High (84%)	Contribution
6 <u>M</u> AP-101 Melter Feed in Simulant	2.8	5.3	7.8	53%	10.8	15.0	19.2	47%
6 <u>M</u> AP-101 Melter Feed in Simulant after Sonication	2.4	4.8	7.3	58%	10.8	15.0	19.2	42%
6 <u>M</u> AP-101 Melter Feed in DIW	2.4	5.5	8.7	56%	13.3	20.8	28.4	44%
6 <u>M</u> AP-101 Melter Feed in DIW after Sonication	1.0	4.1	7.1	58%	14.6	21.5	28.4	42%
LAWA-126 Glass Former Mix in DIW	0.6	1.2	1.8	18%	5.3	22.7	40.0	82%
LAWA-126 Glass Former Mix in DIW After Sonication	0.4	1.0	1.6	19%	5.6	22.5	39.4	81%

Surface area and number basis distributions are shown in Figures 6.3 to 6.6. These distributions are weighted heavily towards smaller particles and indicate that most of the particles in these samples are between 0.1 and 10 μm in diameter. UPA data indicates that no particles smaller than 0.1 μm were measured in the material. Consequently, the X100 data represents the complete particle size distribution for the 6 M Na melter feed sample.

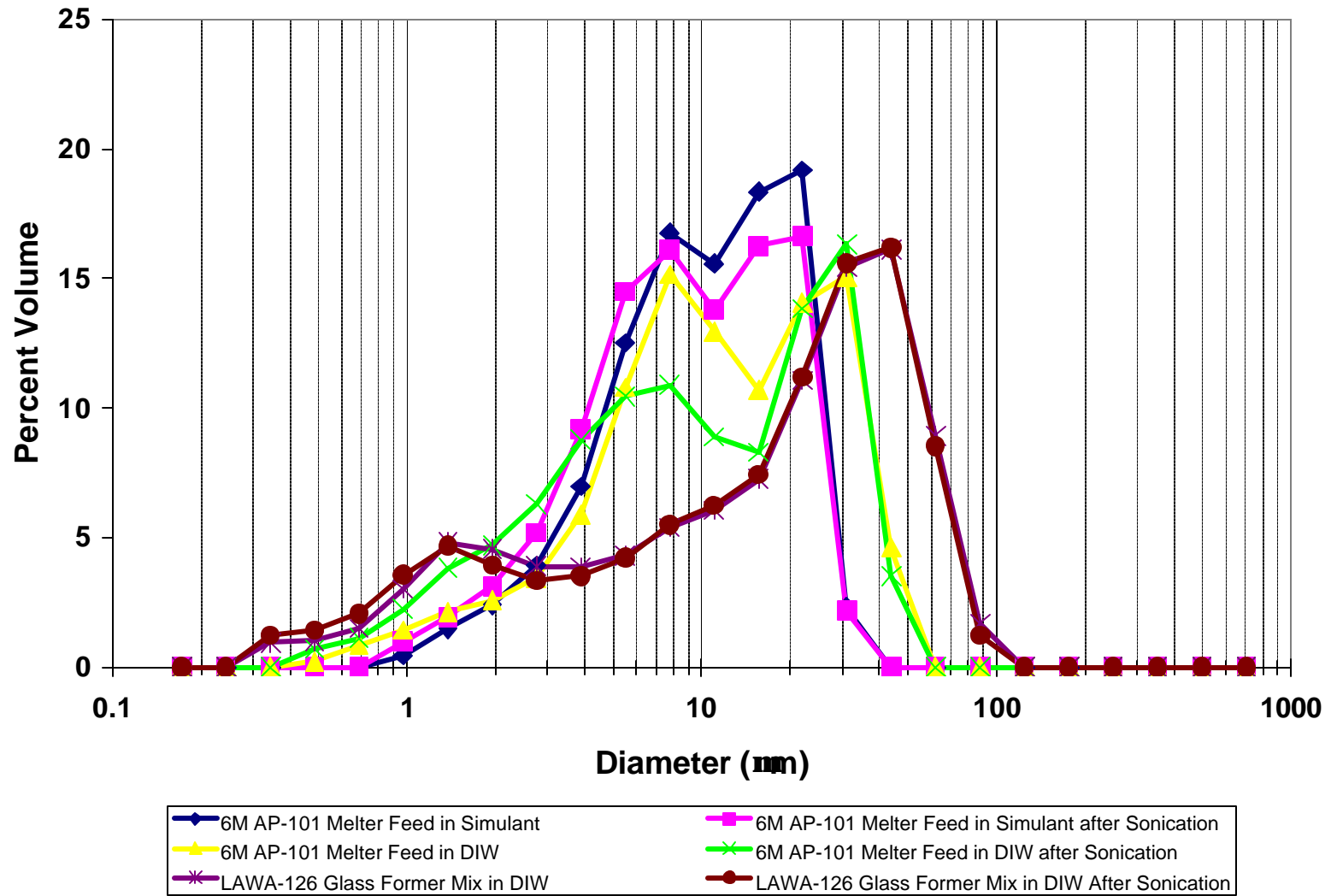


Figure 6.1. Particle Size Distribution on a Volume Basis

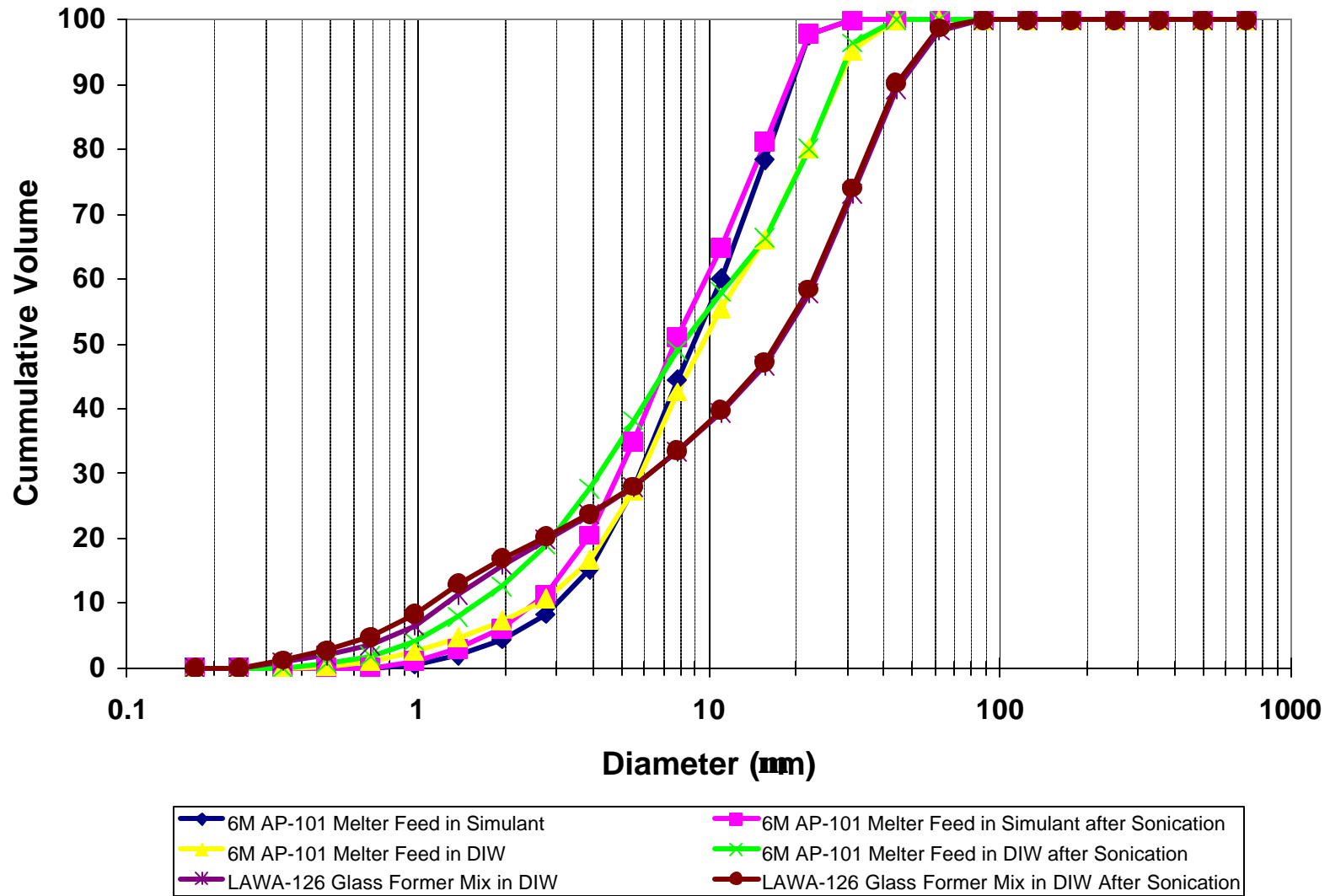


Figure 6.2. Cumulative Particle Size Distribution on a Volume Basis

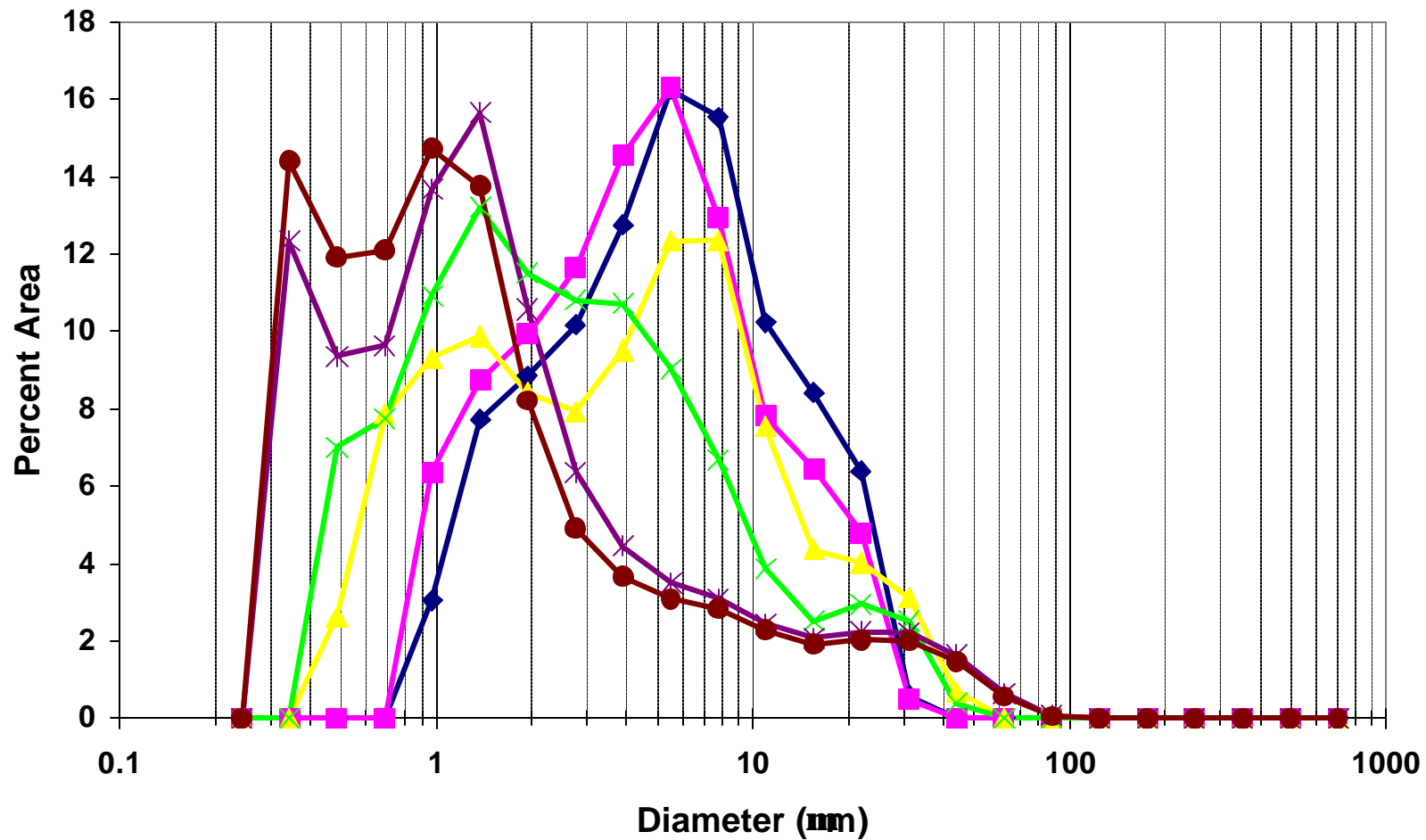


Figure 6.3. Particle Size Distribution on an Area Basis

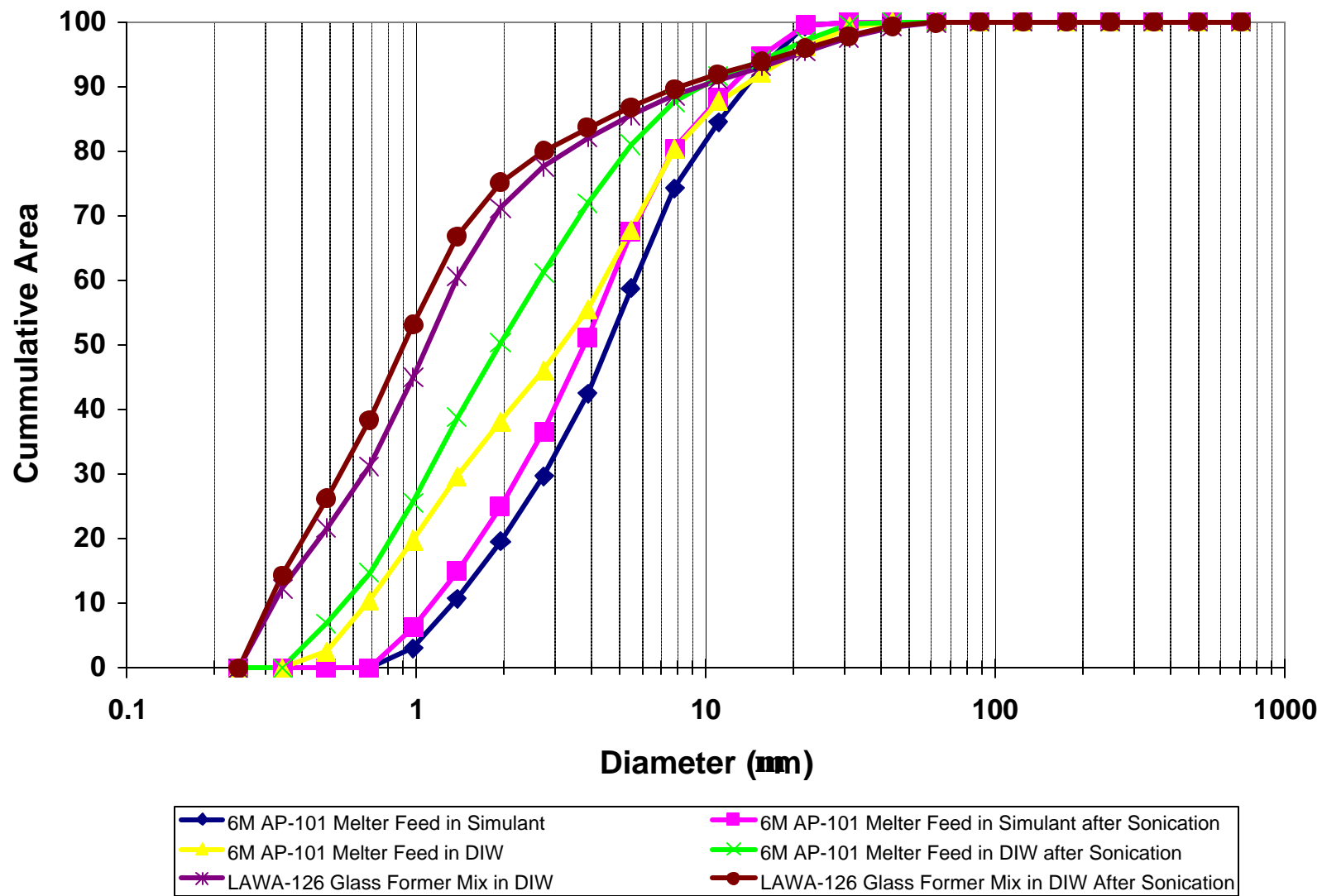


Figure 6.4. Cumulative Particle Size Distribution on an Area Basis

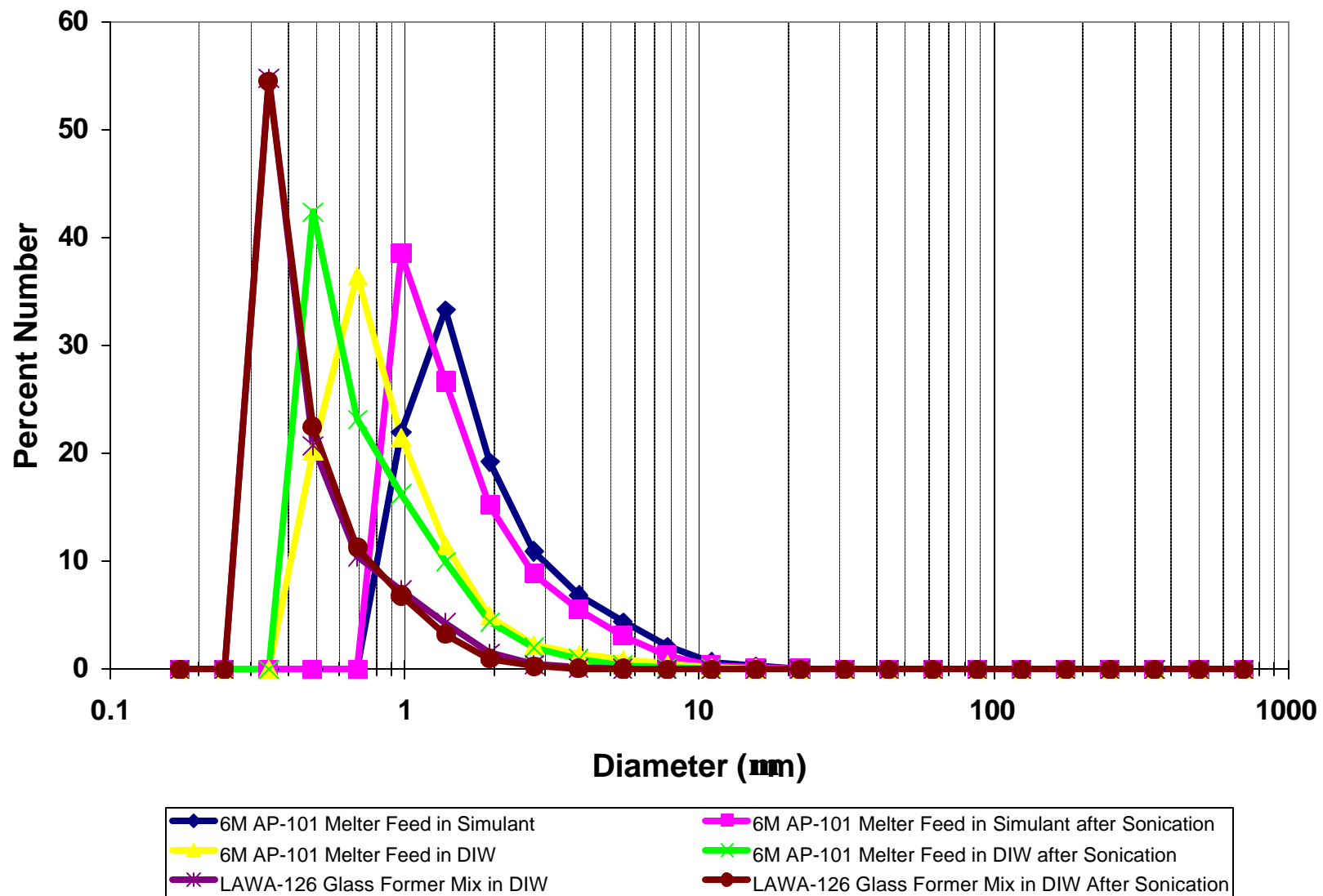


Figure 6.5. Particle Size Distribution on a Number Basis

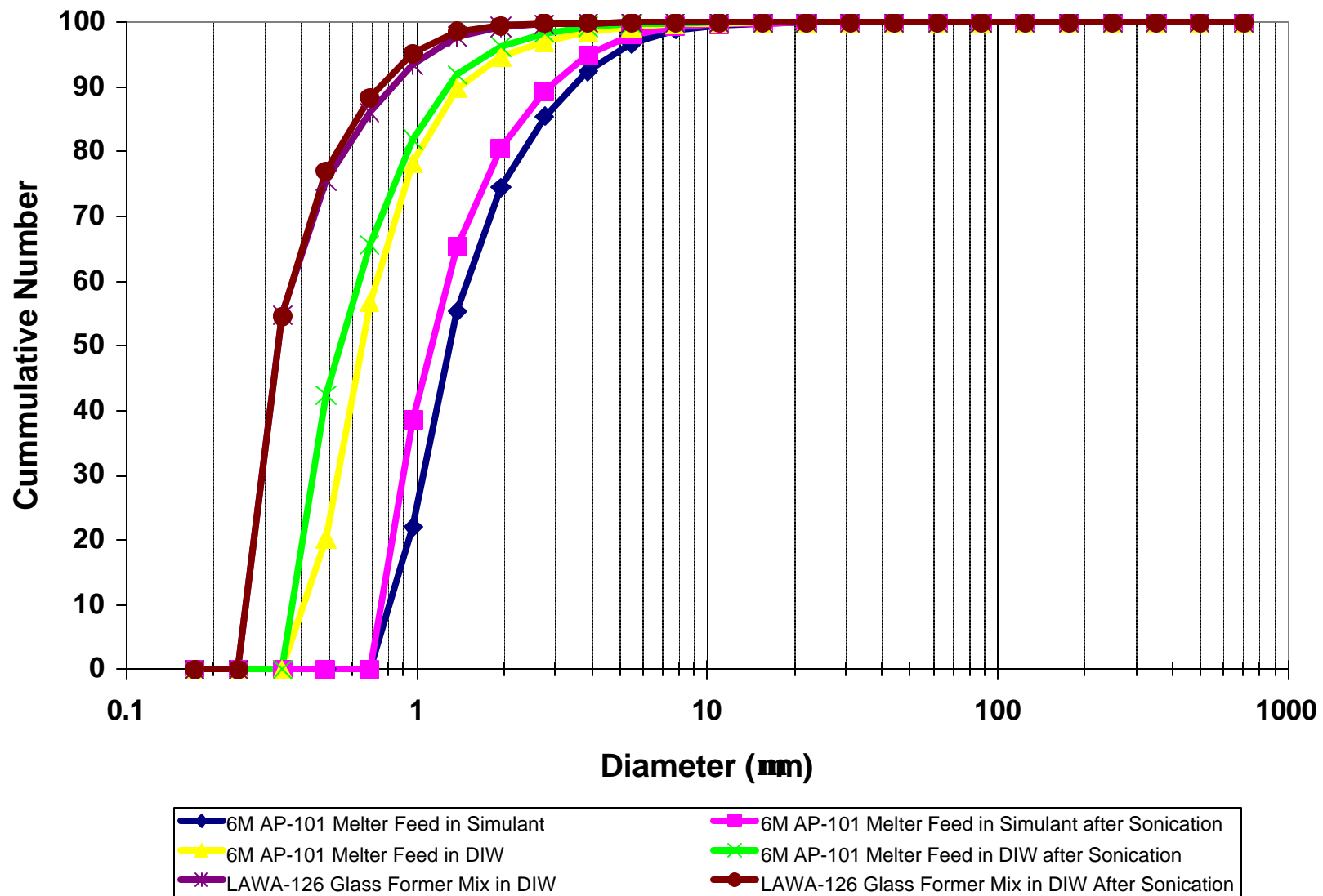


Figure 6.6. Cumulative Particle Size Distribution on a Number Basis

7.0 Identification of Solids

7.1 Introduction

This section details the characterization of the solid phase which precipitated during the evaporation of the AP-101 pretreated feed from 4.9 M Na to 6, 8, and 10 M Na. Phase characterization was accomplished with Scanning Electron Microscopy (SEM), Polarized Light Microscopy (PLM), Infrared Spectroscopy (IR), Raman, X-Ray Diffraction (XRD), and Nuclear Magnetic Resonance (NMR) data from the samples and comparing the known phase reported in the literature as well as to standards analyzed at the time of this investigation.

The SEM tends to examine much smaller size samples than the XRD due to sample handling issues. SEM images are created by rastering a focused electron probe across a sample while simultaneously measuring various secondary- and backscattered-electron signals as a function of beam position. Elastic and inelastic scattering spread the incident electron beam within the sample yielding an interaction volume, the dimensions of which depend on the electron beam energy and the sample composition (i.e., atomic number), rather than the focused probe size. As the energy of the beam increases, the interaction volume also increases. When electrons of adequate energy hit the sample, characteristic x-rays indicative of elemental composition (i.e., atomic number) are produced at intensities proportional to the mass concentration of the given element within the interaction volume.

When monochromatic infrared radiation is passed through a transparent substance, most of the scattered radiation will be of the same incident radiation, called Rayleigh scattering; however, at certain discrete frequencies above and below the incident energy, light will be scattered. This is termed Raman scattering. The shift in frequency of the scattered light is characteristic of the chemical structure of the species under examination. The total area analyzed with Raman was comparable to the area of sample examined with XRD. IR was one of the most representative techniques, as the entire sample bottle was examined non-destructively. Not enough material was available to use NMR on the solids.

7.2 Experimental

7.2.1 Microstructural Analysis of Sub-Samples

The SEM investigations were performed with a JEOL840 equipped with a backscattered detector and ISIS x-ray energy dispersive spectrometer (EDS; Oxford Instruments, X-Ray Technology, Santa Cruz CA) system in the 326 Building. Raman and infrared analyses were performed with a spectrometer in the 325 Building. The X-ray diffraction scans were run on a Scintag diffractometer. In the first part of the study, samples were examined in their 'as-received' state. The samples were then washed to remove the more soluble phases and re-examined with the various micro-analytical techniques.

7.2.1.1 Electron Microscopy

Most SEM images were obtained in backscattered imaging mode with a 20 keV electron beam. This technique is useful for finding different phases and obtaining EDS data over a wide energy range. At times the energy of the beam was reduced and the secondary electrons (SE) were used to form an image that yielded more information about the particle morphology. A carbon coat had to be applied to all samples owing to the type of SEM (JEOL 840, JEOL USA Inc., Boston MA) used in this investigation.

The calibration of the SEM magnification scale was checked with two National Institutes for Standards and Technology (NIST) traceable standards (NIST-4202A and NIST-4250A). Particles from NIST-4202A containing 2.013 ± 0.025 μm polymeric spheres and NIST-4250A containing 50.4 ± 1.0 μm polymeric spheres, were placed on an SEM stub, carbon coated and examined in the SEM. In both cases, the SEM magnification was $<10\%$. This is an acceptable tolerance.

7.2.1.2 X-ray Energy Dispersive Spectroscopy

The EDS system calibration was checked with a known compound (ZrO_2). The agreement between literature and experimental values was excellent, demonstrating that the system was calibrated correctly for analyzing characteristic x-rays at both low and high energies. The error in the peak energy assignments was estimated to be $<1\%$. The carbon conductive coat on the samples also contributed a background signal in all EDS analyses. The SEM instrument was also subject to fluorescence interference from brass components in the column on occasions. Small peaks from Cu-K and Zn-K x-rays were sometimes observed.

7.2.1.3 Infrared and Raman Spectroscopy

Infrared spectroscopy was performed on a Nicolet spectrometer (ThermoNicolet, Madison WI). This instrument is designed with an extended optical cable for remote viewing of samples. For these spectra 0.1 mg of solid was added to 5 mg of KBr. The mixtures were pulverized with an agate motor and pestle. The thin disks were produced using a pellet press.

7.2.1.4 X-ray Diffraction

The X-ray diffraction scans were run on a Scintag (ThermoARL, Germany) instrument from 5° to 65° with a 0.05° step size. The XRD samples were deposited on a silicon crystal wafer that has a much lower background contribution than glass slides.

7.3 Characterization Results of AP-101 Precipitated Solids

7.3.1 Scanning Electron Microscopy of the Solids

In backscattered imaging mode with a 20 keV electron beam, two distinct phases were observed in all three samples. Compositional analysis with EDS revealed that the brighter material (higher average atomic number) contained potassium; whereas, the darker regions (lower average atomic number) were rich in sodium. Both regions contained oxygen. There was a hint of a small nitrogen peak in the sodium region; however, the EDS detector used was inefficient at detecting any lines below about 1 keV, including carbon and nitrogen. Carbon was observed in all analyses but this is due to the carbon coat used to make the sample conductive. At times the energy of the beam was reduced and the secondary electrons were used to form an image that yielded more information about the particle morphology.

7.3.1.1 AP-101-A (6 M Na) and AP-101-B (8 M Na)

Typical micrographs from samples AP-101-A (6 M Na) and AP-101-B (8 M Na) are shown in Figure 7.1. The material contained two distinct regions; although these two regions were intermingled. The white material was rich in potassium and the gray material was rich in sodium. No heavier elements were observed at significant levels; however, a silicon-bearing phase was observed in sample AP-101-B (8 M Na; see Figure 7.4). Although the sodium material was consistent with being sodium nitrate, it was not possible to prove the occurrence of this phase with just the SEM.

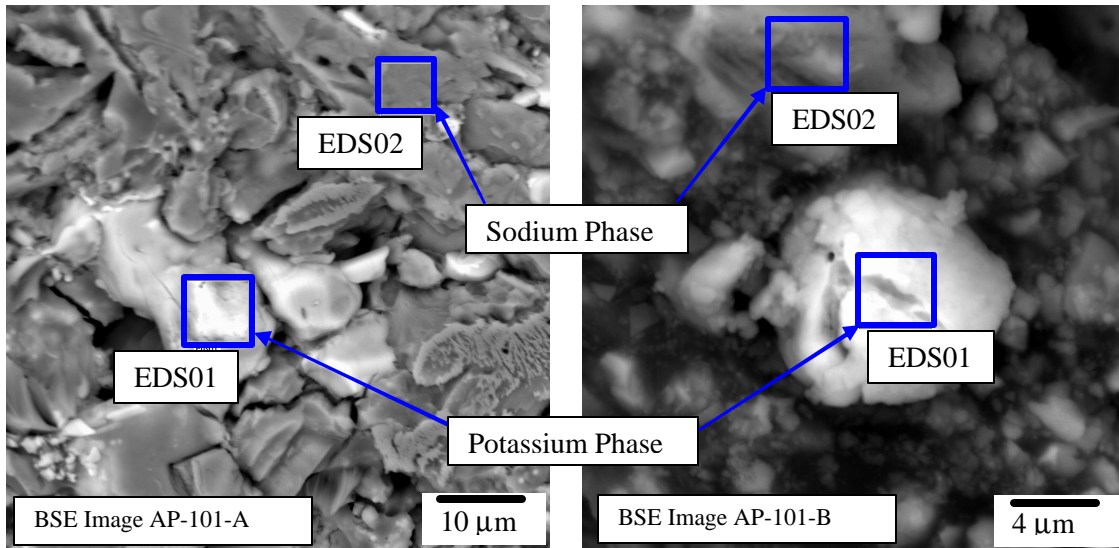


Figure 7.1. Scanning Electron Micrographs of Sodium- and Potassium-Bearing Phases in AP-101-A (6 M Na) and AP-101-B (8 M Na)

7.3.1.2 AP-101-C (10 M Na)

There was much more precipitated material in AP-101-C (10 M Na) than in the other two samples. In this sample, more euhedral (well formed crystal with regular shape) precipitates of the potassium phase were observed. In Figure 7.2, a hexagonal rod of the potassium phase can be seen. The EDS scans of the two different phases in Figure 7.2 are shown in Figure 7.3. Although carbon can be seen in the EDS, this is mainly from the carbon coat. There was little or no evidence of nitrogen in any of the phases.

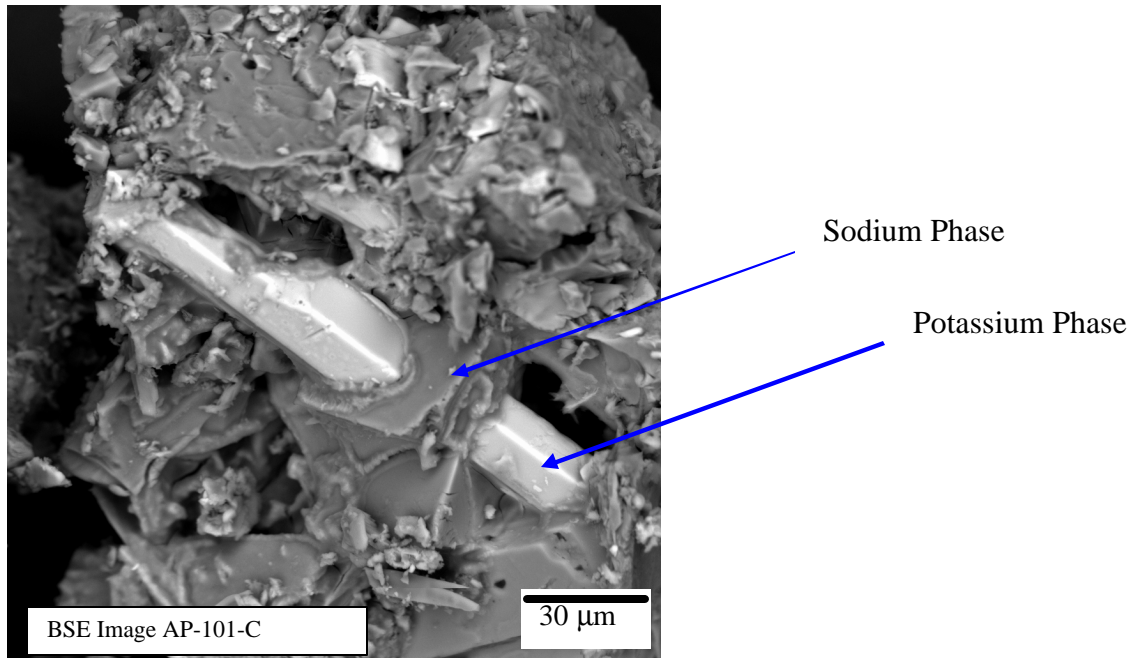


Figure 7.2. Sodium and Potassium Phase in AP-101-C (10 M Na)

Similar sodium- and potassium- bearing phases were observed in AP-101-A (6 M Na) and AP-101-B (8 M Na); however, the only conclusion from the SEM-EDS analyses is that one phase contained potassium and oxygen and the other sodium and oxygen. In one instance, an aluminosilicate particle was observed (see Figure 7.4). This material appeared to be an agglomerate of smaller particles. After washing the solid precipitates to remove the more soluble phases, this type of aluminosilicate phase dominated (see Section 7.3.1.3).

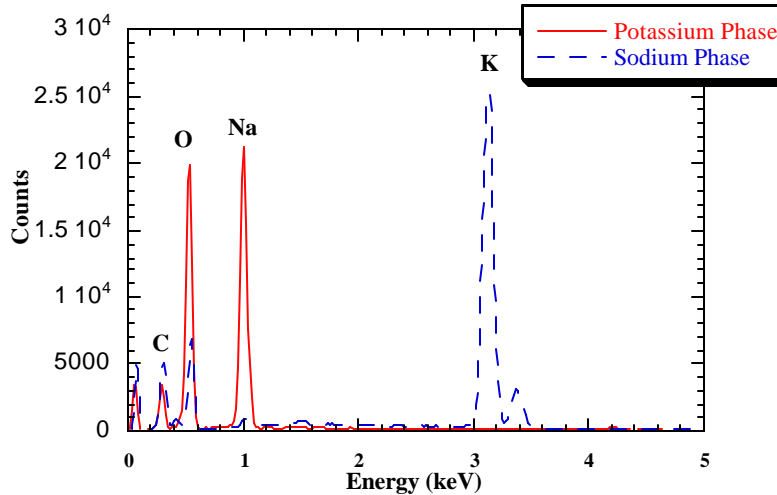


Figure 7.3. EDS Analysis of Sodium and Potassium Phase in AP-101-C (10 M Na)

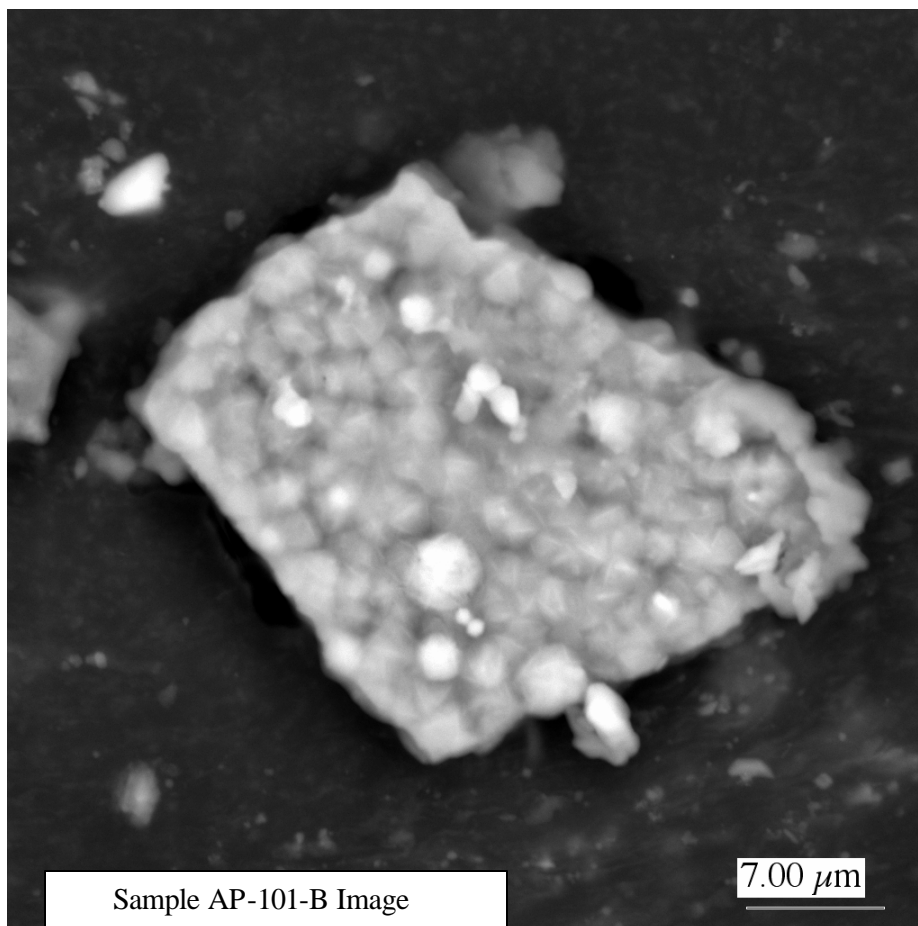


Figure 7.4. An Aluminosilicate Phase was Observed in AP-101-B (8 M Na)

7.3.1.3 Washed Samples

The precipitated solids were washed with de-ionized water three times to remove the more soluble solids. The resulting material appeared to have a higher specific radioactivity. Different particle morphologies were observed during the SEM investigation. Under the PLM, the particles were confirmed to be non-isotropic; however, their small size prevented any further analysis. At low magnification in the SEM, the same particle morphology observed in the PLM could be seen (see Figure 7.5a and 7.5b). With backscattered imaging and spot EDS analysis, it was possible to demonstrate that the composition of the particles was more or less constant. All particles were a sodium aluminosilicate with a trace amount of potassium.

At higher magnification the particles appeared to be botryoidal (A globular growth of minerals) aggregates (see Figures 7.6a and 7.6b and 7.7); however, some particles were acicular (crystals with an elongated or needle-like form) in nature. These elongated particles exhibited the same backscattered contrast and, according to EDS, had the same Na-Al-Si composition (see Figure 7.8). There was no evidence of any phosphorus in any of the precipitated phases. Phosphorus was present in the AP-101 tank supernatant but at low levels relative to aluminum.

By lowering the beam voltage and using secondary electrons to form the images, the ball-like precipitates appeared more like “balls of twine”. In Figure 7.6a and 7.7b, the change in microscope conditions reveals the actual morphology of the alumino-silicate phase. In Figure 7.7, a high magnification image of an individual “ball of twine” is shown. Again, because these images were taken with carbon-coated specimens, the true morphology may be slightly different. However, comparison of these images with those reported in the literature suggests that the “twin-like” morphology is not an artifact.

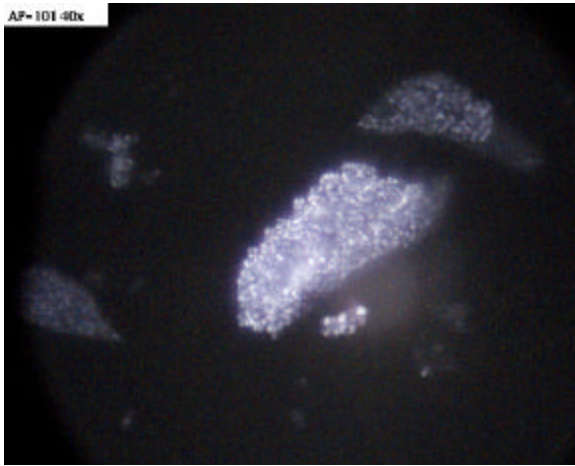


Figure 7.5a. Polarized Light Microscopy Image of Particles of Washed Solids

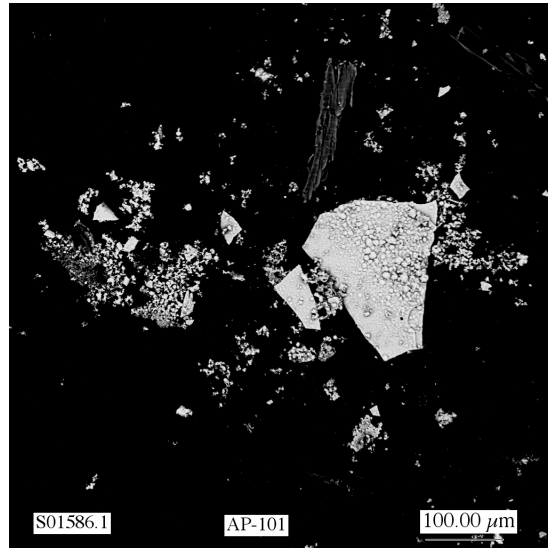


Figure 7.5b. Low magnification SEM Image of particles

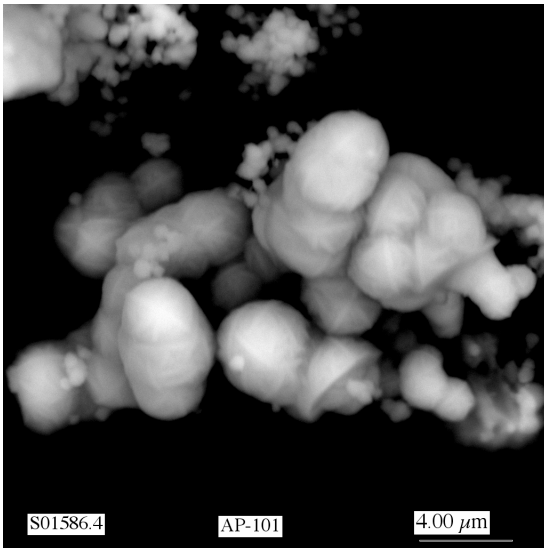


Figure 7.6a. Backscattered SEM Image of Particles at 20keV

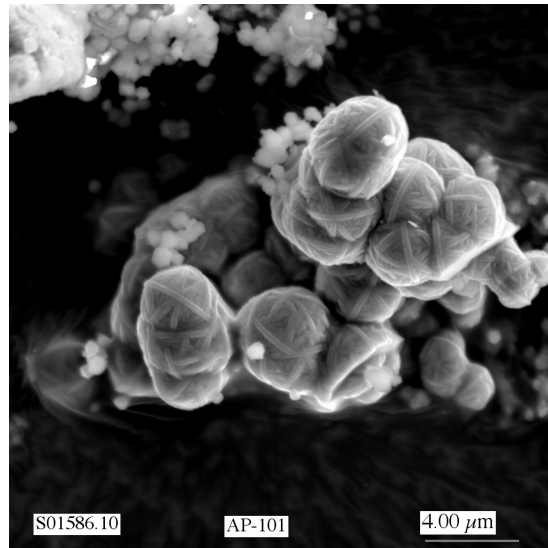


Figure 7.6b. Secondary SEM Image of the Same Particles at 10keV

The spectra similar to that shown in Figure 7.8 were quantified and the estimated compositions of the phases are shown in Table 7.1. As the EDS spectra were obtained from non-ideal samples, these values carry a large error; however, these phases had a composition consistent with either cancrinite $((\text{Na,Ca,K})_7\text{Al}_6\text{Si}_6\text{O}_{24}(\text{CO}_3)_{1.6}\cdot 2.1\text{H}_2\text{O})$ or zeolites.

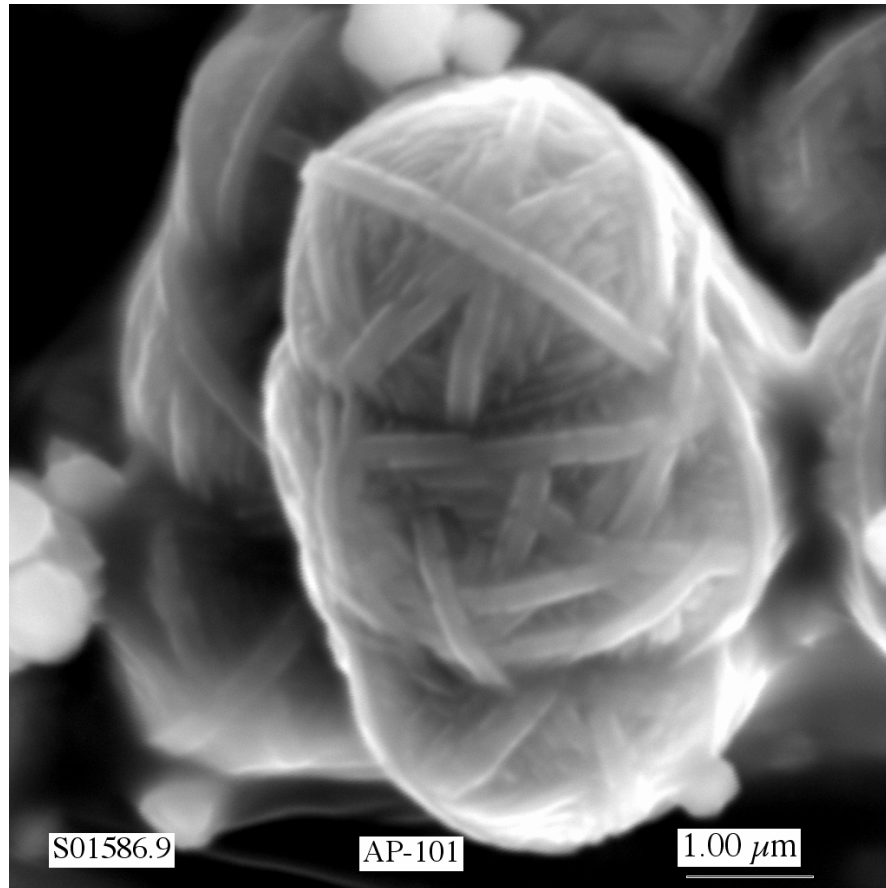


Figure 7.7. SE Higher Magnification Image of “twine -like’ material shown in Figure 7.6b. The image was obtained at 10keV to enhance the particle morphology

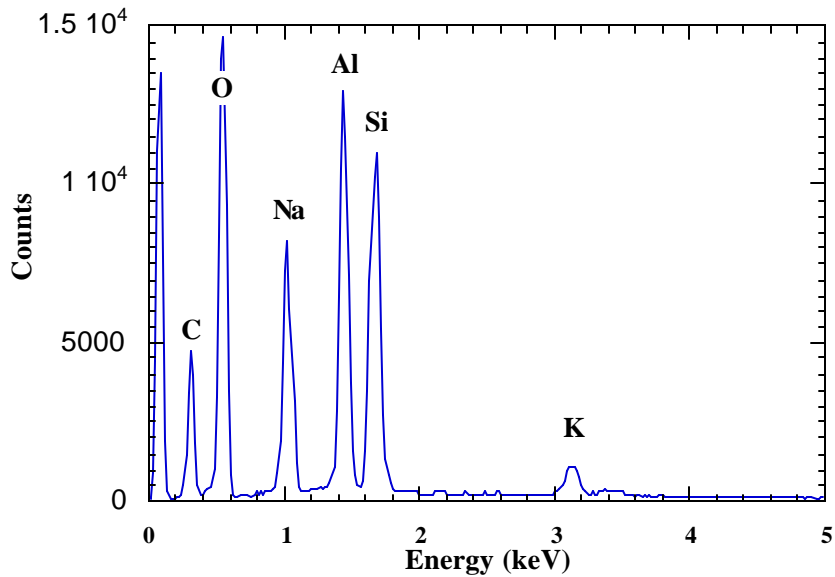


Figure 7.8. X-ray Energy Dispersive Spectrum of “Twine -Like” Particles
 The peak at near 0 keV is an artifact from the instrument.

Table 7.1. EDS Compositional Analysis

Element	Eds04 (Atomic Percent)	Eds05 (Atomic Percent)	Average (Atomic Percent)
Na	18.2±1.8	24.4±2.4	21.3±2.1
Al	33.2±3.3	36.9±3.7	35.0±3.5
Si	38.9±3.9	42.3±4.2	40.6±4.1
K	3.5±0.7	2.7±0.5	3.1±0.6

Almost identical morphologies have been reported for nitrate-cancrinite phases formed in laboratory experiments with simulated Hanford tank wastes by Bickmore et al. (2001). In these experiments, simulated waste was reacted with quartz, eventually precipitating the nitrate form of cancrinite (nitrate-cancrinite). These studies failed to explain the mechanism for the irregular precipitates.

7.3.2 Infrared Spectroscopy of the Solids

Figure 7.9 shows the as received AP101 solids A, B, and C (6 M, 8 M, 10 M Na respectively). Sample vial A had the least amount of precipitated solids with [Na] = 6 M. Solution B had more precipitated solid with [Na] = 8 M and sample vial C had the most precipitated solid at [Na] = 10 M. The IR shows qualitatively the relative amounts of nitrate and carbonate in the dried solids increased with addition of more salt.

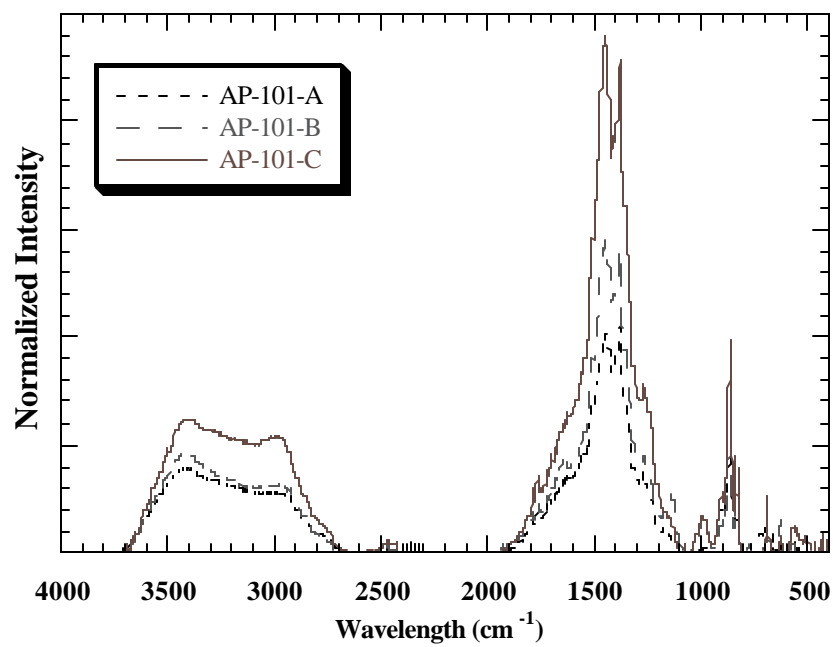


Figure 7.9. Infrared Spectra of AP-101 Dried Solids A, B, and C (6 M, 8 M, 10 M Na, respectively)

The major solids appeared to be carbonate and nitrate in all three samples (6 M, 8 M, and 10 M Na). Neither sulfate nor phosphate was present but another species, possibly an aluminate, was detected. The precipitated solids (100 mg) were washed twice with about 5 mL of deionized water. In Figure 7.10 the effect of this washing can be seen. There was a significant reduction in the carbonate and nitrate signal strength after the first and second wash. The spectrum from the second wash used to obtain a reasonable signal of the low intensity band at 998 cm^{-1} . The two washes removed about 75% by volume of the soluble solids. Figure 7.10 shows the expanded spectrum in the region 640 to 1780 cm^{-1} .

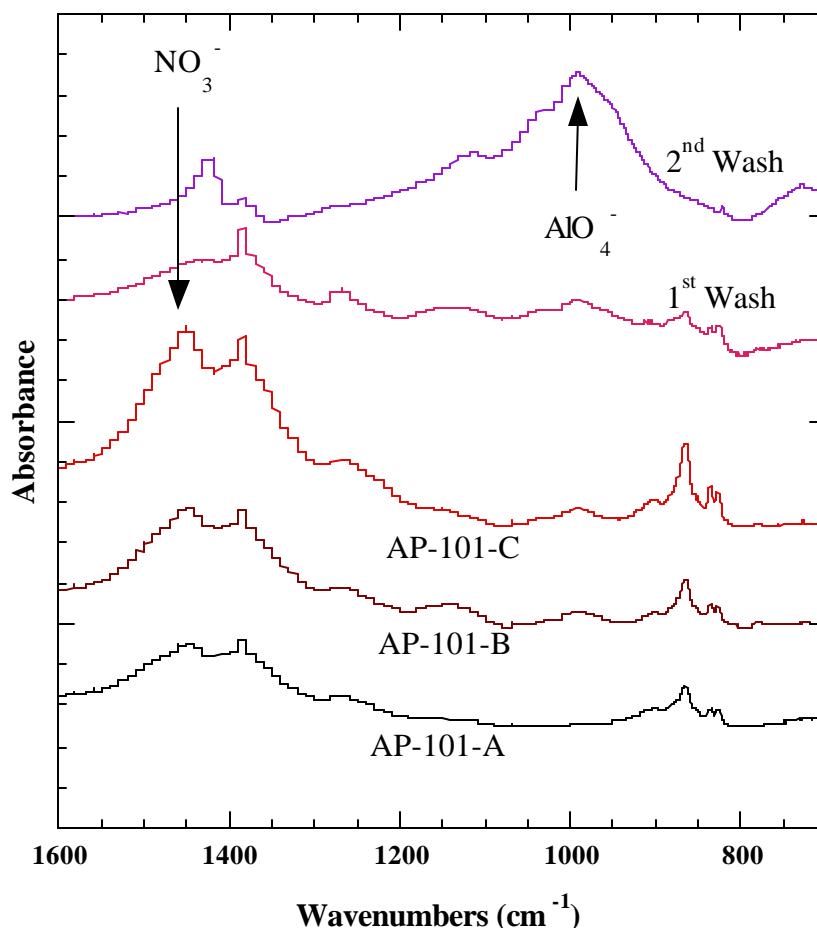


Figure 7.10. Infrared Spectra of AP-101 Solids A (6 M Na), B (8 M Na), C (10 M Na), and C (10 MNa) Washed Twice

7.3.3 Raman Data of the Washed Solids

The Raman spectra show a similar pattern (see Figure 7.11). Liquids A (6 M Na), B (8 M Na), and C (10 M Na) and also the precipitated solids through the bottom of the vial were looked at. Then some of the solids were dried and put on a microscope slide. The liquids spectra are compared to liquids standards, which incorporate the effects of hydroxide and ionic strength in the spectra. The solids are compared to solid standards, NaAlO_4 , $\text{Al}(\text{OH})_3$, NaNO_3 , Na_2CO_3 , Na_2SO_4 , Na_3PO_4 , and some double salts $\text{NaF}(\text{Na}_3\text{PO}_4) \cdot 19\text{H}_2\text{O}$, Na_3FSO_4 , and $\text{Na}_3\text{CO}_3\text{SO}_4$.

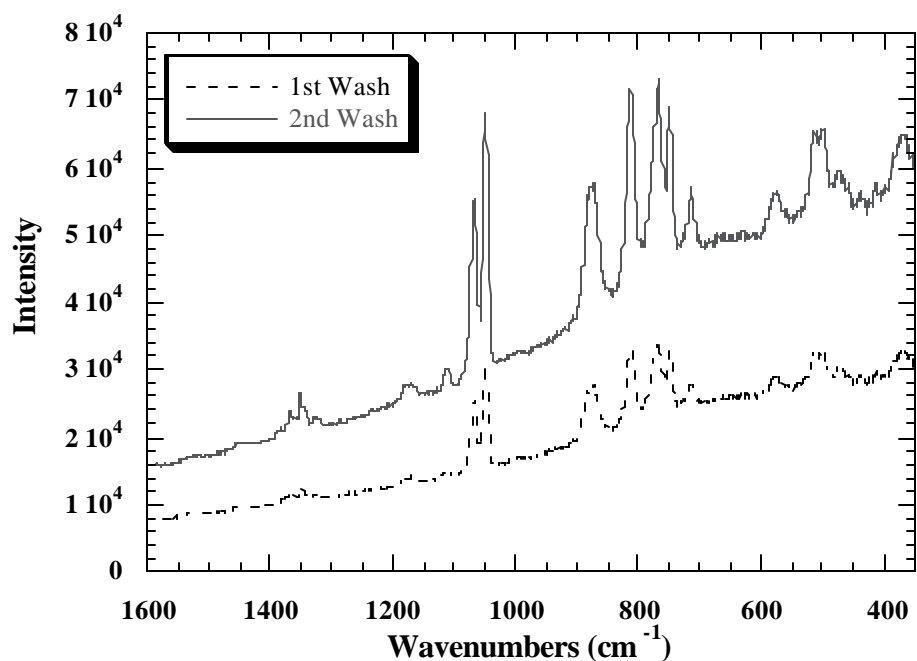


Figure 7.11. The Raman Spectra of AP-101 Solids: 1st and 2nd Wash of Solids C (10 M Na)

As shown in Table 7.2, the Raman shift will change position with respect to phase, and for most species, with respect to the hydroxide concentration. Bands that absorb strongly are listed first in Table 7.2. Comparisons made with the strong bands allow a tentative exclusion sulfate and phosphate species as candidates for the insoluble precipitate in liquids A (6 M Na), B (8 M Na), and C (10 M Na).

Phosphate and aluminate were not clearly seen in the AP101 liquids by Raman although they were detected in the NMR spectra of the native AP101 tank waste (see Section 7.4). The characteristic yellow colored chromate anion was evident, as well, but similarly it was below the detection limit of the Raman experiment.

Table 7.2. Compounds Used For Interpreting Raman Data

LIQUID STANDARDS	RAMAN BANDS (CM ⁻¹)	SOLID STANDARDS	RAMAN BANDS (CM ⁻¹)
AlO ₄ ⁻	619, 912w, 548, 283b	NaAlO ₄	1067vw, 913w, 621s, 543w
NO ₃ ⁻	1049s, 1350w, 749w	Al(OH) ₃	569w, 540, 319
CO ₃ ²⁻	1066s, 1366vw, 768w	AlOOH	655, 674w, 495, 357
SO ₄ ²⁻	970s, 1274vw, 680w, 751w, 447w	Sea Sand (SiO ₂)	878w, 811w, 764w, 465s
PO ₄ ³⁻	998s, 1284w, 698w, 386w	NaNO ₃	1668s, 1385w, 1366w, 766w, 720w
CrO ₄ ²⁻	848s, 1144w, 549w, 345w	KNO ₃	1047s, 1349w, 750w, 714w, 413w,
C ₂ O ₄ ²⁻	1455s, 1753, 1642w, 1614, 1158w, 883, 571w, 483vw	Na ₂ CO ₃	1078s, 1378vw, 781w
		KHCO ₃	1028s, 1329vw, 1280w, 972w, 929 w, 728 w, 675w, 635w
		K ₂ CO ₃	ND*
		Na ₂ SO ₄	992s, 691s, 1294, 1286w, 1151w, 1130w, 1102w, 631b, 464b
		Na ₃ PO ₄	942s, 1003w, 1238w, 643w, 544w, 410w
		Na ₂ CrO ₄	1340vw, 1310vw, 1178w, 1155s, 880s, 778vw, 479w
		NaF(Na ₃ PO ₄).19H ₂ O	932s, 995 w, 1230w, 628w, 538w
		Na ₃ FSO ₄	994s, 1293w, 1131w, 697, 633, 466
		Na ₃ NO ₃ SO ₄	1064s, 995s, 1386w, 1368w, 766w, 724w, 696w

b – broad; s – strong; vw – very weak; v – weak, ND* – Not Determined

7.3.4 Multinuclear NMR of Supernatant

There was an insufficient amount of the solid product to perform NMR; however, ²⁷Al and ³¹P NMR spectra of the native AP-101 tank supernatant were obtained. The ²⁷Al spectrum is shown in Figure 7.12. In the aluminum spectrum, an extremely strong singlet appears at 6258 Hz. The chemical shift of the peak from zero to 6258 Hz indicated that the aluminum in solution has tetrahedral symmetry (i.e., AlO₄⁻(aq)). The phosphorus spectrum was much weaker; although, it did suggest that PO₄²⁻ species were in solution, but this does explain why phosphate was not observed in the precipitated solids.

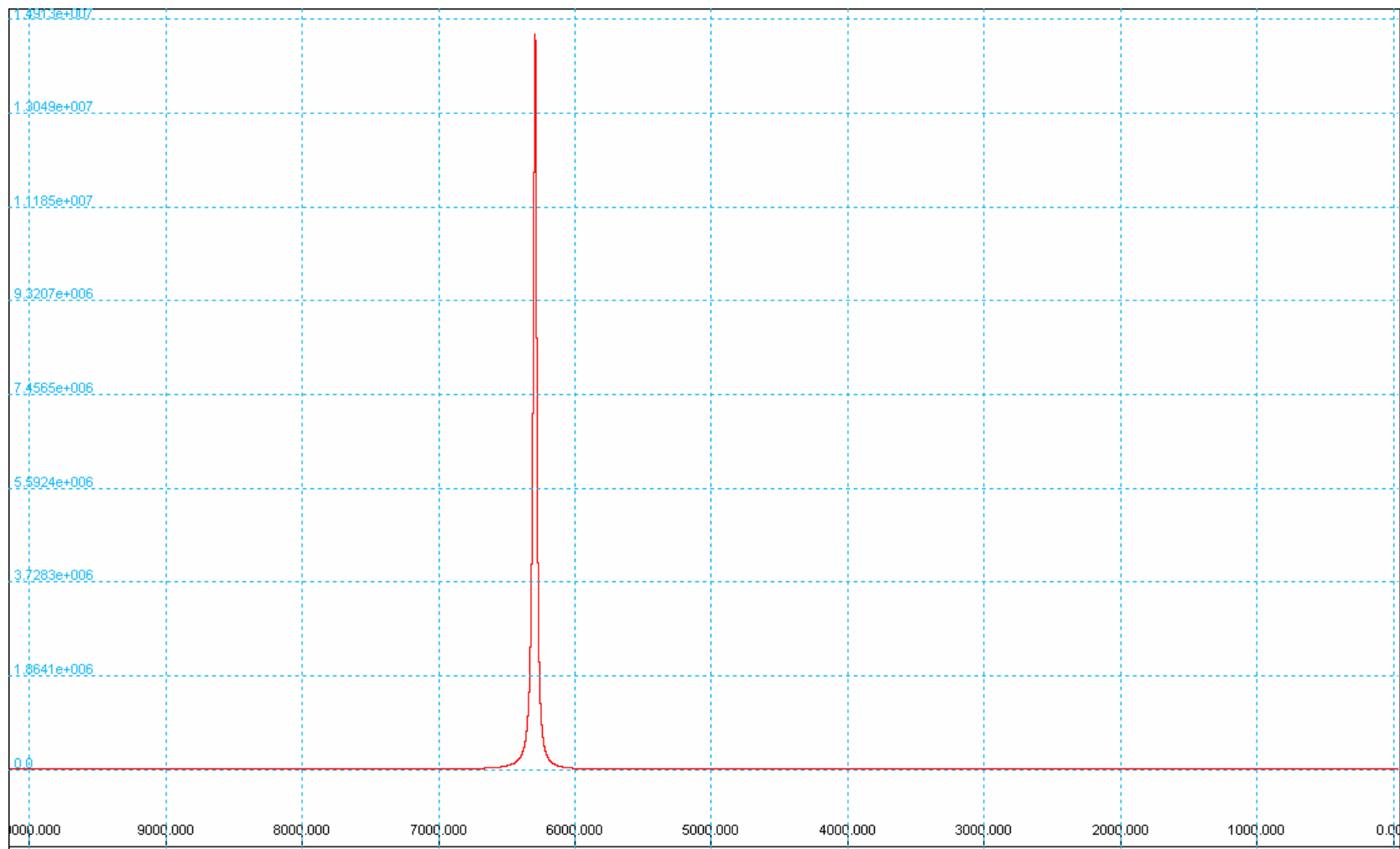


Figure 7.12. ^{27}Al NMR Spectrum of Native AP101 Tank Supernatant

In Figure 7.12, the position of the peak at 6000 Hz indicates that this is tetrahedrally coordinated aluminum in solution ($\text{Al}(\text{OH})_4^-$). The hexa-coordinated aqueous species, for example the nitrate, $\text{Al}(\text{NO}_3)_3 \cdot 9\text{H}_2\text{O}$, would be near zero.

7.3.5 X-ray Diffraction of the Solids

X-ray diffraction of the solids that had precipitated at 10 M Na is shown in Figure 7.13. The major sodium phase was confirmed to be nitratine (sodium nitrate; NaNO_3); however, the identity of the potassium phase was not conclusive. A match was made to potassium nitrate, but the match to potassium carbonate was weak.

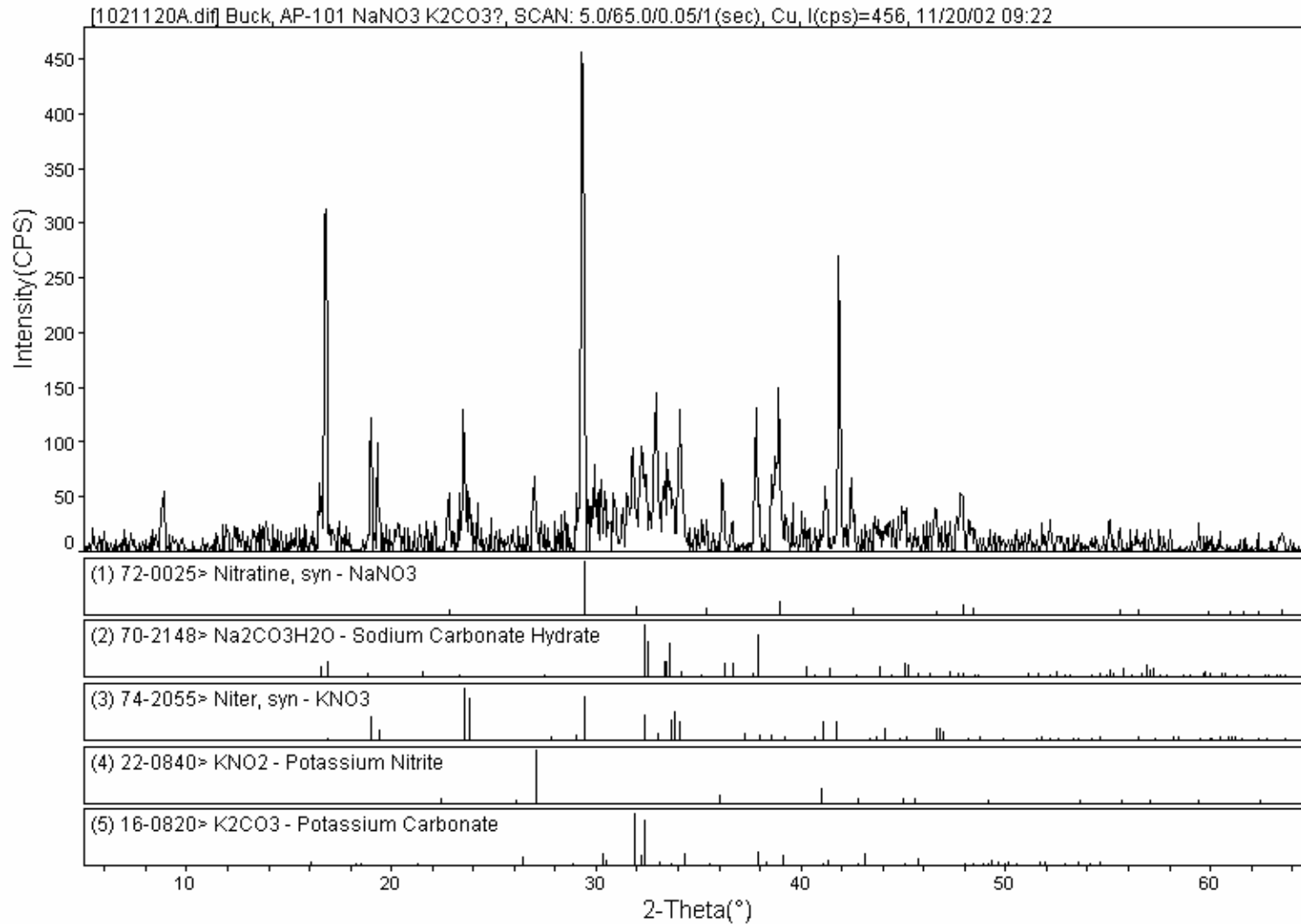


Figure 7.13. Comparison of the X-ray Diffraction Analysis of the Sodium and Potassium Phases in AP-101-C (10M Na) with Reference Spectra of NaNO₃, Na₂CO₃•H₂O, KNO₃, and K₂CO₃

As only a small amount of the washed material from AP-101-C was available. A low background silicon wafer slide mount was used. The spectrum appeared to be single phase shown in Figure 7.14, in agreement with the SEM investigation of the washed material. Based on the composition revealed with the SEM, a search of the XRD database revealed matches with some zeolites (faujasite) and feldspathoids, including cancrinite.

The major d-spacings (lattice spacings obtained with XRD) from hydroxyl-cancrinite (JCPDS 31-1272; $\text{Na}_{14}\text{Al}_{12}\text{Si}_{13}\text{O}_{51}\cdot 6\text{H}_2\text{O}$) and synthetic Na-faujasite (Joint Commission for Powder Diffraction (JCPDS) 28-1036) matched very well with the observed d-spacings from the alumino-silicate phase observed in washed sample AP-101-C. Table 7.3 shows the match to the nitrate-cancrinite reported by Buhl et al. (2000). Buhl et al. have performed complete structural characterization of these types of phases. A nitrate-cancrinite was also reported by Krumhansl et al. (1999).

Table 7.3. Major Peaks in AP-101-C in the XRD Scan of the Alumino-Silicate

Observed d-spacings d_{obs} (nm)	2·Theta	Intensity, I (counts)	Nitrate- Cancrinite d-spacings d_{lit} (nm) ^a	Lattice Indices, <i>hkl</i>
0.63431	13.95	2199	0.63353	110
0.27121	33	1504	--	--
0.36598	24.3	1450	0.36589	300
0.46915	18.9	642	0.46906	101
0.32465	27.45	566	0.32393	211
0.27486	32.55	491	0.27439	400
0.41392	21.45	426	0.41483	210
0.21158	42.7	394	0.21166	302
0.45255	19.6	329	--	--
0.40643	21.85	278	--	--
0.4414	20.1	246	--	--
0.25975	34.5	219	0.25951	002
0.42874	20.7	213	--	--
0.51216	17.3	193	--	--
0.49513	17.9	181	--	--

a Taken from data reported by J-C Buhl et al., *J. Alloys and Compds*, 305 (2000) 93-102.

The XRD of the alumino-silicate precipitate in the washed solids could be matched to a zeolite, Na-faujasite and the feldspathoid phase, hydroxy-cancrinite (see Figure 7.14). These were the only phases available in the JCPDS database. Compositionally, there was little difference, both phases had Al/Si ratios close 1.0, based on quantification with SEM-EDS. The overlap between these two phases reported in the powder diffraction database was almost perfect. There was a good match to nitrate-cancrinite phases reported by Buhl et al. (2000); although, these phases are not reported in the JCPDS to date. Faujasite and related structures are cubic; whereas, cancrinite is hexagonal and slightly birefringent. In addition, cancrinite is denser at 2.4 g/cm³ than faujasite at 1.86 g/cm³. The XRD also showed that there was no crystalline sodium nitrate remaining in the washed solid. Both the IR and Raman data indicated that the NO₃⁻ and CO₃²⁻ species were still present in the washed sample. The polarized light microscopy of the washed solids clearly indicated that the alumino-silicate phase was not isotropic, supporting the identification of cancrinite.

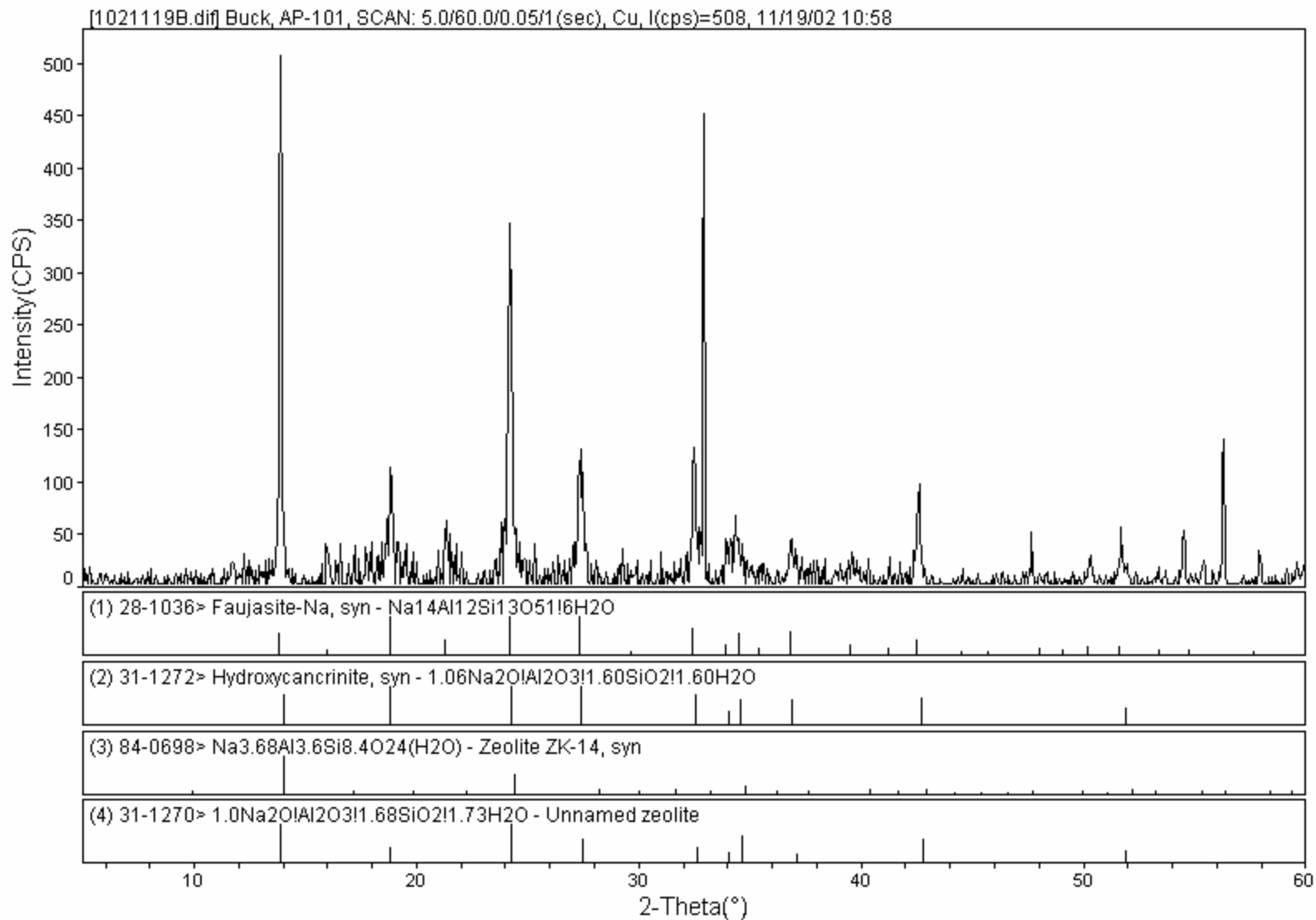


Figure 7.14. Comparison of the X-ray Diffraction Analysis of the Aluminosilicate Phase in AP-101-C (10M Na) with a match to Hydroxy-Cancrinite and other Zeolites

The observations in this study are similar to those reported by Jantzen and Laurinat (2001) in tank waste evaporators at the Savannah River Site. They reported the formation of sodium aluminosilicate (NAS) hydrogel that converts to zeolite-A (ideally $\text{Na}_{12}\text{Al}_2\text{Si}_{12}\text{O}_{48}\cdot 27\text{H}_2\text{O}$) under hydrothermal conditions at elevated temperatures, and eventually to sodalite (cubic; $\text{Na}_4\text{Al}_3\text{Si}_3\text{O}_{12}\text{Cl}$), and finally, cancrinite (hexagonal). The final phases were nitrated as appears to be the case with the AP-101 precipitated solids. Krumhansl et al. (1999) have also predicted that nitrate-cancrinite not zeolites should occur in tank wastes.

7.4 Discussion

7.4.1 Nitrate-Cancrinite

The mineral cancrinite is a feldspathoid but can sometimes be regarded as a zeolite owing to its porous aluminosilicate framework structure. The framework structure of cancrinite results in the formation of a large channel that is able to accommodate OH^- , Cl^- , SO_4^{2-} , NO_3^- , and CO_3^{2-} . Potentially, other anions could be incorporated into the cancrinite channel structure, such as TcO_4^- . Synthetic cancrinites have also been shown to take up cesium ions into non-exchangeable sites (Bickmore et al. 2001). Indeed, we observed a significant increase in the specific radioactivity of the aluminosilicate relative to a similar volume of the unwashed material that contained mainly sodium nitrate. The “balls of twine” morphology of the aluminosilicate phase has been observed in laboratory synthesized cancrinite from a simulated Hanford tank waste by Bickmore et al. (2001). The SEM images, carried out on a more powerful field-emission microscope at the Environmental Molecular Science Laboratory in Richland, show the same characteristic bent crystal morphology. The particles observed in the simulant study of Bickmore et al. (2001) were larger than the particles observed in this study. This investigation was greatly assisted by a number of Environmental Management Science Program (EMSP) studies on Hanford related issues that have addressed the role of cancrinite.

7.4.2 Nitrates

Evidence for nitrate phases was found with IR and Raman spectroscopy and the presence of sodium nitrate was confirmed with XRD. With IR, it was demonstrated that nitrite was not present in the precipitated solids. Because NaNO_2 consists of an ionic lattice with Na^+ ions and NO_2^- ions arranged in an infinite and very regular array, the crystal consists of essentially isolated Na^+ ions and NO_2^- ions. Thus, the vibrational modes of the cation and anion can be considered independently of one another. sodium nitrate is more complex, as there are six normal vibrational modes; however, the IR spectrum, exhibits only three fundamental bands, at 831, 1405, and 692 cm^{-1} . In the case of a planar, triangular ion such as NO_3^- , the symmetric stretch, is not IR active, because the motion does not cause a change in the dipole moment of the ion, and hence cannot give rise to absorption of IR radiation. Among the remaining five modes, there are two sets of doubly degenerate vibrations, (i.e., two instances in which two vibrations occur with exactly the same frequency).

7.4.3 Carbonates

The identity of the potassium phase observed in the precipitated solids remains questionable. The XRD analysis did not provide definitive proof of a potassium carbonate. Undoubtedly, some potassium was present as the nitrate; however, the IR and Raman, indicated a significant fraction of the precipitated solids were carbonates.

7.5 Conclusion

The major phases falling out of solution with increasing sodium concentration is sodium nitrate and possibly a potassium carbonate. The quantity of these phases precipitating increased with increasing sodium concentration. A minor phase, nitrate-cancrinite, increased in concentration with increasing sodium concentration. There were no differences in the solid phase composition at the different sodium concentrations based on the phases observed. This investigation points to the continued importance of understanding the solubility of nitrate-cancrinite and related phases.

8.0 Conclusions

The AP-101 pretreated LAW sample appeared to be near saturation when it was received at a sodium concentration of 4.9 M. White solids precipitated in the 6 M, 8 M, and 10 M Na samples as evaporation proceeded. The 2 wt% undissolved solids process bound was exceeded with 6.7 wt% undissolved solids in the 10 M Na sample. A design basis for this AP-101 pretreated LAW stream should limit the sodium concentration to a maximum of approximately 8 M which should limit the undissolved solids content to approximately 1.2 wt%. Solids precipitated from the LAW pretreated waste during evaporation activities were sodium nitrate and possibly a potassium carbonate. The quantity of these phases precipitating increased with increasing sodium concentration, but the ratio of these individual solid phases within the bulk solid specimens appeared relatively constant. A minor phase, nitrate-cancrinite, increased in concentration with increasing sodium concentration.

When glass former chemicals were added to the AP-101 pretreated LAW, the pH of the solution dropped from above pH 14 to approximately 12.3-12.5. This is most likely due to the relatively large quantity of boric acid in the LAWA-126 melter feed formulation. Such a large change in pH can result in significant solids precipitation. This solids precipitation was observed when preparing an AP-101 simulant suspending medium for particle size measurement purposes. When soluble glass former chemicals (e.g. boric acid) were added to the AP-101 simulant (Russell et al., 2002) a large amount of white solids precipitated. These solids are most likely aluminum hydroxide.

The undissolved solids present in the AP-101 LAW pretreated waste samples settle in a particulate type settling regime (i.e. the settled solids accumulate from the bottom of the sample upward). The AP-101 melter feed settled in a hindered settling regime (i.e. settled solids compress from the top of the sample downward). The settling rate and packing efficiency of the melter feed materials significantly decreased when temperature was increased from 25°C to 40°C.

The AP-101 pretreated LAW samples exhibited Newtonian rheological behavior. Depending on solution concentration and temperature, the viscosity of the samples range from 2 cP to 12 cP. This is within the pretreated LAW process bounding recommendations of 0.4-15 cP discussed by Poloski et al. (2002).

The AP-101 LAW melter feed exhibited Newtonian rheological behavior. Depending on sodium concentration and temperature, the viscosity of the samples range from 10 cP to 40 cP. This is well within the LAW melter feed bounding recommendations of Bingham plastic consistency index between 0.4 cP and 90 cP and yield index below 15 Pa (Poloski et al., 2002). No significant viscosity or pH changes were observed when an 8 M Na AP-101 LAW melter feed sample was mixed and aged for periods of 1-hr, 1-day, and 1-week. The 1-week mixed, 8 M Na AP-101 LAW melter feed settled solids exhibited Bingham plastic behavior with Bingham consistency and yield indices that exceed the LAW melter feed bounding recommendations (Poloski et al., 2002).

The yield strength of the melter feed settled solids were measured at 40°C; 790 Pa for the 6 M Na sample and 79 Pa for the 8 M Na sample. The significantly higher shear strength for the 6 M Na sample is not expected. One possible explanation for this observed decrease with increasing sodium concentration could be the higher degree of precipitated solids in the 8 M Na system. These solids could lower the high settled solids network strength observed in the 6 M Na system. However, after a week mixing period, the settled solids shear strength of the 8 M Na melter feed sample dramatically increased to approximately 610 Pa at 40°C. When cooled to room temperature, the shear strength increased further

to 2600 Pa. Shear strength measurements above approximately 625 Pa may cause difficulties in WTP processing operations (Poloski et al., 2002).

The particle size distribution of a 6 M Na melter feed sample was measured. The particle size distribution exhibits two major peaks, one in approximately the 2 to 7 μm range and the other in approximately the 10 to 20 μm range. The resulting mean particle size on a volume basis is 9.2 μm . Approximately 10 vol% of the particles are below 2.6 μm , 50 vol% (i.e., median value) below 7.6 μm , 90 vol% below 18.2 μm , and 95 vol% below 20.2 μm . The particle size distribution of a LAWA-126 glass former mix in deionized water sample was also measured. The particle size distribution exhibits two major peaks, one in approximately the 0.5 to 1.5 μm range and the other in approximately the 5 to 40 μm range. The resulting mean particle size on a volume basis is 19.9 μm . Approximately 10 vol% of the particles are below 1.1 μm , 50 vol% (i.e., median value) below 17.2 μm , 90 vol% below 43.8 μm , and 95 vol% below 50.8 μm . With particle sizes well below 100 μm , no significant process challenges with respect to particle settling are anticipated.

9.0 References

- Alderman, N.J., G.H. Meetenm, and J.D. Sherwood. 1991. "Vane rheometry of bentonite gels" *J. Non-Newtonian Fluid Mech.*, 39(1991) 291-310.
- Avramidis K.S. and R.M. Turain. 1991. "Yield Stress of Laterite Suspensions", *J. Colloid Interface Sci.*, 143(1991) 54-68.
- Barnes, H A; Carnali, J O. 1990. 'The vane-in-cup as a novel rheometer geometry for shear-thinning and thixotropic materials', *J. Rheol.* 34(6), 841-866.
- Bickmore, BR, KL Nagy, JS Young, and JW Drexler. 2001. "Nitrate-Cancrinite Precipitation on Quartz Sand in Simulated Hanford Tank Solutions". *Environ. Sci. Technol.* Vol. 35, pp. 4481-4486.
- Bowles, J.E. 1977. *Foundation, Analysis and Design*, 2nd Ed., McGraw-Hill, New York, 1977 pg 99.
- Buhl, J-C, S Stief, M Fechtelkord, TM Gesing, U Taphorn, and C Taake. 2000. "Synthesis, X-ray Diffraction and MAS NMR Characteristics of Nitrate Cancrinite $\text{Na}_{7.6}[\text{AlSi}_4\text{O}_{14}]_6(\text{NO}_3) \cdot 1.6(\text{H}_2\text{O})_2$ *J. Alloys and Compds.* Vol. 305, pp. 93-102.
- Burgeson IE, JR Deschane, and DL Blanchard Jr. 2002. *Small Column Testing of Superlig® 639 for Removal of ⁹⁹Tc from Hanford Tank Waste Envelope A (241-AP-101)*, PNWD-3222, Battelle Pacific Northwest Division, Richland, Washington.
- Dabak T. and O Yucel. 1987. "Modeling of the concentration and particle size distribution effects on the rheology of highly concentrated suspensions," *Powder Technology.* 52(1987):193-206.
- Dzuy, N.Q. and D.V. Boger. 1985. "Direct Yield Stress Measurement with the Vane Method," *Journal of Rheology*, Volume 29, 335-347, 1985.
- Fiskum SK, ST Arm, DL Blanchard, and BM Rapko. 2002. *Small Column Ion Exchange Testing of Superlig® 644 for Removal of ¹³⁷Cs from Hanford Waste Tank 241-AP-101 Diluted Feed (Envelope A)*, PNWD-3198, Battelle Pacific Northwest Division, Richland, WA.
- Goheen SC, PR Brecht, OT Farmer, III, SK Fiskum, KA Gaither, LR Greenwood, LK Jagoda, AP Poloski, RD Scheele, CZ Soderquist, RG Swoboda, MP Thomas, MW Urie, and JJ Wagner. 2002. *Chemical Analysis and Physical Property Testing of Diluted 241-AP-101 Tank Waste*, PNWD-3174, Battelle Pacific Northwest Division, Richland, WA.
- James, A.E., D.A. Williams, and P.R. Williams. 1987. *Rheol. Acta.*, 26(1987) 437-446.
- Jantzen, C. M., J. E. Laurinat, and K. G. Brown. 2002. "Thermodynamic modeling of the SRS Evaporators: Part I. The 2H and 2F Systems (U)," Westinghouse Savannah River Company Report, WSRC-TR-2000-00293, Rev 1, Aiken, SC.
- Keentok, M. 1982. "The measurement of the yield stress of liquids" *Rheol. Acta*, 21(1982) 325-332.
- Keentok, M., J.F. Milthorpe, and E. O'Donovan. 1985. "On the shearing zone around rotating vanes in plastic liquids: theory and experiment", *J. Non-Newtonian Fluid Mech.*, 17(1985) 23-35.

Krumhansl, JL, PV Brady, PC Zhang, HL Anderson, SE Arthur, SK Hutcherson, MA Molecke, C Jove-Colon, J Liu, M Qian, KL Nagy, and B Wakoff. 1999. "Final Report: Phase Chemistry of Tank Sludge Residual Components." DOE Environmental Management Science Program Report, Project No. 60403.

Liddell, P.V. and D.V. Boger. 1996. "Yield Stress Measurements With the Vane" *J. Non-Newtonian Fluid Mech.*, 63(1996) 235-261 991) 54-68.

Nguyen, Q.D and D.V. Boger. 1983. "Yield Stress Measurement For Concentrated Suspensions" *Rheol. Acta.*, 27 (1983) 321-349.

Nguyen, Q.D and D.V. Boger. 1985a. "Thixotropic Behavior of Concentrated Bauxite Residue Suspensions" *Rheol. Acta.*, 24 (1985a) 427-437.

Nguyen, Q.D and D.V. Boger. 1985b. "Direct Yield Stress Measurements With the Vane Method" *Rheol. Acta.*, 29 (1985b) 335-347.

Perry and Green. 1997. *Perry's Chemical Engineer's Handbook*, 7th Ed 1997, McGraw Hill, New York.

Poloski A, Smith H, Smith G, Calloway G. 2002. *Development of LAW and HLW Vitrification Physical Property Bounding Conditions and Simulant Verification Criteria*, WTP-RPT-075, Rev. A, Battelle Pacific Northwest Division, Richland, WA.

Russell R.L., Fiskum S.K., Jagoda L.K., Poloski A.P., 2002. *AP-101 Diluted Feed (Envelope A) Simulant Development Report*, WTP-RPT-057, Rev A, Battelle Pacific Northwest Division, Richland, WA.

Smith, G.L. and K. Prindiville. 2002. *Guidelines for Performing Chemical, Physical, and Rheological Properties Measurements*, 24590-WTP-GPG-RTD-001 Rev 0, Bechtel National, Inc., Richland, WA.

Schumacher R.F. and E.K. Hansen. 2002. *Selection of HLW and LAW Glass Formers*, SRT-RPP-2002-00034, Savannah River Technology Center, Aiken, SC.

Appendix A – Guideline Rheology Reporting

This section consists of rheology data that is consistent with reporting requirements in the physical property guidelines developed by Smith and Prindiville. (2002). A singular representative data run has been selected for this reporting format (see Tables A.1-A.20).

Table A.1. AP-101 4.9 M Na Pretreated Waste Rheology Data at 25° C (File Name: 061902a)

Model/model Parameter	Parameter Value
Shear Strength (by Vane Method):	
t_o - Shear Strength (Pa)	n/a
Newtonian:	
η – Newtonian viscosity (cP)	3.4
R^2 – correlation coefficient	0.9932
Ostwald (or Power Law):	
m – the consistency coefficient (mPa·s ⁻ⁿ)	6.1
n – the power law exponent	0.9129
R^2 – correlation coefficient	0.9970
Bingham Plastic:	
t_o^B - the Bingham yield stress (Pa)	0.09669
η_p - the plastic viscosity (cP)	3.3
R^2 – linear correlation coefficient	0.9958
Herschel-Bulkley:	
t_o^H - the yield stress (Pa)	0
k - the Herschel-Bulkely consistency coefficient (mPa·s ^{-b})	6.1
b - the Herschel-Bulkely power law exponent	0.9129
R^2 – correlation coefficient	0.9970
n/a – not applicable	

Table A.2. AP-101 4.9 M Na Pretreated Waste Rheology Data at 40° C (File Name: 061902e)

Model/model Parameter	Parameter Value
Shear Strength (by Vane Method):	
t_o - Shear Strength (Pa)	n/a
Newtonian:	
η – Newtonian viscosity (cP)	2.5
R^2 – correlation coefficient	0.9978
Ostwald (or Power Law):	
m – the consistency coefficient (mPa·s ⁻ⁿ)	3.2
n – the power law exponent	0.9621
R^2 – correlation coefficient	0.9986
Bingham Plastic:	
t_o^B - the Bingham yield stress (Pa)	0.030
η_p - the plastic viscosity (cP)	2.5
R^2 – linear correlation coefficient	0.9982
Herschel-Bulkley:	
t_o^H - the yield stress (Pa)	0
k - the Herschel-Bulkely consistency coefficient (mPa·s ^{-b})	3.2
b - the Hershel-Bulkely power law exponent	0.9621
R^2 – correlation coefficient	0.9986
n/a – not applicable	

Table A.3. AP-101 6 M Na Pre treated Waste Rheology Data at 25° C (File Name: 062002a)

Model/model Parameter	Parameter Value
Shear Strength (by Vane Method):	
τ_o - Shear Strength (Pa)	n/a
Newtonian:	
η – Newtonian viscosity (cP)	5.1
R^2 – correlation coefficient	0.8442
Ostwald (or Power Law):	
m – the consistency coefficient (mPa·s ⁻ⁿ)	27.7
n – the power law exponent	0.7432
R^2 – correlation coefficient	0.8894
Bingham Plastic:	
τ_o^B - the Bingham yield stress (Pa)	0.6220
η_p - the plastic viscosity (cP)	4.2
R^2 – linear correlation coefficient	0.9034
Herschel-Bulkley:	
τ_o^H - the yield stress (Pa)	0.6430
k - the Herschel-Bulkely consistency coefficient (mPa·s ^{-b})	3.8
b - the Hershel-Bulkely power law exponent	1.015
R^2 – correlation coefficient	0.9034
n/a – not applicable	

Table A.4. AP-101 6 M Na Pretreated Waste Rheology Data at 40° C (File Name: 062002e)

Model/model Parameter	Parameter Value
Shear Strength (by Vane Method):	
τ_o - Shear Strength (Pa)	n/a
Newtonian:	
η – Newtonian viscosity (cP)	3.5
R^2 – correlation coefficient	0.9569
Ostwald (or Power Law):	
m – the consistency coefficient (mPa·s ⁻ⁿ)	11.0
n – the power law exponent	0.8266
R^2 – correlation coefficient	0.9750
Bingham Plastic:	
τ_o^B - the Bingham yield stress (Pa)	0.2235
η_p - the plastic viscosity (cP)	3.2
R^2 – linear correlation coefficient	0.9712
Herschel-Bulkley:	
τ_o^H - the yield stress (Pa)	0.008968
k - the Herschel-Bulkely consistency coefficient (mPa·s ^{-b})	10.66
b - the Hershel-Bulkely power law exponent	0.8312
R^2 – correlation coefficient	0.9750
n/a – not applicable	

Table A.5. AP-101 8 M Na Pretreated Waste Rheology Data at 25° C (File Name: 062002i)

Model/model Parameter	Parameter Value
Shear Strength (by Vane Method):	
t_o - Shear Strength (Pa)	n/a
Newtonian:	
η – Newtonian viscosity (cP)	8.1
R^2 – correlation coefficient	0.9359
Ostwald (or Power Law):	
m – the consistency coefficient (mPa·s ⁻ⁿ)	25.0
n – the power law exponent	0.8291
R^2 – correlation coefficient	0.9530
Bingham Plastic:	
t_o^B - the Bingham yield stress (Pa)	0.6540
η_p - the plastic viscosity (cP)	7.2
R^2 – linear correlation coefficient	0.9600
Herschel-Bulkley:	
t_o^H - the yield stress (Pa)	0.7452
k - the Herschel-Bulkely consistency coefficient (mPa·s ^{-b})	5.4
b - the Hershel-Bulkely power law exponent	1.040
R^2 – correlation coefficient	0.9602
n/a – not applicable	

Table A.6. AP-101 8 M Na Pretreated Waste Rheology Data at 40° C (File Name: 062002m)

Model/model Parameter	Parameter Value
Shear Strength (by Vane Method):	
t_o - Shear Strength (Pa)	n/a
Newtonian:	
η – Newtonian viscosity (cP)	5.3
R^2 – correlation coefficient	0.9837
Ostwald (or Power Law):	
m – the consistency coefficient (mPa·s ⁻ⁿ)	10.4
n – the power law exponent	0.8976
R^2 – correlation coefficient	0.9892
Bingham Plastic:	
t_o^B - the Bingham yield stress (Pa)	0.1821
η_p - the plastic viscosity (cP)	5.0
R^2 – linear correlation coefficient	0.9876
Herschel-Bulkley:	
t_o^H - the yield stress (Pa)	0
k - the Herschel-Bulkely consistency coefficient (mPa·s ^{-b})	10.4
b - the Hershel-Bulkely power law exponent	0.8976
R^2 – correlation coefficient	0.9892
n/a – not applicable	

Table A.7. AP-101 10 M Na Pretreated Waste Rheology Data at 25°C (File Name: 062002u)

Model/model Parameter	Parameter Value
Shear Strength (by Vane Method):	
t_o - Shear Strength (Pa)	n/a
Newtonian:	
η - Newtonian viscosity (cP)	12.2
R^2 - correlation coefficient	0.6959
Ostwald (or Power Law):	
m - the consistency coefficient (mPa·s ⁻ⁿ)	78.6
n - the power law exponent	0.7161
R^2 - correlation coefficient	0.7436
Bingham Plastic:	
t_o^B - the Bingham yield stress (Pa)	1.177
η_p - the plastic viscosity (cP)	10.44
R^2 - linear correlation coefficient	0.7235
Herschel-Bulkley:	
t_o^H - the yield stress (Pa)	0
k - the Herschel-Bulkely consistency coefficient (mPa·s ^{-b})	78.6
b - the Hershel-Bulkely power law exponent	0.7161
R^2 - correlation coefficient	0.7436
n/a - not applicable	

Table A.8. AP-101 10 M Na Pretreated Waste Rheology Data at 40°C (File Name: 062002r)

Model/model Parameter	Parameter Value
Shear Strength (by Vane Method):	
τ_o - Shear Strength (Pa)	n/a
Newtonian:	
η – Newtonian viscosity (cP)	7.5
R^2 – correlation coefficient	0.016
Ostwald (or Power Law):	
m – the consistency coefficient (mPa·s ⁻ⁿ)	568.0
n – the power law exponent	0.3361
R^2 – correlation coefficient	0.1122
Bingham Plastic:	
τ_o^B - the Bingham yield stress (Pa)	2.394
η_p - the plastic viscosity (cP)	3.9
R^2 – linear correlation coefficient	0.1190
Herschel-Bulkley:	
τ_o^H - the yield stress (Pa)	2.583
k - the Herschel-Bulkely consistency coefficient (mPa·s ^{-b})	1.2
b - the Hershel-Bulkely power law exponent	1.171
R^2 – correlation coefficient	0.1191
n/a – not applicable	

Table A.9. AP-101 6 M Na Melter Feed Rheology Data at 25°C (File Name: 073002c)

Model/model Parameter	Parameter Value
Shear Strength (by Vane Method):	
t_o - Shear Strength (Pa)	n/a
Newtonian:	
η - Newtonian viscosity (cP)	12.4
R^2 - correlation coefficient	0.9986
Ostwald (or Power Law):	
m - the consistency coefficient (mPa·s ⁻ⁿ)	16.9
n - the power law exponent	0.9530
R^2 - correlation coefficient	0.9996
Bingham Plastic:	
t_o^B - the Bingham yield stress (Pa)	0.2350
η_p - the plastic viscosity (cP)	12.1
R^2 - linear correlation coefficient	0.9996
Herschel-Bulkley:	
t_o^H - the yield stress (Pa)	0.1603
k - the Herschel-Bulkely consistency coefficient (mPa·s ^{-b})	13.7
b - the Hershel-Bulkely power law exponent	0.9816
R^2 - correlation coefficient	0.9998
n/a - not applicable	

Table A.10. AP-101 6 M Na Melter Feed Rheology Data at 40° C (File Name: 073002h)

Model/model Parameter	Parameter Value
Shear Strength (by Vane Method):	
t_o - Shear Strength (Pa; 072302a)	790
Newtonian:	
η – Newtonian viscosity (cP)	9.0
R^2 – correlation coefficient	0.9918
Ostwald (or Power Law):	
m – the consistency coefficient (mPa·s ⁻ⁿ)	3.7
n – the power law exponent	1.134
R^2 – correlation coefficient	0.9980
Bingham Plastic:	
t_o^B - the Bingham yield stress (Pa)	0
η_p - the plastic viscosity (cP)	9.0
R^2 – linear correlation coefficient	0.9918
Herschel-Bulkley:	
t_o^H - the yield stress (Pa)	0.3400
k - the Herschel-Bulkely consistency coefficient (mPa·s ^{-b})	1.7
b - the Hershel-Bulkely power law exponent	1.241
R^2 – correlation coefficient	0.9994

Table A.11. AP-101 8 M Na Melter Feed Rheology Data at 25° C (File Name: 073102c)

Model/model Parameter	Parameter Value
Shear Strength (by Vane Method):	
t_o - Shear Strength (Pa)	n/a
Newtonian:	
η – Newtonian viscosity (cP)	39.4
R^2 – correlation coefficient	0.9954
Ostwald (or Power Law):	
m – the consistency coefficient (mPa·s ⁻ⁿ)	21.0
n – the power law exponent	1.096
R^2 – correlation coefficient	0.9990
Bingham Plastic:	
t_o^B - the Bingham yield stress (Pa)	0
η_p - the plastic viscosity (cP)	39.4
R^2 – linear correlation coefficient	0.9954
Herschel-Bulkley:	
t_o^H - the yield stress (Pa)	0.9813
k - the Herschel-Bulkely consistency coefficient (mPa·s ^{-b})	13.1
b - the Hershel-Bulkely power law exponent	1.161
R^2 – correlation coefficient	0.9994
n/a – not applicable	

Table A.12. AP-101 8 M Na Melter Feed Rheology Data at 40° C (File Name: 073102k)

Model/model Parameter	Parameter Value
Shear Strength (by Vane Method):	
t_o - Shear Strength (Pa; 072302b)	79
Newtonian:	
η – Newtonian viscosity (cP)	25.9
R^2 – correlation coefficient	0.9930
Ostwald (or Power Law):	
m – the consistency coefficient (mPa·s ⁻ⁿ)	54.0
n – the power law exponent	0.8883
R^2 – correlation coefficient	0.9998
Bingham Plastic:	
t_o^B - the Bingham yield stress (Pa)	1.003
η_p - the plastic viscosity (cP)	24.4
R^2 – linear correlation coefficient	0.9980
Herschel-Bulkley:	
t_o^H - the yield stress (Pa)	0
k - the Herschel-Bulkely consistency coefficient (mPa·s ^{-b})	54.0
b - the Hershel-Bulkely power law exponent	0.8883
R^2 – correlation coefficient	0.9998

**Table A.13. AP-101 8 M Na Melter Feed Rheology Data at 25° C
one hour after Glass Former Chemical Addition (File Name: 082202a)**

Model/model Parameter	Parameter Value
Shear Strength (by Vane Method):	
t_o - Shear Strength (Pa)	n/a
Newtonian:	
η – Newtonian viscosity (cP)	23.7
R^2 – correlation coefficient	0.9982
Ostwald (or Power Law):	
m – the consistency coefficient (mPa·s ⁻ⁿ)	18.0
n – the power law exponent	1.042
R^2 – correlation coefficient	0.9990
Bingham Plastic:	
t_o^B - the Bingham yield stress (Pa)	0
η_p - the plastic viscosity (cP)	23.7
R^2 – linear correlation coefficient	0.9982
Herschel-Bulkley:	
t_o^H - the yield stress (Pa)	0.4566
k - the Herschel-Bulkely consistency coefficient (mPa·s ^{-b})	12.8
b - the Hershel-Bulkely power law exponent	1.09
R^2 – correlation coefficient	0.9992
n/a – not applicable	

**Table A.14. AP-101 8 M Na Melter Feed Rheology Data at 40° C
one hour after Glass Former Chemical Addition (File Name: 082202e)**

Model/model Parameter	Parameter Value
Shear Strength (by Vane Method):	
t_o - Shear Strength (Pa)	n/a
Newtonian:	
η – Newtonian viscosity (cP)	19.0
R^2 – correlation coefficient	0.9984
Ostwald (or Power Law):	
m – the consistency coefficient (mPa·s ⁻ⁿ)	16.6
n – the power law exponent	1.021
R^2 – correlation coefficient	0.9986
Bingham Plastic:	
t_o^B - the Bingham yield stress (Pa)	0.02001
η_p - the plastic viscosity (cP)	19.0
R^2 – linear correlation coefficient	0.9984
Herschel-Bulkley:	
t_o^H - the yield stress (Pa)	0.5572
k - the Herschel-Bulkely consistency coefficient (mPa·s ^{-b})	9.81
b - the Hershel-Bulkely power law exponent	1.094
R^2 – correlation coefficient	0.9994
n/a – not applicable	

**Table A.15. AP-101 8 M Na Melter Feed Rheology Data at 25° C
one day after Glass Former Chemical Addition (File Name: 082302a)**

Model/model Parameter	Parameter Value
Shear Strength (by Vane Method):	
t_o - Shear Strength (Pa)	n/a
Newtonian:	
η – Newtonian viscosity (cP)	30.0
R^2 – correlation coefficient	0.9990
Ostwald (or Power Law):	
m – the consistency coefficient (mPa·s ⁻ⁿ)	31.7
n – the power law exponent	0.9916
R^2 – correlation coefficient	0.9990
Bingham Plastic:	
t_o^B - the Bingham yield stress (Pa)	0.255
η_p - the plastic viscosity (cP)	29.6
R^2 – linear correlation coefficient	0.9992
Herschel-Bulkley:	
t_o^H - the yield stress (Pa)	0.6848
k - the Herschel-Bulkely consistency coefficient (mPa·s ^{-b})	21.4
b - the Hershel-Bulkely power law exponent	1.046
R^2 – correlation coefficient	0.9994
n/a – not applicable	

**Table A.16. AP-101 8 M Na Melter Feed Rheology Data at 40° C
one day after Glass Former Chemical Addition (File Name: 082302e)**

Model/model Parameter	Parameter Value
Shear Strength (by Vane Method):	
t_o - Shear Strength (Pa)	n/a
Newtonian:	
η – Newtonian viscosity (cP)	20.8
R^2 – correlation coefficient	0.9934
Ostwald (or Power Law):	
m – the consistency coefficient (mPa·s ⁻ⁿ)	42.6
n – the power law exponent	0.8907
R^2 – correlation coefficient	0.9998
Bingham Plastic:	
t_o^B - the Bingham yield stress (Pa)	0.7562
η_p - the plastic viscosity (cP)	19.7
R^2 – linear correlation coefficient	0.9978
Herschel-Bulkley:	
t_o^H - the yield stress (Pa)	0
k - the Herschel-Bulkely consistency coefficient (mPa·s ^{-b})	42.6
b - the Hershel-Bulkely power law exponent	0.8907
R^2 – correlation coefficient	0.9998
n/a – not applicable	

**Table A.17. AP-101 8 M Na Melter Feed Rheology Data at 25° C
one week after Glass Former Chemical Addition (File Name: 082902a)**

Model/model Parameter	Parameter Value
Shear Strength (by Vane Method):	
t_o - Shear Strength (Pa)	n/a
Newtonian:	
η – Newtonian viscosity (cP)	29.2
R^2 – correlation coefficient	0.9960
Ostwald (or Power Law):	
m – the consistency coefficient (mPa·s ⁻ⁿ)	15.7
n – the power law exponent	1.095
R^2 – correlation coefficient	0.9994
Bingham Plastic:	
t_o^B - the Bingham yield stress (Pa)	0
η_p - the plastic viscosity (cP)	29.2
R^2 – linear correlation coefficient	0.9960
Herschel-Bulkley:	
t_o^H - the yield stress (Pa)	0.6235
k - the Herschel-Bulkely consistency coefficient (mPa·s ^{-b})	10.5
b - the Hershel-Bulkely power law exponent	1.15
R^2 – correlation coefficient	0.9998
n/a – not applicable	

**Table A.18. AP-101 8 M Na Melter Feed Rheology Data at 40° C
one week after Glass Former Chemical Addition (File Name: 090302c)**

Model/model Parameter	Parameter Value
Shear Strength (by Vane Method):	
t_o - Shear Strength (Pa)	n/a
Newtonian:	
η – Newtonian viscosity (cP)	28.3
R^2 – correlation coefficient	0.9920
Ostwald (or Power Law):	
m – the consistency coefficient (mPa·s ⁻ⁿ)	16.0
n – the power law exponent	1.087
R^2 – correlation coefficient	0.9950
Bingham Plastic:	
t_o^B - the Bingham yield stress (Pa)	0
η_p - the plastic viscosity (cP)	28.3
R^2 – linear correlation coefficient	0.9920
Herschel-Bulkley:	
t_o^H - the yield stress (Pa)	0.7993
k - the Herschel-Bulkely consistency coefficient (mPa·s ^{-b})	9.4
b - the Hershel-Bulkely power law exponent	1.16
R^2 – correlation coefficient	0.9956
n/a – not applicable	

**Table A.19. AP-101 8 M Na Melter Feed Settled Solids Rheology Data at 25° C
one week after Glass Former Chemical Addition (File Name: 092502f)**

Model/model Parameter	Parameter Value
Shear Strength (by Vane Method):	
t_o - Shear Strength (Pa; 092402a_ss)	2624
Newtonian:	
η – Newtonian viscosity (cP)	246.6
R^2 – correlation coefficient	0.9305
Ostwald (or Power Law):	
m – the consistency coefficient (mPa·s ⁻ⁿ)	1367
n – the power law exponent	0.7391
R^2 – correlation coefficient	0.9801
Bingham Plastic:	
t_o^B - the Bingham yield stress (Pa)	26.4
η_p - the plastic viscosity (cP)	207.3
R^2 – linear correlation coefficient	0.9771
Herschel-Bulkley:	
t_o^H - the yield stress (Pa)	11.31
k - the Herschel-Bulkely consistency coefficient (mPa·s ^{-b})	742.1
b - the Hershel-Bulkely power law exponent	0.8216
R^2 – correlation coefficient	0.9813

**Table A.20. AP-101 8 M Na Melter Feed Settled Solids Rheology Data at 40° C
one week after Glass Former Chemical Addition (File Name: 092502g)**

Model/model Parameter	Parameter Value
Shear Strength (by Vane Method):	
t_o - Shear Strength (Pa; 091902f_ss)	609
Newtonian:	
η – Newtonian viscosity (cP)	179.0
R^2 – correlation coefficient	0.9894
Ostwald (or Power Law):	
m – the consistency coefficient (mPa·s ⁻ⁿ)	329.2
n – the power law exponent	0.9074
R^2 – correlation coefficient	0.9940
Bingham Plastic:	
t_o^B - the Bingham yield stress (Pa)	7.569
η_p - the plastic viscosity (cP)	167.7
R^2 – linear correlation coefficient	0.9954
Herschel-Bulkley:	
t_o^H - the yield stress (Pa)	8.104
k - the Herschel-Bulkely consistency coefficient (mPa·s ^{-b})	156.7
b - the Hershel-Bulkely power law exponent	1.01
R^2 – correlation coefficient	0.9954

Distribution

No. of Copies		No. of Copies
	OFFSITE	ONSITE
2	<u>Savannah River Technology Center</u> Jim Marra PO Box 616, Road 1 Building 773-43A Aiken, South Carolina 29808 Harold Sturm PO Box 616, Road 1 Building 773-A Aiken, South Carolina 29808	11 <u>Battelle – Pacific Northwest Division</u> B.W. Arey P8-16 P.R. Bredt P7-25 E.C. Buck P7-27 C.H. Delegard P7-25 D.E. Kurath P7-28 B.K. McNamara P7-25 A.P. Poloski P7-25 R.G. Swoboda P7-22 Project Office P7-28 Information Release (2) K1-06
1	<u>Vitreous State Laboratory</u> Ian Pegg The Catholic University of America 620 Michigan Ave., N.E. Washington, DC 20064	5 <u>Bechtel National, Inc.</u> W.L. Graves H4-02 H.R. Hazen H4-02 K. Prindiville H4-02 W.L. Tamosaitis H4-02 WTP PDC Coordinator H4-02